Prepared in cooperation with the Ministry of Petroleum, Energy and Mines, Islamic Republic of Mauritania

Second Projet de Renforcement Institutionnel du Secteur Minier de la République Islamique de Mauritanie (PRISM-II)

Mineral Potential for Nickel, Copper, Platinum Group Elements (PGE), and Chromium Deposits Hosted in Ultramafic Rocks in the Islamic Republic of Mauritania:

Phase V, Deliverable 67

By Cliff D. Taylor, Erin E. Marsh, and Eric D. Anderson

Open-File Report 2013–1280 Chapter G

U. S. Department of the Interior
U. S. Geological Survey

U. S. Department of the Interior
SALLY JEWELL, Secretary

U. S. Geological Survey
Suzette M. Kimball, Acting Director

U. S. Geological Survey, Reston, Virginia: 2015

For more information on the USGS—the Federal source for science about the Earth, its natural and living resources, natural hazards, and the environment, visit http://www.usgs.gov or call 1–888–ASK–USGS.

For an overview of USGS information products, including maps, imagery, and publications, visit http://www.usgs.gov/pubprod

To order this and other USGS information products, visit http://store.usgs.gov

Suggested citation:
Taylor, C. D., Marsh, E. E., and Anderson, E. D., 2015, Mineral potential for nickel, copper, platinum group elements (PGE), and chromium deposits hosted in ultramafic rocks in the Islamic Republic of Mauritania (phase V, deliverable 67), chap. G *of* Taylor, C.D., ed., Second projet de renforcement institutionnel du secteur minier de la République Islamique de Mauritanie (PRISM-II): U. S. Geological Survey Open-File Report 2013–1280-G, 85 p., http://dx.doi.org/10.3133/ofr20131280. [In English and French.]

Any use of trade, firm, or product names is for descriptive purposes only and does not imply endorsement by the U. S. Government.

Although this information product, for the most part, is in the public domain, it also may contain copyrighted materials as noted in the text. Permission to reproduce copyrighted items must be secured from the copyright owner.

Multiple spellings are used in various literatures, and may be reflected in the text.

This report is preliminary and has not been reviewed for conformity with U. S. Geological Survey editorial standards or for stratigraphic nomenclature.

The report is being released in both English and French. In both versions, we use the French-language names for formal stratigraphic units.

ISSN 2331-1258 (online)

Contents

Figures

Tables

Conversion Factors

SI to Inch/Pound

Multiply	By	To obtain
	Length	
centimeter (cm)	0. 3937	inch (in.)
millimeter (mm)	0. 03937	inch (in.)
decimeter (dm)	0. 32808	foot (ft)
meter (m)	3. 281	foot (ft)
kilometer (km)	0. 6214	mile (mi)
	Area	
hectare (ha)	2. 471	acre
square meter (m^2)	0. 0002471	acre
square kilometer (km^2)	0. 3861	square mile (mi^2)
	Volume	
cubic kilometer (km^3)	0. 2399	cubic mile (mi^3)
	Mass	
gram (g)	0. 03527	ounce, avoirdupois (oz)
kilogram (kg)	2. 205	pound avoirdupois (lb)
megagram (Mg)	1. 102	ton, short (2,000 lb)
megagram (Mg)	0. 9842	ton, long (2,240 lb)
metric ton per day	1. 102	ton per day (ton/d)
megagram per day (Mg/d)	1. 102	ton per day (ton/d)
metric ton per year	1. 102	ton per year (ton/yr)
	Pressure	
kilopascal (kPa)	0. 009869	atmosphere, standard (atm)
kilopascal (kPa)	0. 01	bar
	Energy	
joule (J)	0. 0000002	kilowatt hour (kWh)

ppm, parts per million; ppb, parts per billion; Ma, millions of years before present; m.y., millions of years; Ga, billions of years before present; 1 micron or micrometer (µor µm) = 1×10^{-6} meters; Tesla (T) = the field intensity generating 1 Newton of force per ampere (A) of current per meter of conductor

Temperature in degrees Celsius (°C) may be converted to degrees Fahrenheit (°F) as follows:

°F=(1.8×°C)+32

Temperature in degrees Fahrenheit (°F) may be converted to degrees Celsius (°C) as follows:

°C=(°F-32)/1.8

Coordinate information is referenced to the World Geodetic System (WGS 84)

Acronyms

AMT	Audio-magnetotelluric
ASTER	Advanced Spaceborne Thermal Emission and Reflection Radiometer
AVIRIS	Airborne Visible/Infrared Imaging Spectrometer
BIF	Banded iron formation
BLEG	Bulk leach extractable gold
BGS	British Geological Survey
BRGM	Bureau de Recherches Géologiques et Minières (Mauritania)
BUMIFOM	The Bureau Minier de la France d'Outre-Mer
CAMP	Central Atlantic Magmatic Province
CGIAR-CSI	Consultative Group on International Agricultural Research-Consortium for Spatial Information
DEM	Digital Elevation Model
DMG	Direction des Mines et de la Géologie
EC	Electrical conductivity
EMPA	Electron Microprobe Analysis
EM	Electromagnetic (geophysical survey)
EOS	Earth Observing System
eU	Equivalent uranium
GGISA	General Gold International
GIF	Granular iron formation
GIFOV	Ground instantaneous field of view
GIS	Geographic Information System
HIF	High grade hematitic iron ores
IHS	Intensity/Hue/Saturation
IAEA	International Atomic Energy Agency
IOCG	Iron oxide copper-gold deposit
IP	Induced polarization (geophysical survey)
IRM	Islamic Republic of Mauritania
JICA	Japan International Cooperation Agency
JORC	Joint Ore Reserves Committee (Australasian)
LIP	Large Igneous Province
LOR	Lower limit of reporting
LREE	Light rare-earth element
METI	Ministry of Economy, Trade and Industry (Japan)
MICUMA	Société des Mines de Cuivre de Mauritanie
MORB	Mid-ocean ridge basalt
E-MORB	Enriched mid-ocean ridge basalt
N-MORB	Slightly enriched mid-ocean ridge basalt
T-MORB	Transitional mid-ocean ridge basalt
Moz	Million ounces

MVT	Mississippi Valley-type deposits
NASA	United States National Aeronautics and Space Administration
NLAPS	National Landsat Archive Processing System
OMRG	Mauritanian Office for Geological Research
ONUDI	(UNIDO) United Nations Industrial Development Organization
PRISM	Projet de Renforcement Institutionnel du Secteur Minier
PGE	Platinum-group elements
RC	Reverse circulation drilling
REE	Rare earth element
RGB	Red-green-blue color schema
RTP	Reduced-to-pole
SARL	Société à responsabilité limitée
SEDEX	Sedimentary exhalative deposits
SIMS	Secondary Ionization Mass Spectrometry
SNIM	Société National Industrielle et Minière (Mauritania)
SP	Self potential (geophysical survey)
SRTM	Shuttle Radar Topography Mission
SWIR	Shortwave infrared
TDS	Total dissolved solids
TIMS	Thermal Ionization Mass Spectrometry
TISZ	Tacarat-Inemmaudene Shear Zone
TM	Landsat Thematic Mapper
UN	United Nations
UNDP	United Nations Development Program
US	United States
USA	United States of America
USGS	United States Geological Survey
UTM	Universal Transverse Mercator projection
VHMS	Volcanic-hosted massive sulfide
VisNIR	Visible near-infrared spectroscopy
VLF	Very low frequency (geophysical survey)
VMS	Volcanogenic massive sulfide deposit
WDS	Wavelength-dispersive spectroscopy
WGS	World Geodetic System

Second Projet de Renforcement Institutionnel du Secteur Minier de la République Islamique de Mauritanie (PRISM-II)

Mineral Potential for Nickel, Copper, Platinum Group Elements (PGE), and Chromium Deposits Hosted in Ultramafic Rocks in the Islamic Republic of Mauritania:

Phase V, Deliverable 67

By Cliff D. Taylor,[1] Erin E. Marsh,[1] and Eric D. Anderson[1]

1 Summary

PRISM-I summary documents mention the presence of mafic-ultramafic igneous intrusive rocks in several areas of Mauritania and a number of chromium (Cr) and copper-nickel (Cu-Ni (±Co, Au)) occurrences associated with them. Permissive geologic settings generally include greenstone belts of any age, layered mafic-ultramafic and unlayered gabbro-anorthosite intrusive complexes in cratonic settings, ophiolite complexes, flood basalt provinces, and fluid-rich shear zones cutting accumulations of mafic-ultramafic rocks. Regions of Mauritania having these characteristics that are discussed in PRISM-I texts include the Mesoarchean greenstone belts of the Tasiast-Tijirit terrane in the southwestern Rgueïbat Shield, two separate layered ultramafic complexes in the Amsaga Complex west of Atar, serpentinized metadunites in Mesoarchean rocks of the Rgueïbat Shield in the Zednes map sheet, several lateritized annular mafic-ultramafic complexes in the Paleoproterozoic northwestern portion of the Rgueïbat Shield, and the serpentinized ophiolitic segments of the Gorgol Noir Complex in the axial portion of the southern Mauritanides. Bureau de Recherches Géologiques et Minières (BRGM) work in the "Extreme Sud" zone also suggests that small copper occurrences associated with the extensive Jurassic microgabbroic intrusive rocks in the Taoudeni Basin of southeastern Mauritania could have potential for magmatic Cu-Ni (PGE, Co, Au) sulfide mineralization. Similarly, Jurassic mafic intrusive rocks in the northeastern Taoudeni Basin may be permissive. Known magmatic Cu-Ni deposits of these types in Mauritania are few in number and some uncertainty exists as to the nature of several of the more important ones.

[1]U.S. Geological Survey, Denver Federal Center, Denver, Colorado 80225 U.S.A.

2 Introduction

Chromium and other mafic-ultramafic rock hosted metal deposits, including those rich in nickel, copper, platinum-group elements (PGEs), or vanadium, are generally found in layered mafic-ultramafic (rocks enriched in magnesium and iron) igneous rock complexes.The largest chromite and PGE deposits are in layered mafic-ultramafic complexes like the Bushveld and Great Dike Complexes in the Kalahari Craton of southern Africa and formed during the Precambrian.These layered complexes formed when mafic-ultramafic magmas were repeatedly injected into chambers at relatively shallow levels in the crust and then cooled very slowly.Because the magma in the chambers cooled slowly, different minerals crystallized from the magma at slightly different temperatures and settled at the bottom.At times two or more minerals crystallized simultaneously and settled together.This differential crystallization of minerals led to the development of a series of distinct layers, some of which contain economic concentrations of metals such as chromium, PGEs, and vanadium.

Nickel comes from two general types of deposits: nickel laterite and igneous (magmatic) nickel-sulfide deposits.Nickel laterite forms by the weathering of nickel-bearing rock in areas with a tropical climate and good drainage. During this process, silica and other components are leached from the rocks, leaving a soil enriched in nickel, cobalt, and iron. The principal nickel minerals are garnierite (hydrous nickel silicate) and nickeliferous limonite (hydrated nickel-bearing iron oxide).These types of deposit can be enriched along structures where permeability is increased.

Ni-Co laterite mineralization is a supergene enrichment of Ni and Co from the pervasive weathering of ultramafic rocks.There are three sub-type Ni-Co laterite deposits distinguished by the dominant mineralogy: oxide, clay, and hydrous Mg-silicate (Marsh and Anderson, 2011). Deposits occur in both tectonically active and docile settings such as New Caledonia and Western Australia.Some deposits have been preserved by burial such as those deposits in Albania and Greece.A generalized laterite profile from base to top consists of parent rock, saprolite, limonite, and ferricrust (fig. 1). When the parent rock Ni concentration is >0.3 percent and has been exposed to pervasive chemical and mechanical weathering then there is the potential to form Ni-Co laterite deposits in which the saprolite zone contains Ni-rich hydrous Mg-silicates, the Ni-rich clays occur in the transition horizon between the saprolite and limonite zones, and Ni-rich goethite occurs in the limonite zone (fig. 1).

In areas which are potentially similar to the setting in Mauritania such as Western Australia, Ni-Co laterite deposits have developed into oxide and clay-type deposits in a region that underwent sub-tropical weathering in the past and are preserved by a shift into a more arid climate coupled by remaining in a tectonically stable environment. These three factors have allowed for the development of thick weathered profiles. The Ni-Co laterite deposits of Australia formed by tropical to sub-tropical weathering during the Cretaceous through the mid-Tertiary and have subsequently been altered under arid climate in more recent history by the precipitation of silica and magnesite (Butt, 2005).

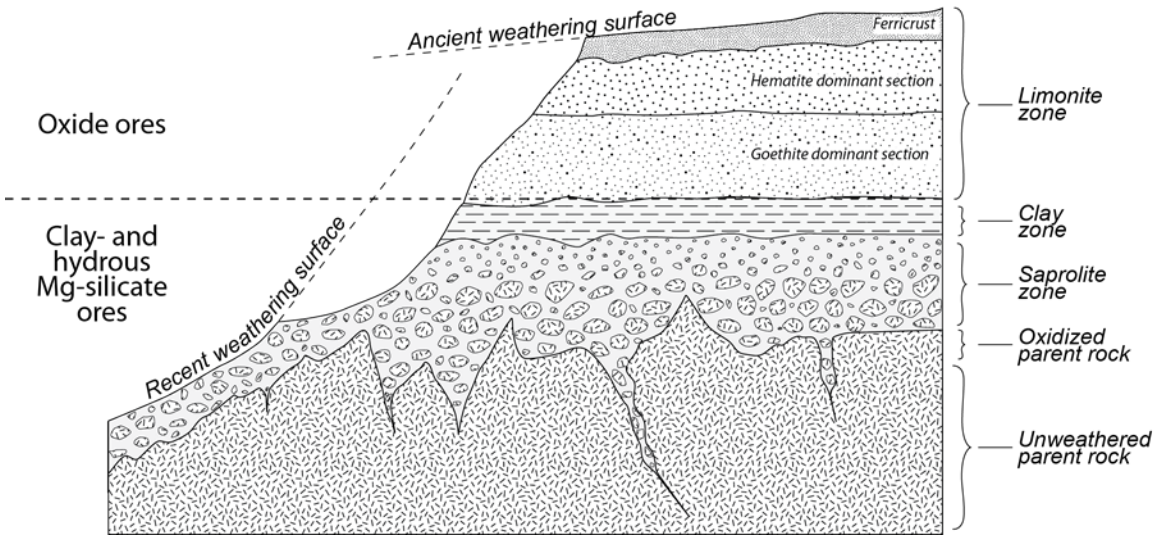

Figure 1. Generalized Ni-Co laterite profile: Idealized cross-section through a Ni-Co laterite weathered profile illustrating all the possible horizons.Natural profiles tend to be much more complex, containing variable sequences of any or all of the layers shown.Modified from Samama (1986).

The potential for such deposits in Mauritania depends on several factors including appropriate parent lithology, key structures, and permissive climate which allows for both the formation and the preservation of the weathered profile. Mauritania has abundant regolith coverage. Looking for the combination of ultramafic country rock, goethite alteration, and structural favorability may be the best approach to finding prospective areas for Ni-Co laterite deposits.

There are several regions in Mauritania that have ultramafic rocks such as harzburgite and dunite that would be appropriate protoliths for a Ni-Co laterite deposit. These areas include the Tasiast-Tijirit region and the southern Mauritanides. It has been noted that northern Mauritania experienced tropical to sub-tropical paleoclimate conditions during the Upper Jurassic (Salpeteur, 2005). The region has since shifted to a semi-arid climate.

Igneous (magmatic) nickel-sulfide deposits are found associated with igneous rocks rich in magnesium, nickel, and chromium; these mafic and ultramafic rocks form as magmas solidify in massive gabbroic and ultramafic igneous complexes like the Sudbury and Duluth Complexes of North America or in flood basalt/sill complexes like the Norilsk Complex in Siberia. As the magmas cool and crystallize, a separate dense liquid rich in sulfur, iron, nickel, copper, and occasionally platinum-group elements, can form within the magma. Once formed, the sulfur-rich liquid, which is denser than the silicate-rich magma, will not remix with the silicate-rich magma. Eventually, the sulfur-iron-nickel-copper-rich liquids accumulate separately and solidify forming a variety of minerals that include pentlandite (iron nickel sulfide), which is mined for its high nickel content. A subtype of the igneous nickel-sulfide deposits is the komatiite-hosted nickel sulfide deposit, such as the Kambalda and Scotia deposits in Australia (Barnes, 2006). Type 1 komatiite-hosted nickel sulfide deposits form as described above, but within lava flow pipes, where they concentrate on the base of the pipes in areas of topographic

variance (Dowling and Hill, 1998). There are known occurrences of komatiitic rocks in the Rgueïbat Shield within the various Birimian dikes, but there are no known extrusive komatiites.

Podiform chromite deposits are lenticular-shaped, pod-like masses of massive coarse-grained to finely disseminated chromitite in the lowermost ultramafic portions of ophiolite complexes (Duke, 1983, 1996; Albers, 1986; Singer and others, 1986). Tabular, rod-shaped, and irregularly shaped bodies are also observed. They form in the lower part of the oceanic lithosphere as magmatic segregation deposits occurring in elongate pockets along spreading plate margins. They are subsequently preserved in collision zones when fragments of oceanic crust are scraped off into the mélange above subduction zones. They are therefore common features of accretion zones at continental margins and, along with their ophiolite host sequences, mark the closure of ocean basins between major crustal blocks.

Rock types present in a complete ophiolite sequence consist of basal tectonized ultramafic rocks (mostly harzburgite), ultramafic cumulates (dunites and harzburgites), non-cumulate and cumulate mafic rocks (gabbros), a basaltic, sheeted dike complex, pillowed basaltic lavas, and a covering of marine sedimentary rocks. The tectonites are thought to represent the residual, partially melted mantle, and the contact with the less deformed, layered ultramafic cumulates has been interpreted to represent the boundary between the mantle and the oceanic crust (the petrological Moho). Discordant bodies of dunite (and chromitite) are suggested to represent intrusions through the upper mantle and lower crust (Cawthorn and others, 2005).The chromite deposits are most common in the uppermost tectonized harzburgites and lower parts of ultramafic cumulates, which are commonly serpentinized. Most podiform chromite deposits worldwide are Phanerozoic in age with important examples in the Phillipines (Tertiary), Albania (Jurassic), Turkey (Paleozoic), and Kazakhstan (Paleozoic). A few Proterozoic examples are known in Egypt and Sudan (Duke, 1996).

Podiform chromite deposits are generally quite small with individual deposits ranging from a few tens to millions of tonnes with deposits greater than 1 million tonnes being rare. The largest known pod in the world contains about 13 million tonnes of high-aluminum chromitite grading 36.5 percent Cr_2O_3. The largest mines generally exploit a number of pods with some mines producing from as many as 20 chromitite pods (Duke, 1996). In terms of dimensions, most podiform chromite bodies are 10 to 100 meters (m) long. A large deposit would be 100–200 m long, 50 m wide, and 10 m thick.

Chromite is the major ore mineral, which when in massive, near-monomineralic aggregates is referred to as the ore-rock chromitite. Ferrichromite, magnetite, ruthenium-osmium-iridium alloys, and the platinum group mineral laurite are possible accessory ore minerals. Gangue minerals in chromitite include olivine, orthopyroxene, clinopyroxene, and plagioclase. Secondary minerals include serpentine, chlorite, tremolite, talc, and carbonate. Chromitite displays a wide range of textures from those clearly related to magmatic processes to those produced during either brittle or ductile deformation. Layering is common and can be a result of cumulate textures, modal grading, and grain size grading. Nodular textured chromite grains are a common and perhaps diagnostic feature of podiform chromite deposits and consist of loosely packed, ellipsoidal chromite nodules 5–20 mm in diameter in dunite matrix (Duke, 1996). Textures produced during deformation include lineation and foliation of chromite and olivine grains, stretching,

boudinage, and fracturing of chromite grains, as well as brecciation and mylonitization. Chromite grains in massive chromitite tend to occur as coarse grained (5–10 mm), interlocking anhedra.

The chemical composition of chromite is variable due to the fact that chrome spinels form a solid solution having the general formula $(Mg, Fe^{2+})(Cr, Al, Fe^{3+})_2O_4$. Naturally occurring chromites have a wide range of chemical compositions that are indicative of the tectonic setting and therefore of the deposit sub-type. Chromite from podiform deposits are low in Fe^{3+} and TiO_2, and the major compositional variation is in the amount of Cr-Al substitution. The $Mg/(Mg+Fe^{2+})$ ratio in chromite from podiform chromite deposits does not vary greatly but does show a slight negative correlation with Cr/(Cr+Al). Systematic variation of chromite compositions across individual deposits has been observed in some deposits and includes the upward decrease in the Cr/Fe ratio in a single lens. A significant increase of both Cr/Fe and Cr/(Cr+Al) with increasing depth below the petrologic Moho has also been documented (Duke, 1983). Podiform chromite deposits are highly resistant to weathering and oxidation.However, despite this characteristic the discovery of a significant number of PGE-bearing podiform chromite deposits has been preceeded by the discovery and exploitation of PGE placer deposits downstream of the podiform chromite deposits. A more thorough description of chromium, nickel, and platinum-group metal deposits related to mafic-ultramafic rocks is found in Naldrett (1989).

Small, annular ultramafic intrusive complexes represent an additional exploration target in Mauritania. Although known in Alaska for almost a century due to their PGE, Cr, Fe, and Ti resource potential (Buddington and Chapin, 1929), they were not recognized as a discrete class of intrusions until the 1960's (Taylor and Noble, 1960; 1969; Noble and Taylor, 1960; Taylor, 1967; Wyllie, 1967; Irvine, 1974) when researchers delineated a group of over 35 intrusions in southeastern Alaska, described their essential characteristics, and noted their similarity to mafic-ultramafic complexes in the Ural Mountains of Russia—sources of the placer PGE deposits of the Urals Platinum Belt (Noble and Taylor, 1960; Krause and others, 2007). The worldwide occurrence of similar Urals/Alaska-type intrusions (in Australia, Canada, China, Colombia, Egypt, and Venezuela) some of which are host to PGE deposits (for example, Gabbro Akarem, Eastern Desert, Egypt; Helmy and Mogessie, 2001), provides a small, but potentially important alternative source of critically important metals other than the larger, well-known layered ultramafic intrusions that occur in Archean-Proterozoic cratonic areas (for example, the Bushveld and Stillwater Complexes of South Africa and the U.S.; the Great Dike of Zimbabwe).

Essential characteristics of annular Alaska/Urals-type intrusions include their small size (meters to as much as 10 kilometers (km) in maximum exposed dimension) and the tendency to occur in belts 20–30 km wide and hundreds of kilometers long.Most of the bodies consist of titaniferous magnetite-bearing hornblende clinopyroxenite or hornblendite, however the larger ones can be zoned and can include chromite-(and PGE) bearing dunite cores surrounded by wehrlites, olivine clinopyroxenites, clinopyroxenites, hornblende clinopyroxenites, and in some cases gabbros. Orthopyroxene- and plagioclase-bearing rocks are conspicuously rare. Mineralogical, chemical, and textural characteristics indicate that they formed from a basaltic parent magma by crystal fractionation and mineral concentration (cumulate) processes, although extensive

layering of cumulates is uncommon. A favored hypothesis suggests they originated from an unfractionated, mantle-derived primary melt such as subalkaline hydrous basalt, common in subduction-related settings such as island arcs. The small size and geometry of the intrusions suggest that they formed as subvolcanic feeder conduits, sills, and small magma chambers at relatively shallow depths of between 3 and 9 km. External contacts of the bodies are generally sharp, steep, and marked by thermal aureoles (Himmelberg and Loney, 1995).However, their exact origins remain contentious. Their tendency to be strongly localized within ~30 km of major terrane-bounding structures and their common juxtaposition and confusion with mafic-ultramafic bodies in adjacent suprasubduction zone ophiolite assemblages, often hampers the discrimination of these types of intrusions (Helmy and Mogessie, 2001; Krause and others, 2007, 2011). When present, mineralization usually consists of Ti-V-rich magnetite, and less commonly chromite and platinum-group minerals or alloys (Taylor and Noble, 1969; Himmelberg and Loney, 1995; Foley and others, 1997; Helmy and Mogessie, 2001; Krause and others, 2007, 2011). Gravity and magnetic highs delineate exposed and buried portions of the intrusions (Barnes, 1986; Brew and others, 1991; Sutphin and others, 1992).

In cases where Alaska/Urals-type intrusions are known to contain PGE resources, they are present in the dunite cores as native platinum, as PGE-bearing bismuth-tellurides and arsenides, or Pt-Fe and Pt-Ir alloys associated with chromite (Cabri, 1981). Erosion of these intrusions and the subsequent concentration of PGEs in placers, accounts for the association of economic PGE placer districts with Alaska/Urals-type intrusive belts.

The potential for the development of economic PGE resources in Cu-Ni-sulfide assemblages within these intrusions is generally regarded as unlikely due to the perception that they are highly oxidized, low-sulfur systems (Himmelberg and Loney, 1995; Helmy and Mogessie, 2001; Johan, 2002; Krause and others, 2007). Controls on the precipitation of PGEs are tied to the concomitant crystallization of olivine and chromite. Rising fO_2 during crystallization lowers the solubility of the PGEs resulting in the entrapment of PGE alloys with chromite grains in dunites. Following the bulk of olivine-chromite crystallization, PGE fractionation trends are largely controlled by fS_2 and the precipitation of PGE-sulfides with greatly enhanced PGE content occurs in association with hornblende-bearing rocks later in the crystallization sequence of the intrusions (Tistl, 1994; Foley and others, 1997).

However, recent work (Urals, Egypt, Columbia and elsewhere; Tistl,1994; Helmy and Mogessie, 2001; Johan, 2002; Krause and others, 2007) has documented significant PGE resources in association with sulfide-bearing assemblages in late (or hydrothermal) phases of zoned intrusions and suggest that perhaps this may be more the usual case when Alaska/Urals-type intrusions contain economic PGE deposits. Ripley and others (2005) suggest that the commonly held assumption that subduction zone settings are not likely to produce large volumes of S-rich mafic magmas may be in error. They point out that ophiolites of suprasubduction zone origin are thought to represent high-degree partial melts of fluid-fluxed mantle wedge material and that the interaction of these magmas with sulfur derived from country rocks could initiate a favorable ore-forming environment. Their observation that the Alaska/Urals-type intrusions may be conduits for the movement of massive amounts of magma responsible for the volcanic rocks in the overlying volcanosedimentary successions provides the mechanism necessary for the throughput and metal exchange needed to form sulfide-rich PGE deposits.

The Alaska/Urals-type intrusions should be highly amenable to exploration targeting and delineation by geophysical methods. High resolution gravity and magnetic data from other mafic intrusions associated with PGE resources (Bushveld, Stillwater) reveal their lateral and vertical extents and in some cases their zonation (Kleinkopf, 1985; Blakely and others, 1985; Blakely and Simpson, 1986; Viljoen, 1999; Cambell, 2011). When combined with mineral occurence, geologic mapping, and remote sensing data, these data can be used to predict the locations and depths of potential intrusion-related deposits.

Aeromagnetic data can be used for mapping the distribution of Alaska/Urals-type intrusions because these complexes tend to be rich in magnetite. Aeromagnetic data provide information on the distribution of magnetic minerals, mainly magnetite. The magnetic property of a rock is quantified by its magnetic susceptibility. In general, rocks with larger concentrations of magnetite have high magnetic susceptibilities and produce magnetic anomaly highs when compared to rocks with low magnetic susceptibilities. Mafic and ultramafic igneous rocks tend to have higher magnetic susceptibilities and produce stronger magnetic anomaly highs relative to felsic igneous rocks (Clark, 1999). Patterns in aeromagnetic anomaly maps can be used to extend the mapping of outcropping lithologic units into the near subsurface.

Several processing techniques can be applied to magnetic data to enhance geologic features. The RTP transform can better align magnetic anomalies with causative geology (Baranov and Naudy, 1964; Blakely, 1995). The RTP transformation recalculates total magnetic intensity data as if the inducing magnetic field had a 90^{o} inclination, as is the case at the north magnetic pole. This operation removes the dependence of magnetic data on the magnetic inclination and thus minimizes anomaly asymmetry due to magnetic inclination and locates anomalies above their causative bodies.

Ultramafic rocks that undergo low-temperature metamorphism are serpentinized. During such processes the ultramafic rocks are hydrated and oxidized which usually results in the formation of magnetite.If magnetite forms in high enough concentration it will appear as an intense positive on a RTP magnetic anomaly map, although differentiating such anomalies from those produced by nearby ultramafic rocks, if present, is difficult.Subsequent geologic processes can destroy the magnetite and the serpentinite may be represented as magnetic anomaly lows.Therefore, interpretation of RTP magnetic anomalies associated with ultramafic and serpentinized rock is complex.The analytic signal calculates the gradient of the magnetic field and can be used to simplify the interpretation of magnetic anomalies (Nabighian, 1972; Roest and others, 1992). This signal exhibits maxima over magnetization contrasts, independent of the ambient magnetic field and source magnetization directions. The resulting anomaly map can be an effective way to map the distribution of ultramafic and serpentized rock.

Magnetic anomaly maps can be used to infer lithologic units at and near the surface. Magnetite-bearing mafic and ultramafic igneous rocks tend to have higher magnetic susceptibilities and produce strong magnetic anomaly highs relative to felsic igneous rocks (Clark, 1999), thereby making differentiation between mafic-ultramafic rocks and felsic rocks relatively straightforward. However, using magnetic anomaly maps to locate ultramafic rocks within mafic rocks is difficult because both can produce magnetic anomaly highs. One way to differentiate mafic and ultramafic rocks is to use

the original flightline data and pick anomalies along the profiles that have characteristic amplitude and wavelength. In this process it is assumed that the ultramafic rocks with higher magnetic susceptibilities produce stronger magnetic anomalies when compared to mafic rocks with lower magnetic susceptibilities (Clark, 1999). The analytic signal calculates the gradient of the magnetic field and can be used to map rapid changes in the magnetic field (Nabighian, 1972; Roest and others, 1992). Ultramafic rocks that have relatively limited aerial extent, such as those associated with podiform chromite deposits and Alaska/Urals-type intrusions, may produce rapid changes in the observed magnetic field making analytic signal helpful in identifying such rocks. Combining magnetic anomaly picks, analytic signal, and mapped geology can be effective for locating ultramafic rocks.

3 Potential for Ni, Cu, PGE, and Cr Deposits in Ultramafic Rocks of Mauritania

3.1 Mesoarchean Greenstone Belts of the Tasiast-Tijirit Terrane

Review of PRISM-I studies by the BGS (Gunn and others, 2004) in the Mesoarchean greenstone belts of the southwestern Rgueïbat Shield suggests that there is abundant evidence for mafic volcanic rock dominated volcano-sedimentary successions that are permissive for Ni-Cu-PGE deposits associated with serpentinized ultramafic bodies within the mafic volcanic rock sequences. In the Tasiast-Tijirit terrane, seven separate greenstone belts should be broadly considered permissive for Ni-Cu-PGE deposits within the supracrustal sequences currently lumped into the Lebzenia Group. More specifically, the Sebkhet Nich Formation encompasses the currently known mafic volcanic sequences within the greenstone belts and is host to known nickel and asbestos occurrences. Areas that are permissive for magmatic Cu-Ni- (PGE, Co-Au) deposits include the southwest Chami Greenstone Belt in the Inkebden area, and at the Khnefissat occurrences in the northwest Chami Belt. An asbestos occurrence at Knefissat Nord provides additional evidence for the presence of permissive serpentinite bodies within the Sebkhet Nich Formation. Thorough analyses of permissive mafic-ultramafic rocks in the other Mesoarchean greenstone belts of the southwestern Rgueïbat Shield appear to be lacking and thus represent untouched exploration targets.

The Rgueïbat Shield in northwestern Mauritania consists of the exposed Archean portion of the West African Craton. Recent mapping by the BGS (Pitfield and others, 2004; O'Connor and others, 2005) divides this part of the shield into two terranes separated by a major arcuate north-northeast- to north-trending shear zone named the Tacarat-Inemmaudene Shear Zone (Key and others, 2008).The eastern Choum-Rag el Abiod terrane consists primarily of granulite facies metamorphic rocks of the Amsaga Complex, which are as old as 3,500 Ma. These rocks are cut by major granitic, and less commonly, by mafic-ultramafic bodies, which range in age from 3,000 to 2,700 Ma. Older fragments of preserved crustal material consisting of greenstone remnants (amphibolites) in migmatitic gneisses are probably about 3,200 Ma in age. This region is interpreted as the dismembered and reworked root zone of a typical granite-greenstone assemblage (Gunn and others, 2004). The western Tasiast-Tijirit terrane consists of a typical Archean granite-greenstone assemblage exposed at shallower levels than the Choum-Rag el Aboid terrane and are thus much less sheared and tectonized than the

similar-age rocks to the east. The oldest rocks are variably migmatized tonalitic gneisses that are cut by younger granitic phases and tectonically or unconformably underlie the greenstone belts (fig. 2).

The Tasiast-Tijirit terrane consists of three major lithologic groups: (1) migmatitic gneisses that are the oldest rocks in the terrane and underlie the greenstone belts, (2) greenstone belt lithologies, and (3) younger granitoid intrusions consisting of gneissic granites, biotite-tonalites-granodiorites (including rocks with abundant secondary epidote) as well as late xenolithic, leucocratic biotite-granites of the Tasiast Suite and gneissic granites of the Tacarat Suite. Intrusions of the Tacarat Suite also intrude the Choum-Rag El Abiod Terrane. Granulite facies rocks of the Choum-Rag El Abiod terrane are not present in the Tasiast-Tijirit terrane (Pitfield and others, 2004).

The migmatitic gneisses consist predominantly of gray tonalitic gneiss cut by up to four generations of intersecting felsic veins, and by much less common metamafic dikes. The metamafic dikes are relatively late intrusions and cut most felsic veins. The veins make up over 20 percent of the rock volume and have a complex history of emplacement separated by periods of ductile shearing. The youngest (muscovite and biotite-bearing) pegmatitic veins post-date the various episodes of ductile shearing, but are cut by brittle fractures. Metamafic dikes are curviplanar features up to about 1m in thickness and can be traced across the larger exposures for tens of meters. Geochemical studies by the BGS on the migmatitic gneisses of both the Tasiast-Tijirit and Choum-Rag El Abiod terrane indicate that the Tasiast-Tijirit gneisses are consistently more silicic, plotting in the rhyolite field of a TAS diagram, and appear more fractionated. They are interpreted as a calc-alkaline magmatic arc crust underlying the greenstone belts (Pitfield and others, 2004). A single U-Pb zircon age of approximately 2,970 Ma (Chardon and others, 1997) and Nd model ages of 3,050 to 3,100 Ma provide the only age contraints on the gneissic basement rocks (Key and others, 2008).

The main greenstone belts in the Tasiast-Tijirit terrane are named, from east to west, the Tijirit, Ahmeyim, Sebkhet Nich, Kreidat, and Chami. Two smaller greenstone belts to the west of the Chami Belt are called the Hadeibt Agheyâne and Hadeibt Lebtheinîyé and are collectively referred to as the Lebzenia Greenstone Belts (fig. 2). These greenstone belts consist predominantly of mafic metavolcanic and siliciclastic metasedimentary rocks metamorphosed at low- to medium-grades. Banded iron formation (BIF) and ultramafic rocks are locally common and intermediate to felsic metavolcanic rocks are rare. The greenstone belts are locally intensely sheared especially along competency contrasts between lithologic units, and major ductile shear zones control both the current shape of the belts as well as folds within the belts.

The greenstone belts are characterized by low to medium-grade metamorphic mineral assemblages in an assortment of metavolcanic and metasedimentary strata. Altered basalts and gabbros that include amphibolite schists, siliciclastic rocks and banded ironstones dominate the various greenstone belts. Ultramafic rocks are locally common (for example, Sebkhet Nich Greenstone Belt). Ferruginous quartzites and banded ironstones are common in the Chami Greenstone Belt and the two westernmost greenstones. Actinolite schists are most common near contacts with intrusions such as syenites, gabbros and late-stage granites. Metasedimentary rocks are locally recrystallized to actinolite-chlorite-quartz, and sericite-quartz schists. The belts are

locally intensely sheared with individual shear zones preferentially following specific lithologies.

Lithologies in the various greenstone belts are lumped into the Lebzenia Group. Four formations are recognized within this group and include: the Talhayet Formation and Tijraj Formation in the Ahmeyim Greenstone Belt, the Aouéoua Formation in the Chami Greenstone Belt, and the Sebkhet Nich Formation from the greenstone belt of the same name. The Tijraj and Aouéoua Formations are dominated by metasedimentary rocks with a significant felsic to intermediate volcanic component. The Talhayet and Sebkhet Nich Formations are characterized by basaltic greenstones and ultramafic rocks with synvolcanic intrusive sheets. In the Ahmeyim Greenstone Belt, the Tijraj Formation is overlain by the Talhayet Formation and exhibits a transitional contact from a dominantly sedimentary to dominantly mafic volcanic assemblage. Mapping by the BGS suggests that the Tijraj Formation was folded about NW-trending axes before deposition of the Talhayet Formation. However, there is no obvious break in the apparent transitional sequence. The Aouéoua Formation forms the fault-bounded synformal core to the contiguous Chami and Kreidat Greenstone Belts and appears to overlie the mafic-ultramafic rocks of the Sebkhet Nich Formation. In the Sebkhet Nich Greenstone Belt, the greenstone sequence is characterised by metasedimentary units structurally overlain by metabasaltic lavas and mafic sheets that are in turn overlain by ultramafic rocks. This same greenstone association flanks the Aouéoua Formation in the Chami and Kreidat Greenstone Belts and characterizes the volcanosedimentary succession in the Hudeibt Agheyâne and Hadeibt Lebtheinîyé Greenstone Belts as well. Thus, if the Talhayet and Sebkhet Nich formations are correlatable, then the most likely depositional sequence assuming no overthrusting or inversion would place the Tijraj Formation at the base, overlain by the Talhayet and Sebkhet Nich formations, with the Aouéoua Formation (dated at 2,968±2Ma) at the top (Pitfield and others, 2004).

Tectonic reconstruction of the southwestern Rgueïbat Shield by the BGS (Pitfield and others, 2004) suggest that amalgamation of two crustal blocks consisting of the western Tasiast-Tijirit terrane and the eastern Choum-Rag el Aboid terrane occurred along the Tacarat-Inemmaudene Shear Zone (TISZ), a transpressive ductile suture zone showing sinistral horizontal offset and east-directed thrusting on its eastern side at about 2,954 Ma. There are no indications of the size of the two crustal blocks prior to their accretion. They are distinguished by differing early Archean geological histories with higher-grade metamorphic rocks including major charnockitic gneiss sheets dominating the Choum-Rag el Abiod terrane and migmatitic tonalite gneisses as the dominant lithology in the Tasiast-Tijirit Terrane. Geochemical characteristics of the tonalite gneisses suggest they represent a calc-alkaline magmatic arc basement to the volcanosedimentary rock successions (greenstone belts) that were emplaced at about 2,968 Ma.

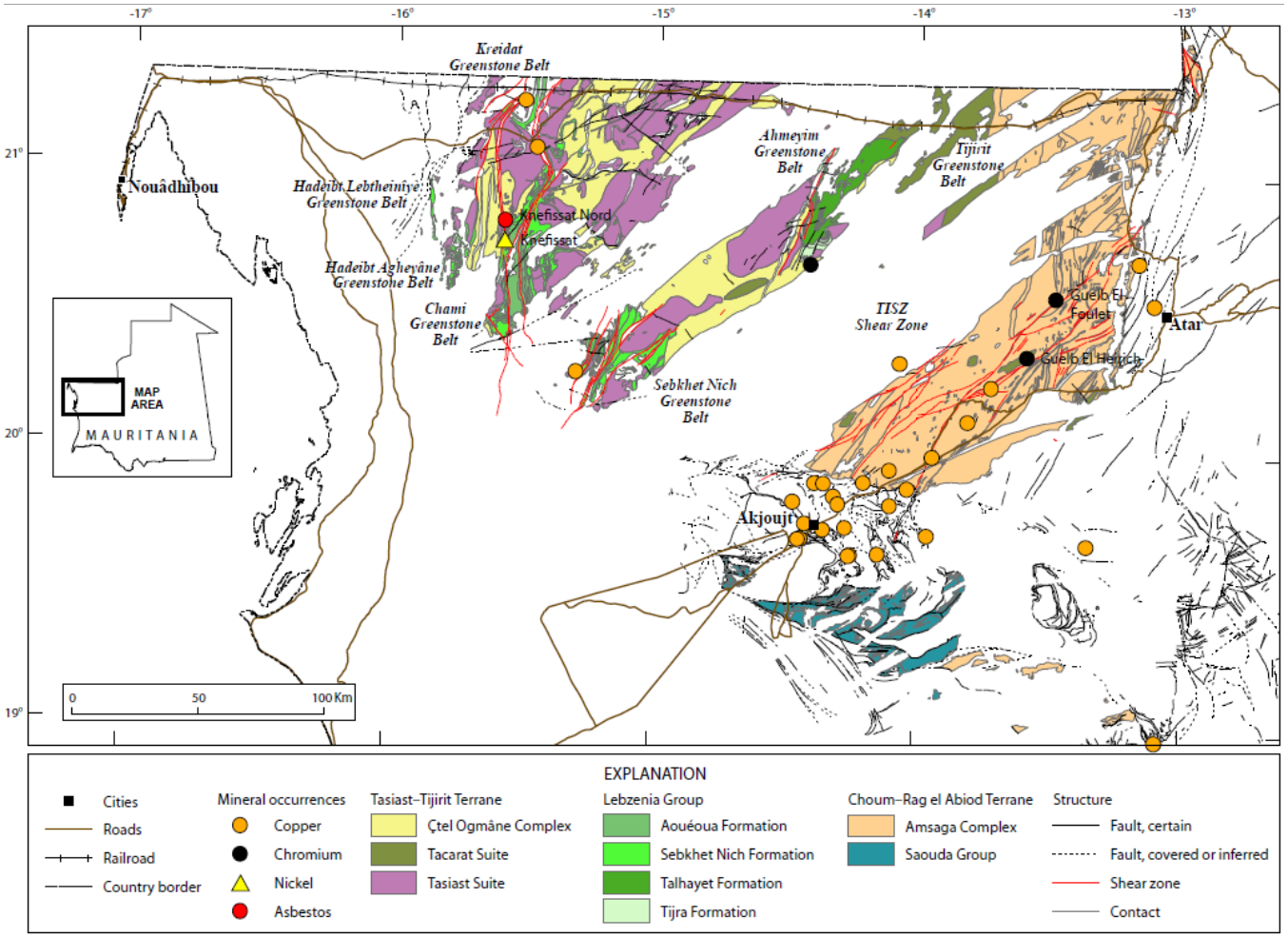

Figure 2. Simplified geologic map of the northwestern Rgueïbat Shield showing the Choum-Rag el Abiod and Tasiast-Tijirit terranes. The principal greenstone belts and mineral occurrences discussed in the text are shown.

Reconstruction of the greenstone belts of the Tasiast-Tijirit terrane suggests that the volcanosedimentary rocks may have originally formed a more continuous carapace over the gneissic basement. The larger greenstone belts may originally have been volcanic centers and display a wide range of volcanic lithologies including felsic volcaniclastics. Geochemical studies of basaltic to intermediate extrusive rocks in the greenstone belt succession exhibit T-MORB to E-MORB affinities followed by subduction-related island arc affinities consistent with initial rifting of the Tasiast-Tijirit terrane basement followed by the development of a more mature island arc setting. The Aouéoua Formation, which forms the fault-bounded core of the contiguous Chami and Kriedat Greenstone Belts, consists predominently of metasedimentary rocks with intermediate and felsic volcanic rocks and is interpreted as a possible transtensional volcanosedimentary basin fill (Pitfield and others, 2004). Neodymium model ages of 3,050 to 3,600 Ma on the felsic rocks suggest derivation from older crustal material (Key and others, 2008).

Available geochronologic constraints suggest that volcanism immediately preceded the collision of the Choum-Rag El Abiod and Tasiast-Tijirit terranes. Volcanism ceased by approximately 2,965 Ma and was followed by collision of the two crustal blocks by approximately 2,954 Ma. Emplacement of voluminous tonalitic plutons at approximately 2,920 Ma occurred throughout the western terrane and shearing in both terranes commenced after amalgamation resulting in significant dismemberment of the greenstone belts. Geochemical studies indicate that the tonalites are metaluminous, calc-alkaline, magmatic arc-type granitoids. Thus, the entire cycle of rifting and island arc formation with subsequent plate collision and post-collision subduction-related arc magmatism took place over a period of about 50 m.y. towards the end of the Mesoarchean. Later anorogenic magmatism at approximately 2,700 Ma occurred throughout both terranes and marks the first period of crustal reworking in the southwestern Rgueïbat Shield (Pitfield and others, 2004).

Very little information is available regarding the size or origins of the two crustal blocks prior to their amalgamation along the TISZ. Based on clear differences in the composition and metamorphic grade of the two juxtaposed gneissic basements, they are suggested to be allochthonous. Westward dipping gneissic fabric within the TISZ suggests that the Tasiast-Tijirit terrane was emplaced on and overlies the Choum-Rag el Abiod terrane (Pitfield and others, 2004; Key and others, 2008). This would imply a continent-continent collision. However, there are no data to suggest that closure of an intervening ocean occurred. A series of small ultramafic bodies of unknown origin, some of which are weakly layered dunites with centimeter-scale layers of chromitite, are present in the Choum-Rag el Abiod terrane and in the eastern portion of the TISZ but not in the Tasiast-Tijirit terrane. These could be interpreted as remnants of oceanic crust except that geophysical data show an absence of features that would indicate the presence of (a rare Archean) ophiolite along the suture (Finn and Anderson, 2015). They may also represent suprasubduction zone ultramafic intrusions or Alaska/Urals-type annular intrusions above an eastward dipping subduction zone. Similarly, all geochemical data available on mafic volcanic rocks in the greenstone belts suggest their derivation from an uncontaminated or slightly contaminated depleted mantle source with the less abundant intermediate and felsic volcanic rocks displaying “subduction-related” signatures. None

of the volcanic rocks analyzed to date exhibit N-MORB geochemistry or primitive radiogenic isotopic signatures indicative of oceanic crust.

The nature of the collision and the environment of formation of the volcanosedimentary successions in the greenstone belts of the Tasiast-Tijirit terrane has direct implications for the types of ultramafic rocks that should be present and on the favorability of the successions. The absence of oceanic crust in the Tasiast-Tijirit terrane clearly eliminates the possibility of discovering ophiolite-related types of Cr-Cu-Ni-PGE-bearing magmatic sulfide segregation or podiform chromite deposits. The presence of mafic-dominated sequences related to island arc volcanism and incipient rifting suggests that the terrane is permissive of ultramafic rock-hosted deposits similar to those found in island arcs and in rifted suprasubduction zone and back-arc settings. Therefore, future exploration for ultramafic rock hosted deposits in the Tasiast-Tijirit terrane should expect to find either magmatic sulfide segregation deposits or Alaska/Urals-type annular ultramafic type deposits that are known to occur in accreted terranes.

The presence of other mineral deposit types in the Tasiast-Tijirit terrane known to be associated with Cu-Ni-PGE and Cr-PGE deposits in accreted terranes is encouraging for exploration (for example, orogenic gold). Due to the clear potential for the discovery of orogenic gold deposits in the region (see Goldfarb and others, 2015), the exploration maturity is relatively high compared to other regions of Mauritania. Since the 1990s the region has been explored for orogenic gold and nickel sulfide by several different companies and agencies resulting in the collection and analysis of over 18,000 geochemical samples followed by a significant amount of drilling (see exploration summary in Gunn and others, 2004). Although the greenstone belts of the Tasiast-Tijirit terrane are regarded as permissive for the occurrence of bimodal-mafic and possibly pelite-mafic types of volcanogenic massive sulfide (VMS) deposits, the complete absence of known VMS occurrences suggests that the favorability for this deposit type is low. The reason for the absence of known VMS occurrences is unclear and may only partially be due to the lack of targeted exploration in the region (see Taylor and Giles, 2015a).

Ultramafic rocks in the Tasiast-Tijirit region in the southwestern Rgueïbat Shield of northwestern Mauritania with potential laterite enrichment were studied by Dumas (1971) and Muller (1972). In this region the weathered profile has been observed to have characteristics similar to the generalized Ni-Co laterite profile described above with the addition of overprinting by secondary silica (fig. 3).One notable difference from deposits in Western Australia (WA) is the depth of the weathered profile; in the Tasiast-Tijirit region it is approximately 10 m deep and in WA it can be up to 100 m deep.

Dumas' (1971) geochemistry for surface samples taken across a silicified laterite at the Inkebden occurrence shows elevated levels of Co and Ni (fig. 4). The geochemistry reported in Dumas (1971) was followed with a more detailed review of the mineralogy at the Kneiffissat and Inkebden occurrences in Muller (1972). The Mineral Deposit Database of the Islamic Republic of Mauritania (Marsh and Anderson, 2015) lists Knefissat (038IND0012) as an occurrence of garnierite, which is a term for amorphous hydrous-Mg silicate common to the saprolite horizon of Ni-Co laterite deposits.Muller (1972) noted a concentration of >1 percent Ni within the laterite profile at the South Inkebden occurrence.He also observed that in this region many of the altered profiles are covered by dolomite, which has no Ni signature or alteration. This observation may indicate that young rock sequences, in this region the dolomite, has covered and

preserved the laterite profile, similar to the limestone capped deposits in Greece and Albania (see Valeton and others, 1987; Economou-Eliopoulus, 2003). In this region there are thin heterogenous occurrences of Ni enrichment that can exceed 1 percent but do not exceed 3m in thickness and these Ni anomalies are Ni-Co laterite deposits rather than Ni-sulfide occurrences (Muller, 1972).These locations in the Tasiast-Tijirit region are moderately prospective for Ni-Co laterite deposits as they have ultramafic parent rocks that have been pervasively weathered to develop residual concentrations of Ni and Co.

Aeromagnetic data collected in the Tasiast-Tijirit region show a complex pattern of magnetic anomalies (fig. 5). The reduced-to-pole (RTP) anomaly map shows through-going linear north-northeast-trending anomalies that are interpreted to reflect dikes. North-northwest trending RTP anomaly highs are also present and are attributed to BIF associated with greenstone belts (Finn and Anderson, 2015). Several broad RTP anomaly highs correlate with mapped Archean granodiorite, gneiss, and mafic metavolcanic rocks in the region. The analytic signal is dominated by the greenstone belts that trend north-northwest. The Mesozoic dikes are also evident in the analytic signal, but their anomalies are more subdued than those associated with the greenstone belts.

The Kneiffissat and Inkebden regions show several isolated analytic signal highs that correlate with actinolite schist and metabasalt units (Dumas, 1971; Muller, 1972). The Inkebden region also shows isolated analytic signal highs associated with mapped metagabbro units. These isolated analytic signal highs represent areas of rapid change in the magnetic field. Such changes may be associated with the production and preservation of magnetite during and after serpentinization of ultramafic parent rock. These areas are interpreted to host favorable parent rocks that may weather to form Ni-laterite deposits. Thus the isolated analytic signal highs, especially when in proximity to mapped laterite units, are favorable for Ni-laterite deposits.

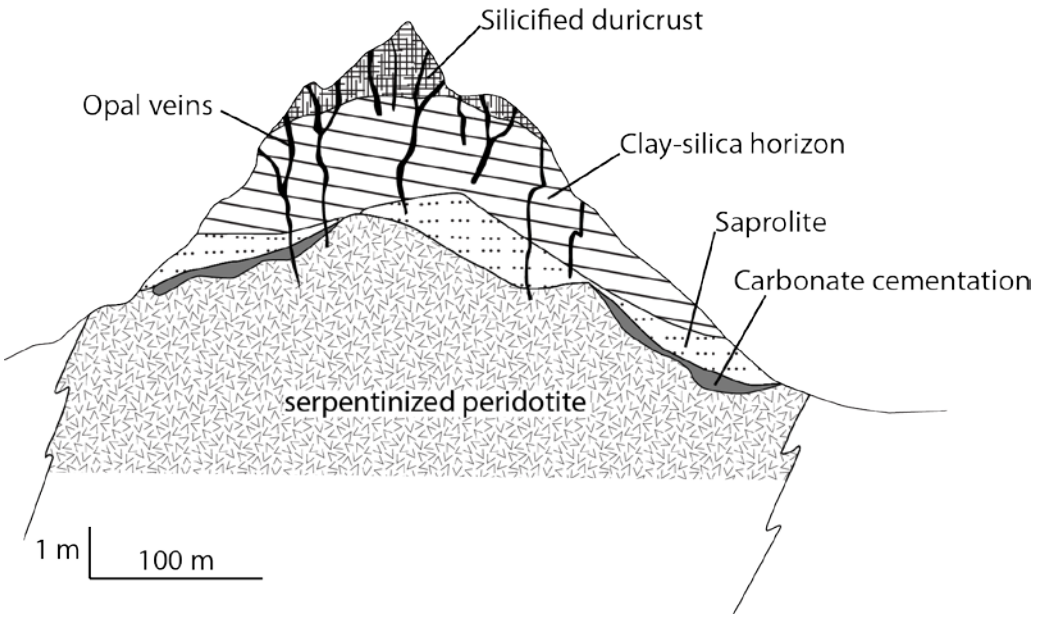

Figure 3. A cross section of a weathered laterite profile from the Tasiast-Tijirit region showing the progressive weathering of the serpentinized peridotite host rock. Modified from Freyssinet (1994).

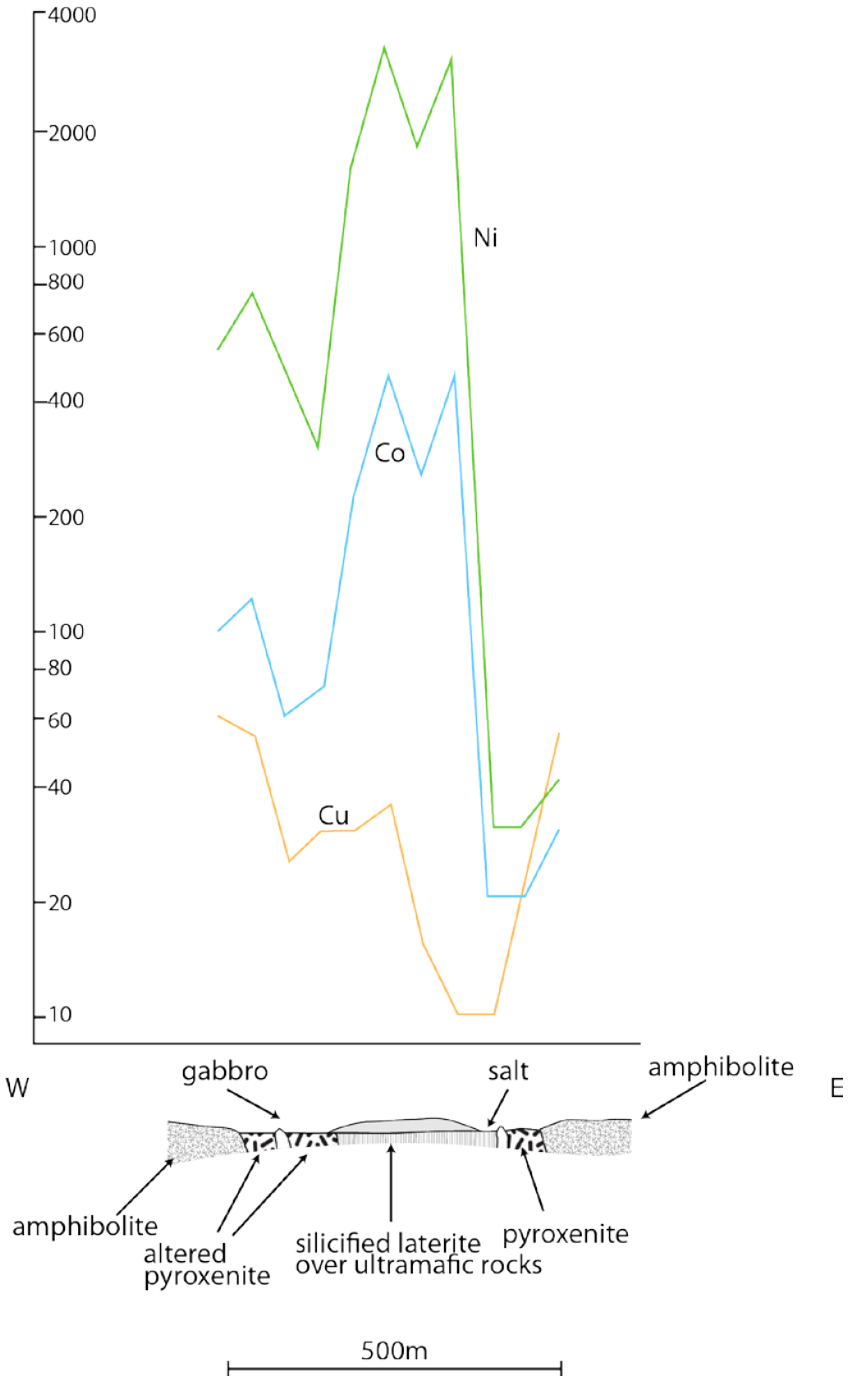

Figure 4. Profile at Inkebden showing a geologic cross section of the sampling transect and the Ni (in green), Co (in blue), and Cu (in orange) geochemistry across the transect (modified from Dumas, 1971). Y axis in parts per million (ppm).

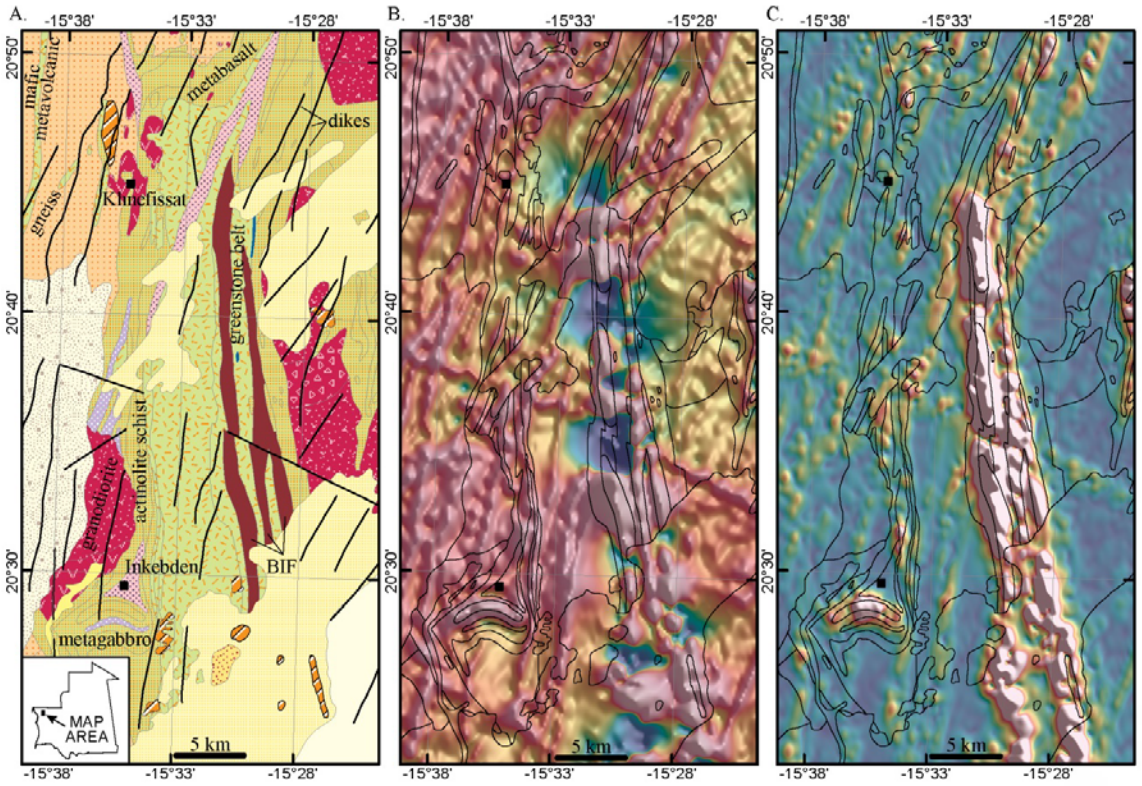

Figure 5. Generalized geology, reduced-to-pole (RTP), and analytic signal maps from the Tasiast-Tijirit region. The Khnefissat and Inkebden Ni-laterite occurrence are shown. *A,* The geology in the region consists of granodiorite, gneiss, mafic metavolcanic, metagabbro, and BIF. Dikes trending mostly north-northeast are also mapped in the region (black lines). *B,* The RTP map shows through-going, linear magnetic anomaly highs associated with the mapped dikes. Broader magnetic anomaly highs are associated with granodiorite and gneiss units. The linear north-northwest magnetic anomaly highs correlate with BIFs. Magnetic highs and lows are shown as warm and cool colors, respectively. *C,* The analytic signal map highlights the greenstone belt between the BIFs. Also shown are several, more isolated analytic signal highs that correlate with mafic metavolcanic, actinolite schist, and metagabbro units which are considered favorable parent rock for Ni-laterite deposits. Analytic signal highs and lows are shown as warm and cool colors, respectively.

3.2 Ultramafic Bodies in the Amsaga Complex

As described above, the Choum-Rag El Abiod terrane is the eastern high grade metamorphic basement of the Mesoarchean southwestern portion of the Rgueïbat Shield. The terrane is characterized as the root zone of a typical Archean granite-greenstone terrane such as is exposed at shallower levels in the Tasiast-Tijirit terrane to the west (Pitfield and others, 2004). The majority of the Choum-Rag El Abiod terrane is composed of amphibolite to granulite facies granitic rocks of the Amsaga Complex that have been tectonically reworked. Ductile shearing is so prevalent that most outcrops are lozenge-shaped and consist of tectonically juxtaposed lithologies that are migmatized to a

greater or lesser extent. Fissile, biotite-bearing quartzofeldspathic gneiss is the dominant lithology within which there are numerous, generally small elliptical bodies of schistose amphibolite, and lesser thinly laminated biotite-carbonate rocks that may represent sheared metabasalts, pyroxenites, metagabbro, banded calc-silicate rocks, BIF, dunite-carbonate breccias, charnockitic gneiss, anorthosite sheets, and other unspecified ultramafic bodies. Individual lozenges of a given lithology are generally up to several hundred meters long and tens of meters thick (Pitfield and others, 2004). Individual mappable units of mylonite and ultramylonite occur in a series of long, thin lozenges that run in a sinuous pattern up the center and eastern portion of the Amsaga Complex from the southern thrust contact with overlying Neoproterozoic rocks of the Inchiri district to the northern border near Choum. These mylonites are "flower structures (Pitfield and others, 2004)" related to the TISZ, which constitutes the western border of the terrane.

The majority of the relatively common amphibolite bodies as well as many of the biotite-carbonate lenses are probably remnants of arc mafic volcanic rocks such as the Saouda Group greenstones present in the southern end of the Choum-Rag el Abiod terrane or the Lebthenia Group rocks in the Tasiast-Tijirit terrrane. However, as described above, there are a number of small ultramafic bodies of unknown origin, some of which are weakly layered dunites with centimeter-scale layers of chromitite.Layered complexes described by the BGS (Gunn and others, 2004) in the Amsaga Complex represent an area of potential for chromite and Cu-Ni-PGE deposits in layered ultramafic complexes. Two occurrences of chromite at Guelb el Foulet and at Guelb El Heirich are hosted by small, tectonized anorthosite complexes containing lenses of serpentinite, pyroxenite, anorthosite, and amphibolite within garnet leptynite, (charnockitic) hypersthene schist, and migmatite of the Amsaga Complex. Although amphibolite and ultramafic units are individually mapped within the 1:200,000 scale geologic mapping by the BGS (Pitfield and others, 2004) in the Amsaga Complex, the lack of correlation of the two known chromite occurrences with existing mapped ultramafic units requires that the entire Amsaga Complex be considered as permissive for these deposits. The BGS report (Gunn and others, 2004) notes that small pods of chromitite are associated with all of the several varieties of ultramafic rocks present. There are no known occurrences of nickel or asbestos within the Amsaga Complex. The majority of the five or six known copper occurrences in this region are either of uncertain setting or are associated with quartz veining in paragneiss and migmatite.

The BGS report (Gunn and others, 2004) mentions the presence of a massive, homogenous metagabbro body in the Iguilid massif in the eastern Choum-Rag el Abiod terrane that also must be considered permissive for chromite and Cu-Ni-PGE. The Iguilid massif is the largest of a series of metagabbro intrusive bodies located throughout the Amsaga Complex. It consists of an arcuate body elongated in the N-S direction underlying a range of large hills and a second smaller north-south elongate body to the east. Smaller metagabbro pods are common in the tectonically interleaved gneisses surrounding the intrusion and all of the metagabbroic rocks in the area are collectively referred to as the Iguilid Suite. The metagabbros are massive, equigranular, medium to coarse-grained, and weather to either a blue-gray or brown color. The main body is described as having little evidence of layering, grain size, or compositional variation and very sparse or absent magmatic sulfides. However, the relatively large size of the two main intrusive bodies (10 × 3 and 7 ×1.2 km respectively) is significant and analogous to

massive gabbroic intrusions, such as the Duluth Complex, which are known hosts to significant Cu-Ni-PGE deposits. An age of approximately 2,730 Ma was obtained on two late tectonic, post-granulite granite and gabbro intrusions (Potrel and others, 1998) and the Iguilid metagabbro yielded a mineral Sm-Nd age of 2,706±54 Ma (Rocci and others, 1991).

The Iguilid massif is cut by tourmaline and muscovite-bearing quartz-feldspar pegmatite veins and sheets similar to those occurring in the Tasiast-Tijirit terrane (Pitfield and others, 2004) and has two beryl occurrences located on the east and west margins of the intrusion (Gunn and others, 2004; Taylor and Giles, 2015b). However, there are no known occurrences of Cu, Ni, Cr, or PGEs associated with the Iguilid Suite. A USGS field team visited the margins of the main intrusion during fieldwork in October 2007 to confirm the locations of the pegmatite occurrences but conducted no work on the massif itself (fig. 6).

Determination of the nature of the host ultramafic bodies at the two chromitite occurrences has implications for their prospectivity and will additionally provide information on the prospectivity of other tectonically dismembered ultramafic bodies in the Amsaga terrane. Gunn and others (2004) describe the Guelb el Heirich occurrence as a northeast-trending area approximately 10 km long and 500 m wide that is located about 20 km to the southwest of the Guelb el Foulet occurrence. This area represents a zone of faulting and mylonitization into which an extensive anorthosite complex with associated serpentinites and amphibolites was emplaced and then dismembered. Individual anorthosite bodies reach dimensions of up to 1 km and chromitites are associated with all of the various mafic-ultramafic lithologies. Chromitite bodies generally are much smaller, occupying areas of a few hundred square meters, and are of limited vertical extent. Twenty eight drill holes of up to 30 meters depth encountered chromitites at depths greater than 10 m in only two holes (BRGM, 1975). Geochemical analyses of 40 samples contained an average of approximately 30 percent Cr_2O_3, low Al_2O_3, and low Cr/Fe ratios (Gunn and others, 2004).

In October 2007, a USGS field team attempted to locate the Guelb el Heirich chromitite occurrence without success. Outcrop at the coordinates published in the Mineral Deposit Database of the Islamic Republic of Mauritania (Marsh and Anderson, 2015) consists of mylonitic granitic rocks and thin layers of very fine crystalline black amphibolite. No ultramafic rocks were present in the vicinity.

Similar to the El Heirich occurrence, Gunn and others (2004) describe the Guelb el Foulet occurrence as a dismembered anorthosite complex containing numerous bodies of anorthosite, serpentinites, pyroxenites, and amphibolites in a zone approximately 4 kilometes long and 300 m wide. The dismembered complex is hosted in faulted and sheared garnet-bearing quartzofeldspathic gneiss close to a faulted contact with hypersthene-bearing gneisses to the west. Drilling in the main area of the occurrence identified a complex series of tectonized chromitite pods in a serpentinite that was formerly a harzburgite body (BRGM, 1975). Chromitites up to a meter thick were intersected primarily in pyroxenites. Geochemical analyses of drill core from 36 holes contained Cr_2O_3 of 30–36 percent with three samples in excess of 40 percent. Samples were low in Al_2O_3 and had low Cr/Fe ratios (Gunn and others, 2004).

Outcrop at the published coordinates of the Guelb el Foulet Cr occurrence consists of a low-standing area in the regolith composed of pyroxenite, anorthosite

(sample CT07RIM-19-2), and semi-massive chromitite (sample CT07RIM-19-1). The location is about 5 km east of the Guelb el Foulet topographic feature (Thiam Baidy Abdoulaye, Department of Mines and Geology, Islamic Republic of Mauritania, oral commun., October 2007). Geologic relationships at this site are unclear due to poor exposure (fig. 7). A second site approximately one km to the north consists of similar rocks in poor outcrop and regolith around a cemented drill hole collar. Sample CT07RIM-20-1 collected from this site consists of semi-massive chromitite with interstitial plagioclase (anorthite). Finally, a low ridge with a second cemented drill collar is located an additional 100 m to the north. At this location, the most abundant lithology is chromite-bearing pyroxenite with variable amounts of plagioclase. A minor amount of light-colored noritic lithologies are present in outcrop and in float near the ridge. Distinct layering on a centimeter-scale is visible in hand samples and in outcrop as well as size grading of crystals within individual layers, suggesting that the anorthosite-pyroxenite host body was emplaced late- to post-tectonically. Bands of semi-massive chromitite 1 to 2 centimeters (cm) thick are interlayered with pyroxenite (sample CT07RIM-21-1) and with anorthosite (sample CT07RIM-21-2). Layered pyroxenite-anorthosite without chromitite (sample CT07RIM-21-3) is also present in outcrop. Chromitite layers and layered ultramafic rocks can be traced for approximately 20 to 30 meters along the crest of the low ridge before being obscured by regolith.

Due to the paucity of information on the small ultramafic bodies in the Amsaga Complex and the corresponding lack of high quality geochemical data, all six of the samples described above were analyzed for detailed bulk rock geochemistry including a full suite of PGEs and Au. Results of these analyses are provided in table 1. Additional petrographic and mineral chemistry (electron microprobe) studies were carried out in an effort to discriminate the tectonic environment of formation of the Guelb el Foulet Cr occurrence. The mineral chemistry of chromite can provide insights into the tectonic setting in which mafic and ultramafic rocks have formed. As a member of the spinel solid solution series, chromite exhibits subtle variation in major element composition that provide the ability to discriminate between different types of host mafic-ultramafic intrusions such as those formed in ophiolites, Alaska/Urals-type or layered stratiform intrusions. Chromite is a refractory mineral that crystallizes early from the melt and remains stable under a variety of post-crystallization environments (Irvine, 1965, 1967; Roeder, 1994). The widespread occurrence of chromite as an accessory mineral in mafic-ultramafic igneous rocks and its resistance to chemical change in the metamorphic and hydrothermal environment makes it a useful discriminant tool in poorly exposed geologic terrains or where geologic relationships are unclear. Microprobe data on Guelb el Foulet chromites are presented in table 2 and the results of tectonic discriminant analyses based on these data are described below.

Figure 6. View along the margin of the Iguilid metagabbro massif. USGS photo.

Figure 7. View looking north at the Guelb el Foulet chromite occurrence. USGS photo.

Table 1. Detailed whole rock geochemical data for samples of mafic-ultramafic lithologies and chromitites from the Guelb el Foulet Cr occurrence and from a quarry in the northern Amsaga Complex near Choum.

		Field No.	CT07RIM19-1	CT07RIM19-2	CT07RIM20-1	CT07RIM21-1	CT07RIM21-2	CT07RIM21-3	CT07RIM24-1	CT07RIM25-1
		Mineral occurrence	Guelb el Foulet	Guelb el Foulet	Guelb el Foulet	Guelb el Foulet	Guelb el Foulet	Guelb el Foulet	SNIM prospect	SNIM quarry
Analytical method	Oxide or element	Lithology	semi-massive chromitite in pyroxenite	norite	chromite-bearing ultramafic	semi-massive chromitite in pyroxenite	banded chromitite-norite	banded norite-pyroxenite	anorthosite	anorthosite
WDXRF	Al2O3	%	22.3	28.9	16.2	15	9.27	1.64		16.2
WDXRF	CaO	%	1.44	13.5	0.08	0.04	0.18	0.22		3.54
WDXRF	Cr2O3	%	31.4	0.02	34.3	25.2	15.5	0.57		<0.01
WDXRF	Fe2O3	%	26.5	2.13	26	23.6	19.7	15		3.41
WDXRF	K2O	%	0.05	0.5	<0.01	<0.01	<0.01	<0.01		1.16
WDXRF	LOI	%	<0.01	1.76	1.27	4.33	6.94	10.8		0.35
WDXRF	MgO	%	10.3	1.29	12.4	18.7	25.5	35		0.92
WDXRF	MnO	%	0.2	0.02	0.29	0.18	0.08	0.07		0.06
WDXRF	Na2O	%	0.17	3.14	0.05	0.03	0.03	0.02		4.9
WDXRF	P2O5	%	0.01	0.02	<0.01	0.01	0.02	0.07		0.09
WDXRF	SiO2	%	7.49	48.7	10.3	13.5	23.4	36.7		68.6
WDXRF	TiO2	%	0.59	0.14	0.25	0.28	0.18	0.08		0.35
Au-Pt-Pd FA	Au	ppb	4	8	4	1	<1	<1	<1	
Au-Pt-Pd FA	Pt	ppb	245	9	18.3	75.5	44.7	7.9	<1	
Au-Pt-Pd FA	Pd	ppb	38	2	21	83	34	4	<0.5	
NiS-FA	Pt	ppb	540	< 20	< 170	89	230	< 20		< 20
NiS-FA	Pd	ppb	150	< 20	98	110	140	< 20		< 64
NiS-FA	Ru	ppb	165	< 50	317	331	220	< 50		< 50
NiS-FA	Ir	ppb	92	< 1	53	80	67	2		1
NiS-FA	Os	ppb	< 22	< 10	< 25	55	43	< 10		< 10
NiS-FA	Rh	ppb	60	< 5	29	82	120	< 5		< 5
ICPAES_MS_55	Al	%	11.7	15.3	8.45	7.82	4.87	0.9	9.01	8.02
ICPAES_MS_55	Ca	%	1	9.6	<0.1	<0.1	0.2	0.2	4.7	2.4
ICPAES_MS_55	Fe	%	17.6	1.41	17.3	16	13.3	10.5	5.93	2.39
ICPAES_MS_55	K	%	<0.1	0.5	<0.1	<0.1	<0.1	<0.1	0.7	1
ICPAES_MS_55	Mg	%	6.32	0.76	7.85	11.5	15.7	21.8	1.64	0.52
ICPAES_MS_55	Mn	%	0.21	0.02	0.28	0.19	0.11	0.05	0.09	0.04
ICPAES_MS_55	P	%	0.02	<0.01	0.01	0.01	0.02	0.03	0.07	0.05
ICPAES_MS_55	Ti	%	0.34	0.08	0.15	0.16	0.1	0.04	0.59	0.19
ICPAES_MS_55	Ag	ppm	<1	<1	<1	<1	<1	<1	<1	<1
ICPAES_MS_55	As	ppm	<30	<30	<30	<30	<30	<30	<30	<30
ICPAES_MS_55	Ba	ppm	41.7	193	19.9	180	32	69.5	310	315
ICPAES_MS_55	Be	ppm	<5	<5	<5	<5	<5	<5	<5	<5
ICPAES_MS_55	Bi	ppm	0.4	0.1	<0.1	<0.1	0.1	<0.1	<0.1	<0.1
ICPAES_MS_55	Cd	ppm	<0.2	<0.2	<0.2	<0.2	<0.2	<0.2	<0.2	<0.2
ICPAES_MS_55	Ce	ppm	1.1	6.1	0.5	1.3	1.2	2.1	65.7	24.2
ICPAES_MS_55	Co	ppm	197	8	270	203	165	118	60.1	8.2
ICPAES_MS_55	Cr	ppm	199000	220	217000	147000	106000	3800	20	<10
ICPAES_MS_55	Cs	ppm	<0.1	0.2	<0.1	<0.1	<0.1	<0.1	0.1	<0.1
ICPAES_MS_55	Cu	ppm	11	23	7	7	7	<5	33	38
ICPAES_MS_55	Dy	ppm	0.31	0.65	0.08	0.24	0.15	0.24	6.24	1.39
ICPAES_MS_55	Er	ppm	0.33	0.39	0.27	0.27	0.15	0.18	3.44	0.78
ICPAES_MS_55	Eu	ppm	0.07	0.31	<0.05	<0.05	<0.05	<0.05	2.03	0.64
ICPAES_MS_55	Ga	ppm	52	20	34	28	19	2	50	20
ICPAES_MS_55	Gd	ppm	0.28	0.66	0.07	0.29	0.15	0.21	6.49	1.95
ICPAES_MS_55	Ge	ppm	<1	<1	<1	<1	<1	1	3	1
ICPAES_MS_55	Hf	ppm	<1	<1	<1	<1	<1	<1	6	3
ICPAES_MS_55	Ho	ppm	0.05	0.13	<0.05	<0.05	<0.05	0.05	1.11	0.28
ICPAES_MS_55	In	ppm	<0.2	<0.2	<0.2	<0.2	<0.2	<0.2	<0.2	<0.2
ICPAES_MS_55	La	ppm	0.6	3.2	0.5	0.6	0.6	1.1	31.3	13.6
ICPAES_MS_55	Li	ppm	<10	<10	<10	<10	<10	<10	20	10
ICPAES_MS_55	Lu	ppm	<0.05	0.06	<0.05	<0.05	<0.05	<0.05	0.57	0.1
ICPAES_MS_55	Mo	ppm	<2	<2	<2	<2	<2	<2	<2	<2
ICPAES_MS_55	Nb	ppm	<1	2	<1	<1	<1	<1	15	4
ICPAES_MS_55	Nd	ppm	0.6	2.5	0.3	1	0.7	1	30.5	10
ICPAES_MS_55	Ni	ppm	1280	29	924	1180	1190	1750	43	26
ICPAES_MS_55	Pb	ppm	23	11	10	<5	<5	<5	10	9
ICPAES_MS_55	Pr	ppm	0.15	0.69	0.08	0.21	0.17	0.27	8.09	2.94
ICPAES_MS_55	Rb	ppm	8.9	11.5	7.1	4.9	4	0.6	7.6	23.7
ICPAES_MS_55	Sb	ppm	<0.1	<0.1	0.2	<0.1	<0.1	<0.1	0.2	<0.1
ICPAES_MS_55	Sc	ppm	13	<5	<5	6	5	8	16	<5
ICPAES_MS_55	Sm	ppm	0.2	0.6	<0.1	0.2	0.1	0.3	6.7	2
ICPAES_MS_55	Sn	ppm	5	1	2	<1	<1	<1	3	<1
ICPAES_MS_55	Sr	ppm	3.4	155	0.5	1.4	6	5.1	267	199
ICPAES_MS_55	Ta	ppm	<0.5	<0.5	<0.5	<0.5	<0.5	<0.5	1	1.1
ICPAES_MS_55	Tb	ppm	<0.05	0.12	<0.05	<0.05	<0.05	<0.05	0.98	0.3
ICPAES_MS_55	Th	ppm	<0.1	0.5	0.2	<0.1	<0.1	0.1	0.7	0.4
ICPAES_MS_55	Tl	ppm	<0.5	<0.5	<0.5	<0.5	<0.5	<0.5	<0.5	<0.5
ICPAES_MS_55	Tm	ppm	<0.05	0.06	<0.05	<0.05	<0.05	<0.05	0.52	0.15
ICPAES_MS_55	U	ppm	0.34	0.39	0.1	0.08	0.1	0.22	0.34	0.29
ICPAES_MS_55	V	ppm	1690	43	882	1020	633	47	151	40
ICPAES_MS_55	W	ppm	<1	<1	<1	1	<1	<1	1	<1
ICPAES_MS_55	Y	ppm	2.3	4.4	1	1.2	0.8	1.5	33.2	9.9
ICPAES_MS_55	Yb	ppm	0.2	0.3	0.1	0.1	<0.1	0.1	3.2	0.8
ICPAES_MS_55	Zn	ppm	1120	7	1340	910	587	65	76	55
ICPAES_MS_55	Zr	ppm	7.8	10.4	4.3	3.6	6.8	8.4	243	123

Table 2. Electron microprobe analytical data on selected unaltered (>98 percent total oxides) chromitites from the Guelb el Foulet Cr occurrence. Data are recalculated based on Fe2+/Fe3+ and Mn corrections obtained from the Open University website (accessed Nov., 2012 at http://www.open.ac.uk/earth-research/tindle/AGT/AGT_Home_2010/Microprobe-2.html).

Chromite recalculation including Fe2+/Fe3+ and Mn correction. MnO correction = empirical calculation.																													
	Sample CT07RIM-19-1							Sample CT07RIM-20-1										Sample CT07RIM-21-1						Sample CT07RIM-21-2					
Raw EMPA data	spot2	spot3	spot4	spot10	spot12	spot13	spot14	spot2	spot3	spot7	spot8	spot9	spot12	spot13	spot14	spot17	spot18	spot1	spot2	spot6	spot7	spot16	spot17	spot4	spot10	spot11	spot13	spot14	spot15
Cr2O3	37.66	38.06	37.72	38.19	37.86	38.03	38.33	42.25	45.43	42.51	42.04	42.05	42.62	42.30	42.66	43.76	42.76	39.02	39.07	38.57	39.47	38.27	38.61	37.63	38.14	38.02	38.40	38.57	38.21
Al2O3	25.28	24.95	25.07	25.57	25.04	24.98	24.89	21.02	8.96	21.00	20.97	21.28	20.61	20.57	20.63	19.70	20.84	22.82	23.09	23.06	23.40	23.54	23.45	23.35	22.77	23.30	21.67	21.85	21.76
TiO2	0.40	0.47	0.44	0.35	0.44	0.31	0.48	0.34	0.49	0.32	0.34	0.34	0.39	0.35	0.34	0.35	0.34	0.39	0.38	0.41	0.34	0.36	0.36	0.34	0.41	0.35	0.47	0.43	0.44
FeO	26.77	26.86	26.87	26.72	27.13	26.82	26.44	24.68	36.45	24.81	24.92	24.78	25.00	25.18	25.00	25.90	25.20	24.87	25.16	25.79	24.62	24.33	25.00	26.83	27.58	27.20	28.29	28.23	28.19
MgO	8.78	8.52	8.62	8.77	8.41	8.67	8.86	9.78	5.59	9.78	9.74	9.83	9.53	9.53	9.46	8.77	9.53	10.30	10.19	9.76	10.77	10.81	10.28	9.60	9.11	9.28	8.66	8.89	8.69
MnO	0.30	0.32	0.30	0.31	0.32	0.32	0.30	0.30	0.49	0.30	0.32	0.31	0.29	0.30	0.30	0.33	0.27	0.32	0.29	0.28	0.34	0.29	0.28	0.31	0.28	0.28	0.32	0.34	0.30
NiO	0.14	0.20	0.18	0.20	0.20	0.18	0.21	0.13	0.20	0.14	0.11	0.12	0.12	0.12	0.16	0.10	0.12	0.10	0.09	0.07	0.13	0.10	0.09	0.10	0.11	0.09	0.11	0.11	0.10
Total	99.33	99.38	99.18	100.12	99.39	99.32	99.51	98.50	97.61	98.85	98.45	98.71	98.57	98.35	98.55	98.92	99.06	97.82	98.27	97.93	99.06	97.70	98.08	98.17	98.39	98.52	97.92	98.43	97.70
MnO corrected	0.15	0.16	0.15	0.16	0.17	0.17	0.15	0.13	0.31	0.13	0.15	0.14	0.12	0.13	0.13	0.15	0.10	0.17	0.13	0.12	0.18	0.14	0.12	0.16	0.12	0.13	0.16	0.19	0.15
Total	99.18	99.23	99.03	99.96	99.24	99.17	99.36	98.33	97.43	98.68	98.28	98.54	98.40	98.18	98.38	98.74	98.89	97.67	98.11	97.78	98.91	97.55	97.93	98.02	98.24	98.37	97.77	98.28	97.54
Corrected Analysis																													
Cr2O3	37.66	38.06	37.72	38.19	37.86	38.03	38.33	42.25	45.43	42.51	42.04	42.05	42.62	42.30	42.66	43.76	42.76	39.02	39.07	38.57	39.47	38.27	38.61	37.63	38.14	38.02	38.40	38.57	38.21
Al2O3	25.28	24.95	25.07	25.57	25.04	24.98	24.89	21.02	8.96	21.00	20.97	21.28	20.61	20.57	20.63	19.70	20.84	22.82	23.09	23.06	23.40	23.54	23.45	23.35	22.77	23.30	21.67	21.85	21.76
TiO2	0.40	0.47	0.44	0.35	0.44	0.31	0.48	0.34	0.49	0.32	0.34	0.34	0.39	0.35	0.34	0.35	0.34	0.39	0.38	0.41	0.34	0.36	0.36	0.34	0.41	0.35	0.47	0.43	0.44
FeO	22.58	22.93	22.75	22.77	23.09	22.58	22.46	20.10	24.82	20.20	20.15	20.14	20.51	20.40	20.52	21.57	20.68	19.46	19.86	20.45	19.14	18.76	19.69	20.74	21.56	21.36	21.94	21.74	21.84
Fe2O3	4.66	4.36	4.58	4.38	4.49	4.72	4.42	5.09	12.93	5.12	5.31	5.15	5.00	5.31	4.98	4.82	5.02	6.01	5.90	5.93	6.09	6.18	5.91	6.77	6.69	6.49	7.05	7.22	7.06
MgO	8.78	8.52	8.62	8.77	8.41	8.67	8.86	9.78	5.59	9.78	9.74	9.83	9.53	9.53	9.46	8.77	9.53	10.30	10.19	9.76	10.77	10.81	10.28	9.60	9.11	9.28	8.66	8.89	8.69
MnO	0.15	0.16	0.15	0.16	0.17	0.17	0.15	0.13	0.31	0.13	0.15	0.14	0.12	0.13	0.13	0.15	0.10	0.17	0.13	0.12	0.18	0.14	0.12	0.16	0.12	0.13	0.16	0.19	0.15
NiO	0.14	0.20	0.18	0.20	0.20	0.18	0.21	0.13	0.20	0.14	0.11	0.12	0.12	0.12	0.16	0.10	0.12	0.10	0.09	0.07	0.13	0.10	0.09	0.10	0.11	0.09	0.11	0.11	0.10
Total	99.65	99.66	99.49	100.40	99.69	99.64	99.80	98.84	98.73	99.20	98.82	99.06	98.90	98.71	98.88	99.22	99.39	98.27	98.70	98.37	99.52	98.17	98.52	98.70	98.91	99.02	98.47	99.00	98.25
Formula units based on 32 oxygens and Fe2+/Fe3+ assuming full site occupancy																													
Cr	7.47	7.58	7.51	7.52	7.54	7.56	7.61	8.54	10.01	8.57	8.50	8.47	8.64	8.59	8.65	8.92	8.62	7.84	7.82	7.76	7.81	7.65	7.72	7.56	7.69	7.63	7.83	7.81	7.80
Al	7.48	7.41	7.44	7.51	7.43	7.41	7.36	6.33	2.95	6.31	6.33	6.39	6.23	6.23	6.24	5.99	6.27	6.84	6.89	6.92	6.90	7.01	6.99	6.99	6.84	6.97	6.59	6.60	6.62
Ti	0.08	0.09	0.08	0.07	0.08	0.06	0.09	0.07	0.10	0.06	0.07	0.07	0.08	0.07	0.07	0.07	0.07	0.08	0.07	0.08	0.06	0.07	0.07	0.07	0.08	0.07	0.09	0.08	0.08
Fe3+	0.88	0.83	0.87	0.82	0.85	0.89	0.84	0.98	2.71	0.98	1.02	0.99	0.96	1.03	0.96	0.93	0.96	1.15	1.12	1.14	1.15	1.18	1.12	1.29	1.28	1.24	1.37	1.39	1.37
Fe2+	4.75	4.84	4.80	4.76	4.87	4.76	4.73	4.31	5.91	4.32	4.33	4.31	4.41	4.40	4.42	4.67	4.43	4.16	4.22	4.37	4.02	3.99	4.19	4.43	4.62	4.56	4.76	4.69	4.75
Mg	3.29	3.20	3.24	3.26	3.15	3.25	3.32	3.73	2.32	3.71	3.72	3.73	3.64	3.65	3.62	3.37	3.62	3.90	3.84	3.70	4.02	4.07	3.88	3.63	3.46	3.51	3.33	3.39	3.34
Mn	0.03	0.03	0.03	0.03	0.04	0.04	0.03	0.03	0.07	0.03	0.03	0.03	0.03	0.03	0.03	0.03	0.02	0.04	0.03	0.03	0.04	0.03	0.03	0.03	0.03	0.03	0.04	0.04	0.03
Ni	0.03	0.04	0.04	0.04	0.04	0.04	0.04	0.03	0.05	0.03	0.02	0.02	0.03	0.02	0.03	0.02	0.02	0.02	0.02	0.01	0.03	0.02	0.02	0.02	0.02	0.02	0.02	0.02	0.02
Total	24.01	24.01	24.01	24.01	24.01	24.01	24.01	24.02	24.12	24.02	24.02	24.02	24.01	24.02	24.01	24.01	24.01	24.02	24.02	24.02	24.02	24.02	24.02	24.03	24.03	24.02	24.03	24.03	24.03
100Cr/Cr+Al	49.97	50.57	50.22	50.03	50.35	50.52	50.81	57.41	77.27	57.58	57.34	56.99	58.09	57.97	58.09	59.83	57.92	53.42	53.16	52.87	53.08	52.16	52.48	51.93	52.90	52.25	54.30	54.21	54.08
100Mg/Mg+Fe2+	40.87	39.78	40.24	40.65	39.29	40.55	41.23	46.35	28.22	46.21	46.19	46.43	45.21	45.34	45.02	41.95	45.01	48.43	47.64	45.84	49.95	50.53	48.09	45.04	42.81	43.51	41.14	42.00	41.34

The new whole rock geochemical data from Guelb el Foulet confirms the moderately low Cr content of the chromitites in drill core reported by the BRGM (1975). Two samples analyzed by the USGS (table 1) contain approximately 34 and 31 percent Cr_20_3, respectively. Al_2O_3 contents are moderately high, at approximately 22 and 16 percent, with correspondingly moderate Cr/Al ratios. SiO_2 contents are in the percent range indicating that the samples contain appreciable quantities of silicate minerals in addition to chromite. The four chromite-bearing samples contain total PGEs + Au values between approximately 598 and 1,022 ppb with maximum values of 540 ppb Pt, 150 ppb Pd, and 8 ppb Au in individual samples. While these values are hundreds of ppb higher in total PGEs +Au than average analyzed values from typical worldwide examples of podiform chromitite, and similar to or less than Alaska/Urals-type chromitites (Crocket, 1981; Economou-Eliopoulos, 1996; Zaccarini and others, 2008; Ahmed and others, 2009) they are well below the ppm to tens of ppm values contained in PGE-bearing chromitite ores that are mined for PGEs in worldwide stratiform mafic-ultramafic complexes such as the Bushveld and Stillwater Complexes (Page and others, 1976; McLaren and De Villiers, 1982; Lee and Parry, 1988; Maier and Barnes, 2008) and several known examples of PGE-enriched deposits in ophiolite complexes (Tsoupas and Economou-Eliopoulos, 2008; Evans and others, 2011).

Petrographic data from thin sections from five samples collected at the Guelb el Foulet occurrence show that primary mineralogy consists almost entirely of pyroxene (augite), plagioclase (andesine), and chromite (fig. 8) with minor biotite and amphibole. No olivines or orthopyroxenes were observed in thin section or indicated by EMPA, indicating that the samples are gabbros, anorthosites, and semi-massive chromitites. Alteration of both the interstitial silicate minerals and chromite grains is variable with minor to almost complete sausseritization of plagioclase and formation of fine grained amphiboles around the pyroxene grains. In general, the chromite grains are relatively unaltered to moderately altered and exhibit typical cracking of equant grains (fig. 9). When alteration of chromite is present, ferrit-chromite appears as dark gray rims along grain boundaries and cracks (fig. 10).

Electron microprobe data for 29 analytical spots on chromite grains in four thin sections of chromite-bearing samples from Guelb El Foulet are shown in table 2. All samples were analyzed in the USGS Denver Microbeam Laboratory with a JEOL JXA 8900 electron microprobe and all samples were carbon-coated before use. Wavelength-dispersive spectroscopy (WDS) was used for all quantitative analyses. Operating conditions were 5 kV and 20nA for all chromites and silicates, with an average beam diameter of 10 microns (μm) and a focused beam. Natural and synthetic standards were run, and count times of 20 seconds were used.

Figure 11 shows these data plotted on the tectonic discriminant diagrams originally developed from the work of Irvine (1965, 1967) and Roeder (1994). The specific fields in the diagrams are taken from Jan and Windley (1990), Arai (1992) and Arif and Jan (2006). In all three plots on figure 11 the chromite data form a relatively tight cluster with one analysis that falls well away from the rest of the data. Reasons for this are unclear, however, we suspect that the data point is anomalous due to alteration or perhaps mixed or non-chromite mineralogy.

In the $100Mg/(Mg+Fe^{2+})$ vs $100Cr/(Cr+Al)$ plot (fig. 11*A*) the data cluster plots well out of the ophiolite (abyssal and alpine peridotites) fields and just below and

overlapping the field of stratiform mafic-ultramafic complexes. In the Al-Fe^{3+}-Cr ternary plot (fig. 11*B*) the data cluster overlaps the fields of ophiolites and stratiform complexes and plots well out of the field of Alaska/Urals-type complexes. In the 100Mg/(Mg+Fe^{2+}) vs TiO_2 plot (fig. 11*C*) the data cluster overlaps the compositional fields of MORB and island arc rocks and plots well out of the field for boninites.We conclude that based on the geologic relationships described above and the combination of tectonic environments and compositional fields indicated by the three discriminant plots in figure 11 that the Guelb El Foulet occurrence is best interpreted as a tectonized remnant of a stratiform mafic-ultramafic complex. This is consistent with the post-metamorphic and relatively pristine rock textures observed in outcrop and hand samples at the occurrence. We suggest that host rocks at Guelb El Foulet belong to the approximately 2,730 Ma suite of anorogenic granites, gabbros, and anorthosites in the Tasiast-Tijirit and Choum-Rag El Abiod terranes such as the Iguilid gabbro and the Ahmeyim Great Dike. We confidently rule out the possibility that the occurrence is of the Alaska/Urals-type based on the tectonic discriminant plots, the lack of boninitic geochemical characteristics and the presence of large amounts of anorthosite, which would be rare for Alaska/Urals-type intrusions. The elimination of an ophiolitic origin is less certain due to some overlap of data on the discriminant plots. However, we note that if an ophiolite origin were proposed that the intrusion would have been emplaced during collision of the Tasiast-Tijirit and Choum-Rag El Abiod terranes at approximately 2,954 Ma. Guelb El Foulet host rocks would have been subject to the intense plastic deformation and granulite-facies metamorphism exhibited by older rocks of the Choum-Rag El Abiod terrane along the TISZ. Examination of geophysical data for the TISZ and Amsaga terrane suggest that there are no large coincident magnetic and gravity anomalies that might suggest the presence of either a significant ophiolite sequence or a large layered mafic-ultramafic complex (Finn and Anderson, 2015). However, aeromagnetic imaging of the Guelb El Foulet area (fig. 12) does show that a relatively large anorthosite body lies under cover just to the west of the occurrence. This suggests that other anorthosite bodies in the Amsaga Complex may be associated with gabbroic layering and may be exploration targets for magmatic segregation deposits of Cr-PGE or Ni-Cu-PGE.

Aeromagnetic data collected along 500-m spaced flightlines over the Amsaga Complex show an intricate pattern of magnetic anomalies (fig. 12). The RTP map shows broad magnetic anomaly highs associated with the charnockite gneiss that is in contrast to magnetic lows associated with the garnet quartzofeldspathic gneiss. Linear northeast trending magnetic highs correlate with mapped BIF and amphibolite units whereas a north trending magnetic high correlated with the metacarbonate unit. Several mapped ultramafic bodies broadly correlate with RTP anomaly highs. The metagabbro associated with the Iguilid massif is assocated with a strong, arcuate RTP anomaly high. The El Foulet and El Heirich Cr occurrences correlate with magnetic highs and lows, respectively.

The gradient of the magnetic field is calculated from the analytic signal and can be used to simplify the interpretation of magnetic anomalies (Nabighian, 1972; Roest and others, 1992). The analytic signal over the Amsaga Complex shows several highs that indicate areas where the magnetic field is rapidly changing. Analytic signal highs correlate with the metagabbro of the Iguilid massif, the linear metacarbonate unit, and BIFs. Several of the smaller mapped ultramafic units also correlate with analytic signal

highs. The El Foulet and El Heirich Cr occurrences show relatively subtle analytic signal highs. Several isolated analytic signal highs occur within the garnet quartzofeldspathic gneiss which may indicate the presence of more ultramafic rocks in the region than is depicted on the geologic maps.

Magnetic anomalies with amplitudes greater than 1,000 nanoteslas were identified along flightlines. Such anomalies may represent magnetic material, such as ultramafic rock, within less magnetic material. Such strong anomalies may be subdued during gridding processes, so using original flightline data to map their distribution is preferred. All of the magnetic anomlies identified correlate with analytic signal highs. These areas may be further focused, by selecting the regions within the analytic signal highs where the most magnetic units occur. Comparing the mapped geology, RTP, analytic signal, and magnetic anomaly picks may help indicate where the more favorable areas for ultramafic rocks within the Amasaga Complex occur.

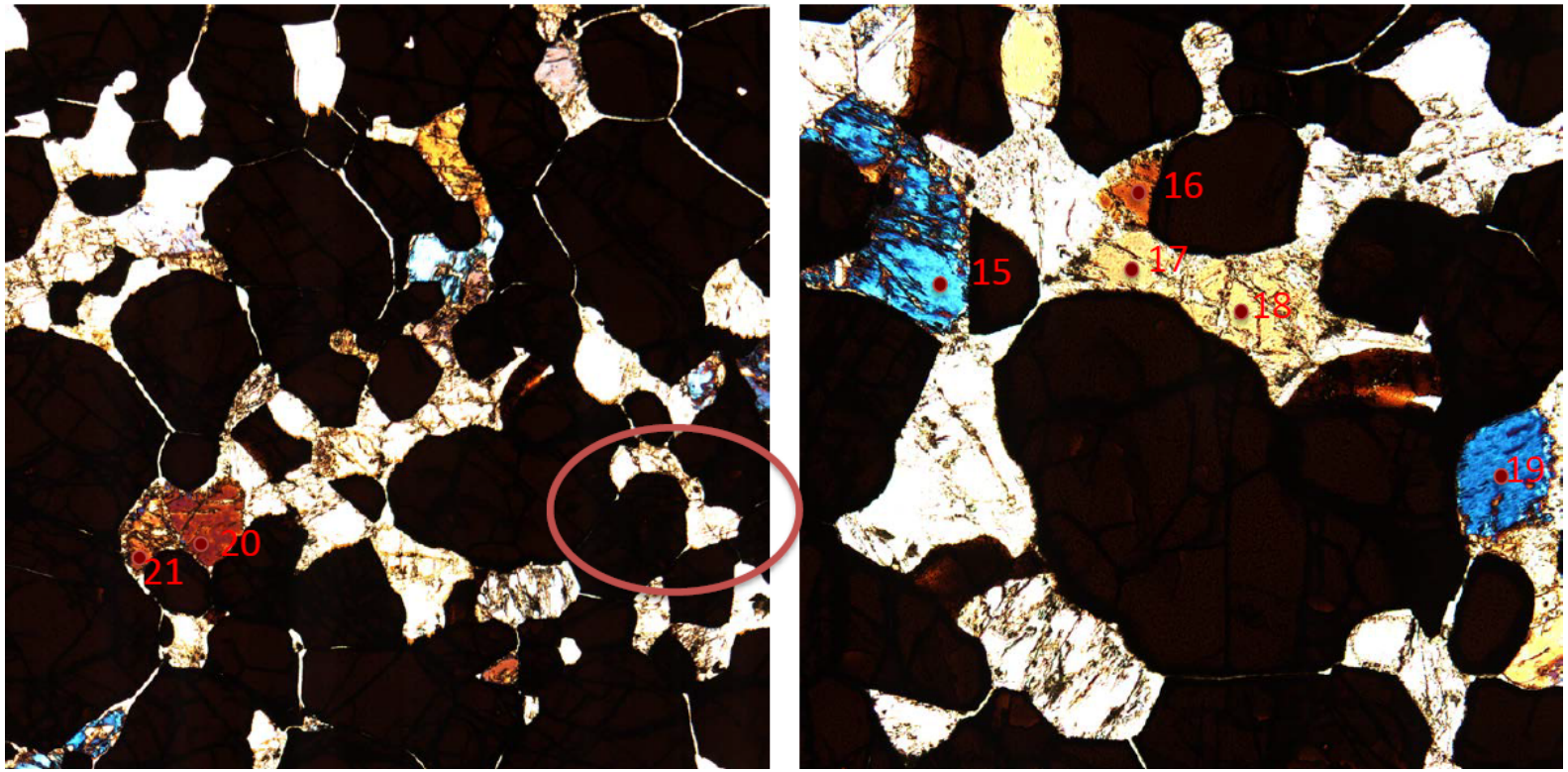

Figure 8. Thin section photomicrograph of sample CT07RIM-19-1 under 5x (left image) and 10x (right image) objectives in plane polarized light. Numbered red spots indicate EMPA sites. Both images show large black chromite grains with interstitial pyroxene and plagioclase. Circled area shows lath-shaped pyroxenes interstitial to chromite.

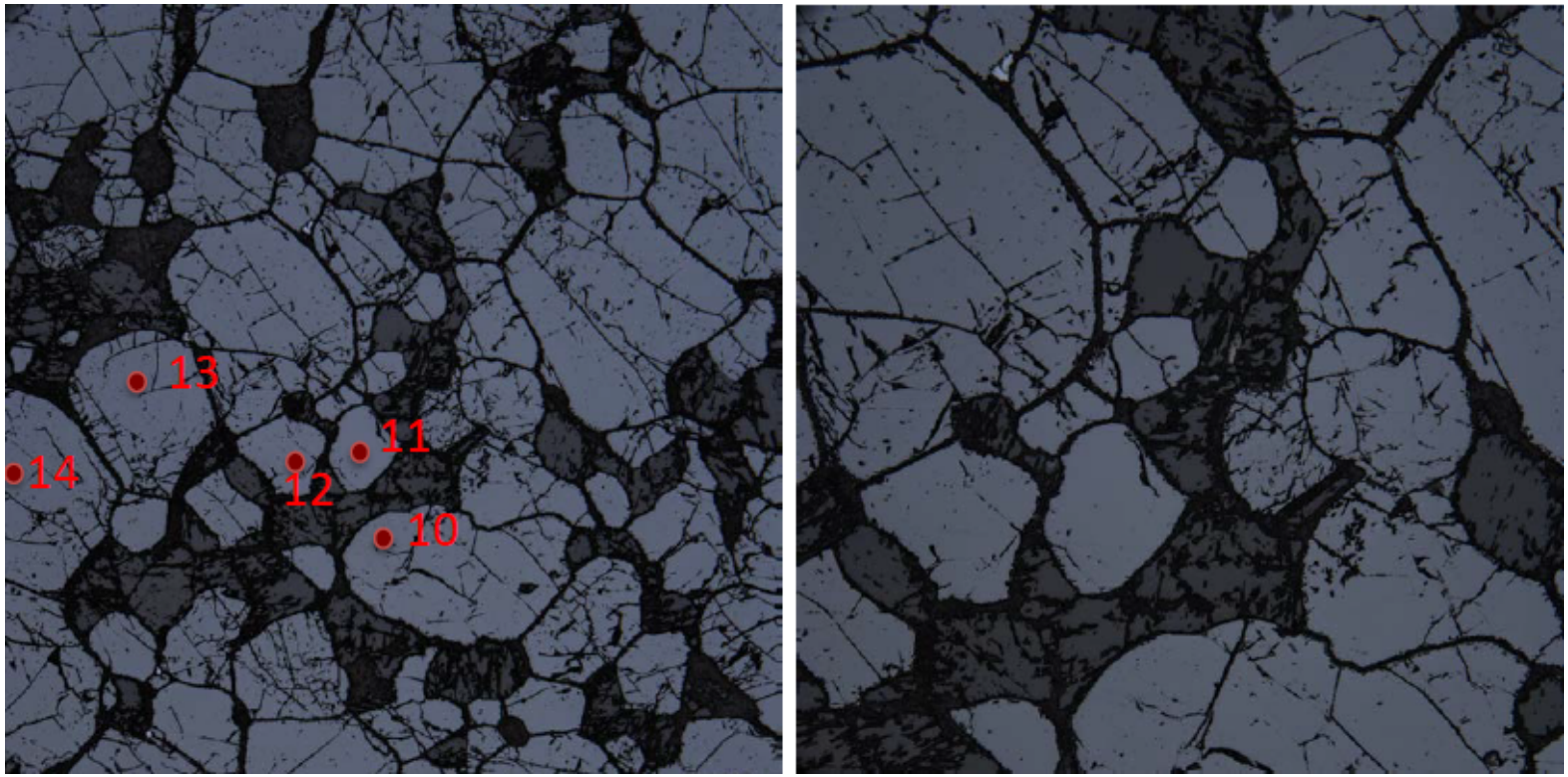

Figure 9. Thin section photomicrograph of sample CT07RIM-19-1 under 5x (left image) and 10x (right image) objectives in reflected light. Numbered red spots indicate EMPA sites. Both images show relatively unaltered light gray chromite grains with interstitial dark gray pyroxene and plagioclase. Minor small opaque grains are bright whitish-gray.

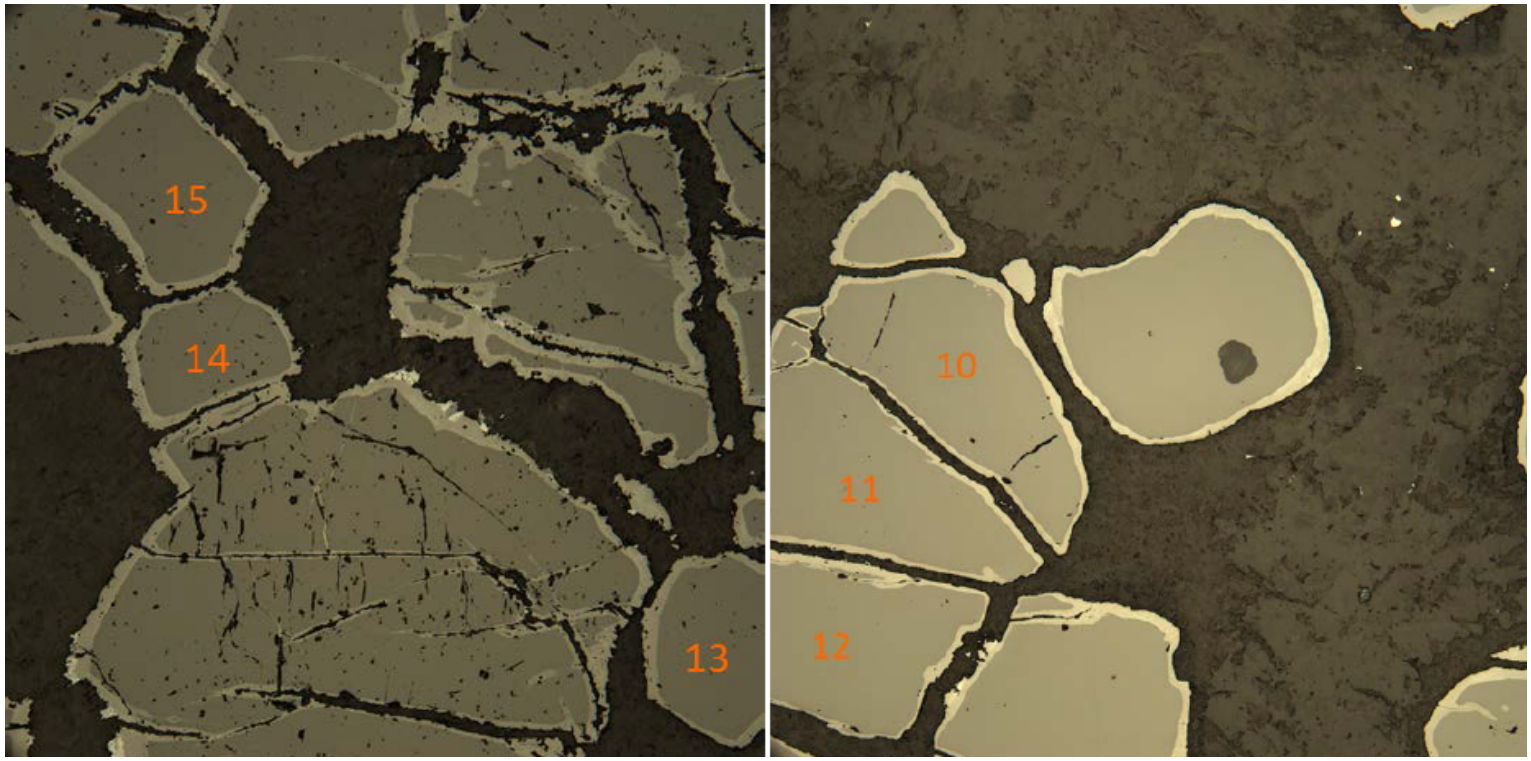

Figure 10. Thin section photomicrograph of sample CT07RIM-21-1 under 10x objective in reflected light. Numbers indicate EMPA sites. Both images show relatively unaltered gray chromite grains with interstitial dark gray pyroxene and plagioclase. Distinctive light gray ferrit-chromite alteration rims are present around all grains and along cracks within grains.

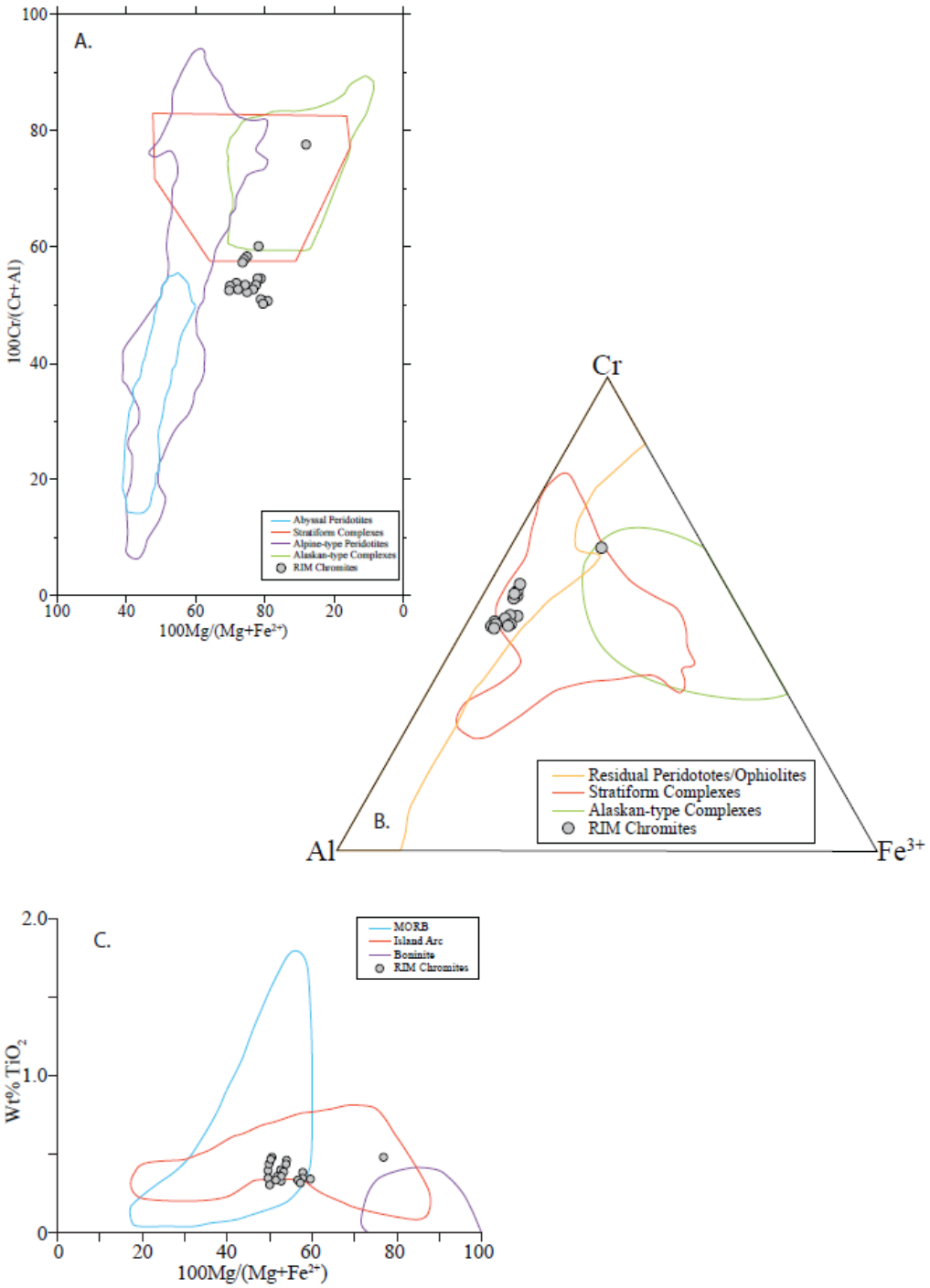

Figure 11. Tectonic discriminant analysis based on electron microprobe data from chromites from the Guelb El Foulet occurrence. *A*, (Cr×100)/(Cr+Al) vs (Mg×100)/(Mg+Fe^{2+}) plot. *B,* Ternary plot of Fe^{3+}, Al, and Cr. C. TiO_2 vs (100×Cr)/(Cr+Al) plot. Compositional fields and tectonic settings after Jan and Windley (1990), Arai (1992), and Arif and Jan (2006).

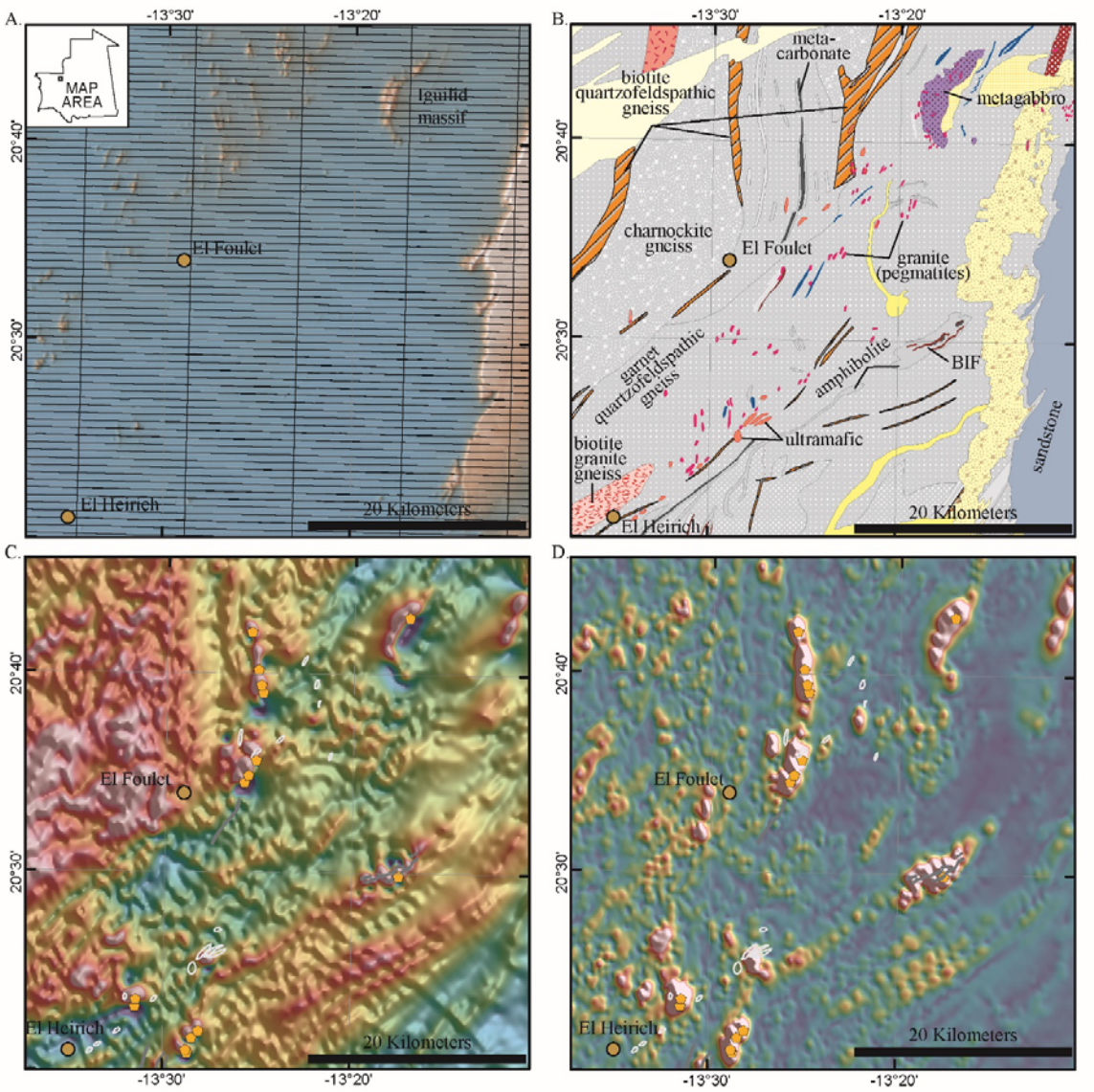

Figure 12. Generalized geology, reduced-to-pole (RTP), and analytic signal maps over the Amsaga Complex. *A,* Shaded-relief of digital elevation model and flightline location for the area. *B,* Generalized geologic map showing the distribution of small mafic-ultramafic intrusions mostly within the garnet quartzofeldspathic gneiss. *C,* RTP map showing a broad magnetic anomaly high associated with the charnockite gneiss in the west. Several linear magnetic anomalies correlate with BIF units (gray polygon) and ultramafic rocks (white polygons). Orange markers indicate magnetic anomalies > 1,000 nanoteslas along flightlines. Magnetic highs and lows are shown as warm and cool colors, respectively. *D,* Analytic signal highlighting several areas where the magnetic field is rapidly changing. Orange markers indicate magnetic anomalies > 1,000 nanoteslas along flightlines. Analytic signal highs and lows are shown as warm and cool colors, respectively.

3.3 Mesoarchean and Neoproterozoic Greenstones of the Inchiri District

Although no Ni-Cu-PGE occurrences are known within the Saouda Group of the southern Choum-Rag El Abiod terrane, the similarity of these rocks to the greenstone belts of the Tasiast-Tijirit terrane and the presence of several gabbroic to ultramafic bodies of Mesoarchean age associated with mafic volcanic sequences indicates that they are permissive for such occurrences. Gabbroic and ultramafic intrusive bodies related to the Neoproterozoic supracrustal sequences are permissive as well.

The area here referred to as the central Mauritanides, consists of the Akjoujt area, also called the Inchiri district. Mineralized host rocks in the district are dominantly Neoproterozoic through lower Paleozoic supracrustal rocks consisting of metabasalts, sediments, BIF, and lesser intermediate to felsic metavolcanics of the Oumachoueima Group. These rocks are host to a large number of copper and gold occurrences thought to be of the iron oxide copper-gold type (IOCG), including the Guelb Mohgrein mine that is currently in production (see Fernette, 2015). Similar to the southern Mauritanides, this region was affected by Pan-African through Hercynian deformation that produced a structurally complex zone of thrust nappes, together referred to as the Akjoujt nappe pile, that juxtaposes slices of the Mesoarchean basement and associated supracrustal rocks with slices of the Proterozoic supracrustal sequence (fig. 13). Current understanding of the age contraints on the supracrustal rocks of the district are conflicting and raise the possibility that both the host rocks and mineral occurrences could be as old as Mesoarchean to as young as Neoproterozoic. Until the ages of these rocks are resolved, the relationship of the central Mauritanides to either the greenstone belts of the Tasiast-Tijirit terrane or to the younger rocks of the southern Mauritanides remains in question. Similarly, uncertainty exists as to the true nature of the copper-gold occurrences in the district. Although current work at Guelb Mohgrein has resulted in its assignment to the IOCG class of mineral deposits, previous work in the district raised the possibility that Guelb Mohgrein and other occurrences may be VMS (Ba Gatta, 1982) or skarn-like deposits related to regional metamorphism (Goldfarb and others, 2015; Fernette, 2015).There are currently no known Cu-Ni sulfide deposits in either the Mesoarchean or Neoproterozoic rocks of the Inchiri district. However, the common association of magmatic sulfide segregation deposits of Cu-Ni±PGEs with orogenic gold deposits and VMS deposits in greenstone belts of all ages suggests that gabbroic and ultramafic bodies associated with the mafic supracrustal sequences of the Inchiri district represent permissive targets for such deposits.

Rocks in the Inchiri district are an allochthonous package consisting of Mesoarchean to Paleoproterozoic gneisses and metamafic volcanosedimentary rocks in tectonic windows within an imbricated supracrustal nappe pile of Paleoproterozoic to Neoproterozoic rocks of wide-ranging lithologies. This infrastructural allochthon (Pitfield and others, 2004) was emplaced over autochthonous to para-autochthonous rocks of the Amsaga Complex and foreland basin sedimentary rocks of the Taoudeni Basin during the Pan African through Hercynian Mauritanide orogeny. The allochthon consists of a basal root zone and three internally imbricated nappes (fig. 13).

The Agoualilet Group, consisting of a mafic melange interspersed with siliciclastic sedimentary rocks, forms the root zone and regionally extensive basal nappe of the allochthon. It forms a western block at the southwestern edge of the Akjoujt nappe pile and an eastern block well to the southeast of the Ijibbitene Group (fig. 13). The Tamagot basement window, or tectonic inlier, and the Bou Kerch Nappe, are located along the eastern edge of the

Agoualilet Group root zone southwest and south of Akjoujt. These rocks consist of the Tamagot orthogneiss and mafic igneous rocks, BIF, and sedimentary rocks of the Saouda Group that together exhibit characteristics of an Archean granite-greenstone association. They are the oldest rocks in the allochthon and are thought to be an eastward-transported southern section of the Mesoarchean Tasiast-Tijirit terrane. In the Bou Kerch Nappe, rocks of the Saouda Group tectonically overlie and are imbricated with quartzitic metasediments of the Agoualilet Group (fig. 13; Pitfield and others, 2004).

To the east and north, the Tamagot window and Bou Kerch Nappe are overthrust by the Choueima Nappe, which comprise the volcanosedimentary host rocks to numerous mineral occurrences of the Inchiri district. The nappe is centered on the town of Akjoujt (fig. 13) and consists of the Eizzene and Oumachoueima Groups separated by an angular unconformity. The older Eizzene Group consists of a lower sequence of mafic volcanic rocks, the Raoui Formation, overlain by the Khmeiyat Formation consisting of BIF and semipelitic schists. The Eizzene Group is unconformably overlain by the Oumachoueima Group, which commences with the Atilis Quartzite member of the clastic Irarchene El Hamra Formation. The Irarchene El Hamra Formation is overlain by volcanogenic sedimentary rocks and BIF of the Atomai Formation, which is in turn overlain by proximal volcanic to distal volcaniclastic rocks of dominantly intermediate composition of the Sainte Barbe Formation. The Sainte Barbe Formation is capped by a widespread marker-unit that consists of chert and BIF of the Lembeitih Formation. The stratigraphy culminates in a monotonous pile of submarine basalts and related microgabbroic intrusive rocks of the Akjoujt Formation (Pitfield and others, 2004). Detailed geology of the Akjoujt nappe pile is shown in figure 14. The stratigraphy of the Akjoujt nappe pile and possible correlations to other rocks described in this section is shown in figure 15.

The uppermost nappe in the Akjoujt nappe pile is the Hajar Dekhen-Kleouat Nappe, which overlies the Cheouima Nappe primarily in areas to the south and west of Akjoujt (fig. 13). Rocks of the Hajar Dekhen-Kleouat Nappe consist of amphibolite facies supracrustal metamorphic and granitic rocks. Previously thought to consist of overthrust basement, the nappe also contains rocks of the Eizzene and Oumachoueima Groups. The age relationship of the rocks in the Hajar Dekhen-Kleouat Nappe depends on the age and correlation of the Eizzene Group (Pitfield and others, 2004).

The task of defining rock packages in the Inchiri district that are permissive of the occurrence of Cu-Ni-PGE deposits is hampered by the structural complexity of the region. Because Cu-Ni-PGE deposits in greenstone belts are generally related to the mafic-ultramafic intrusions that feed extrusive mafic volcanic rock sequences, factors that control their distribution include primary structural and volcanostratigraphic features such as the alignment of the axis of a former magmatic arc, polarity and position of a former subduction zone, identification of preserved ocean floor rocks (ophiolites), and presence, size, and interconnectivity of subvolcanic dikes, sills, and feeder conduits to volcanic edifices. Such primary relationships in the Mesoarchean to Neoproterozoic rocks of the Inchiri district are obscured by Pan African to Hercynian tectonic events.

At the most basic level, rocks considered permissive of magmatic sulfide segregation deposits in the Inchiri district include all mafic volcanic rock sequences. Additional favorable criteria include the presence of gabbroic to ultramafic intrusions, the presence of ophiolites, and the presence of either Cu-Ni-PGE or chromite (±PGE) occurrences.

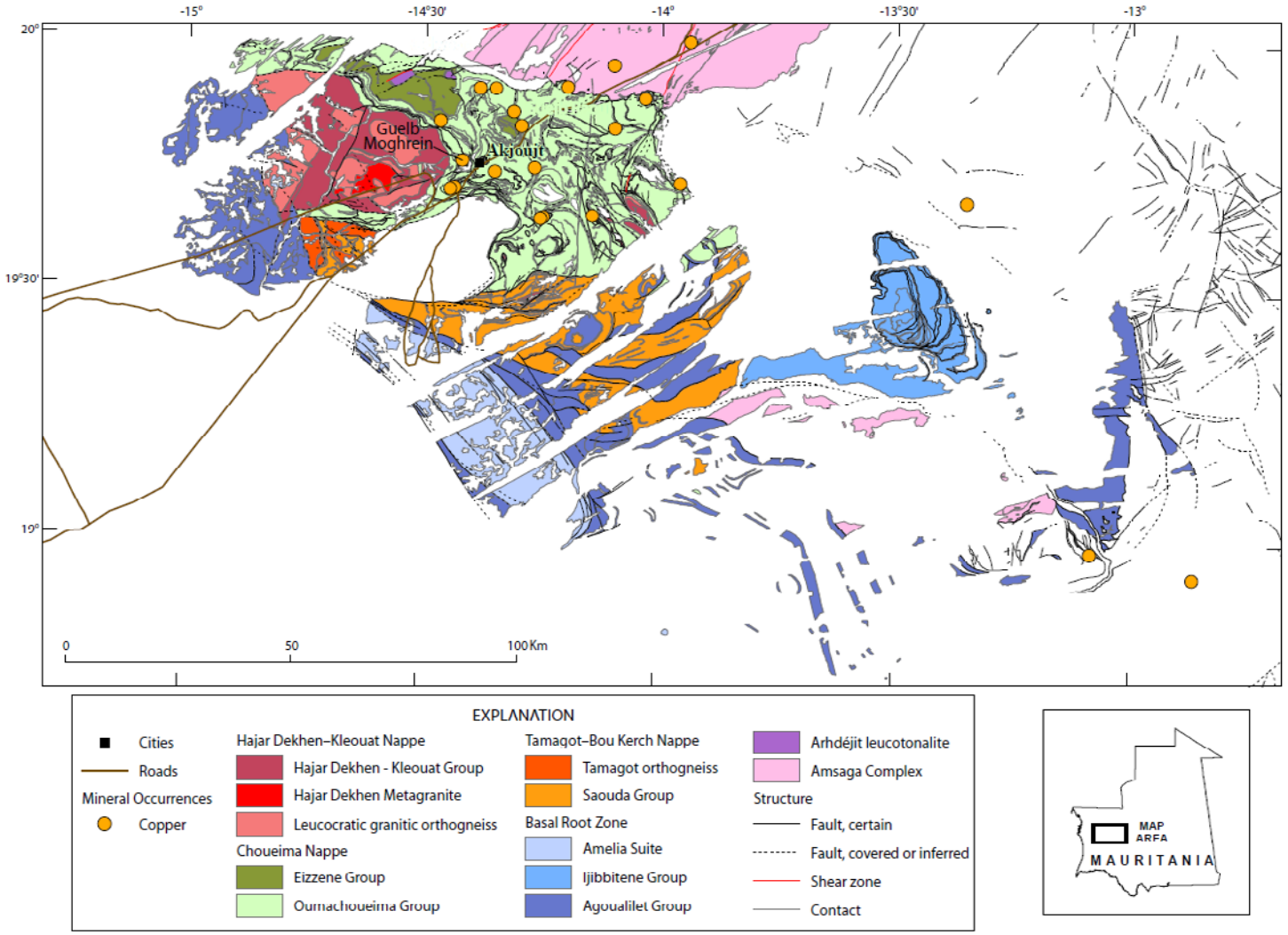

Figure 13. Simplified geology of the Inchiri district showing various nappes and tectonic windows of the Akjoujt nappe pile and mineral deposits and occurrences discussed in text.

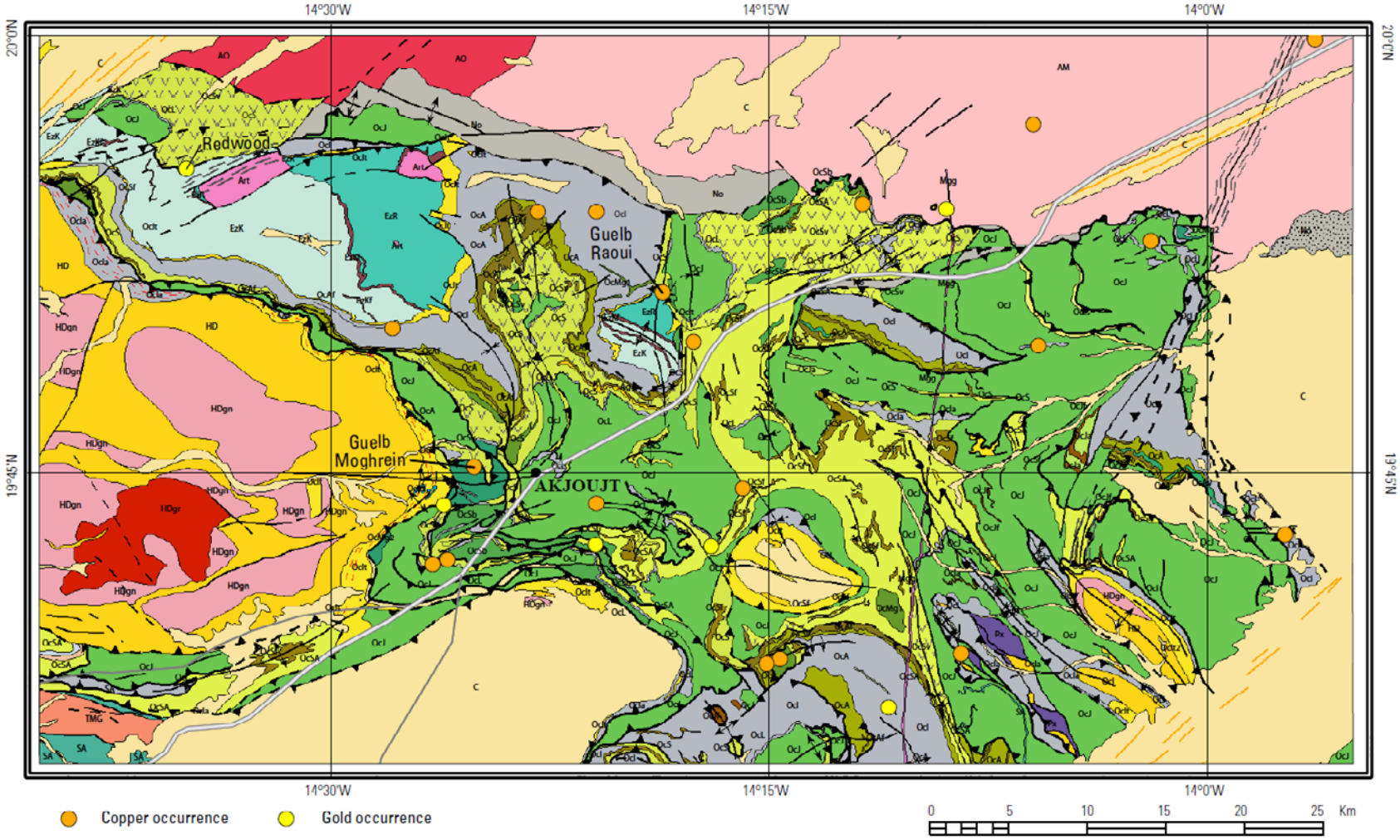

Figure 14. Detailed geology of the Akjoujt nappe pile (from Pitfield and others, 2004). Geologic units shown here are described in figure 15.

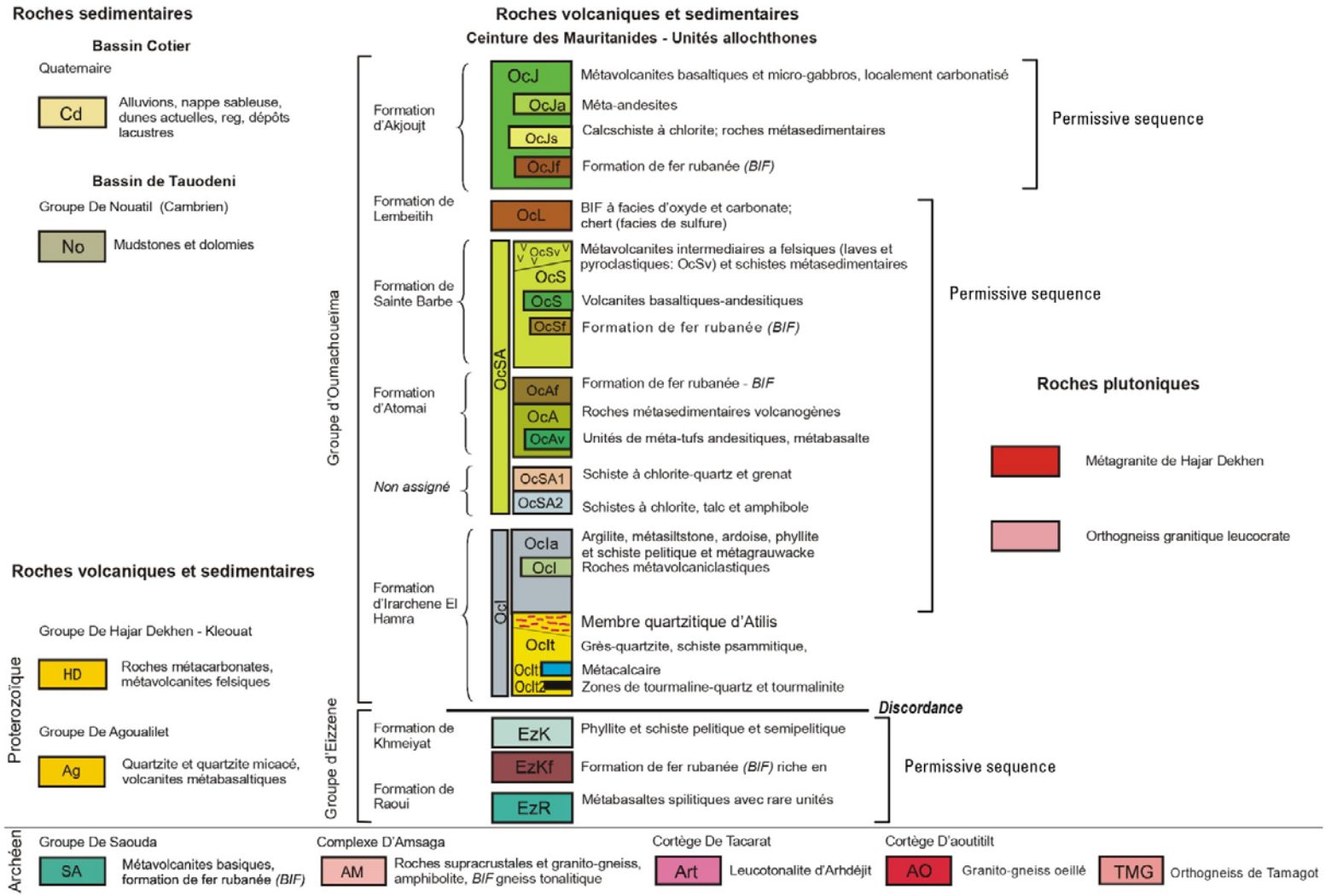

Figure 15. Stratigraphic section and correlation diagram of rocks in the Akjoujt nappe pile (from Pitfield and others, 2004).

Both the western and eastern blocks of the basal nappe composed of the Agoualilet Group contain mafic volcanic rocks and associated co-genetic (?) intrusions that are permissive of Cu-Ni-PGE or chromite (±PGE) deposits. The western block contains a melange of metabasic intrusive rocks with lenses and partitions of metavolcanic, metaultramafic and metasedimentary rocks named the Amleila Suite (currently mapped as a correlative of the Guidamaka Suite) that is overlain along its eastern side by a 2–4 km-wide strip of basaltic metavolcanics and lesser metagabbroic intrusive rocks of the Adam el Bouje Formation (Pitfield and others, 2004). This core of the western block is surrounded on all sides by predominantly quartzites and other sedimentary rocks of the Toueirja Subgroup that are of uncertain relationship to the Agoualilet Group volcanosedimentary rocks, and that extend to the south as individual nappes or slices. They are not regarded as permissive.

The eastern block consists of the polydeformed volcanosedimentary succession of the Treïfiyat Formation.The formation is characterized by an association of metabasaltic lavas and volcaniclastics, calc-chlorite±sericite schists, metasiltstones, calc-quartzites, metalimestones and rare BIF units. It is exposed over a large area to the south of the Ijibbitene Massif and overlies and is imbricated with basement rocks of the Amsaga Complex. For the purposes of this report the entire mapped exposure of the Treïfiyat Formation is considered permissive for the occurrence of Cu-Ni-PGE or chromite (±PGE) deposits.

Correlation of the metamafic igneous suite of the Agoualilet Group with the Gorgol Noir Complex of the Southern Mauritanides (Pitfield and others, 2004) supports the permissive nature of these rocks in the Inchiri district. The submarine metabasaltic volcanics of Adam el Bouje Formation (western block) and Treïfiyat Formation (eastern block) are comparable to the El Gueneiba Group volcanics whereas the fragmented intrusive metamafic-metaultramafic complex paired with quartzites of the Toueirja Subgroup has many similarities with the Gadel Group (Pitfield and others, 2004). The Gueneiba Group is interpreted to be a rift basin assemblage of mafic volcanic rocks and associated sediments and the Gadel Group, an ophiolite mélange composed of a structurally complex assortment of mafic volcanic rocks and sediments juxtaposed with gabbros and ultramafic rocks. The presence of numerous mafic-type (Cyprus-type) VMS occurrences (Taylor and Giles, 2015a) and podiform chromite occurrences as well as these rocks being regarded as permissive of orogenic gold (Goldfarb and others, 2015) in correlative rocks to the south implies favorable potential for Cu-Ni-PGE or chromite (±PGE) in the Agoualilet Group of the Inchiri district. However, there are no geochemical or geochronological data available for rocks of the Agoualilet Group with which to further evaluate either the type of volcanism or correlation with similar rocks in the southern Mauritanides.

The current understanding of the Saouda Group in the Tamagot window and Bou Kerche nappe suggests that these predominantly mafic metavolcanic rocks with ubiquitous BIF represent an Archean (?) granite-greenstone sequence that may be related to the Tasiast-Tijirit terrane. The granite-greenstone-like geometry is primarily based on the complexly interfolded nature of the Saouda Group greenstones with orthogneiss in the Tamagot window and is extrapolated to the mafic metavolcanosedimentary succession of the Bou Kerche nappe. Available geochronologic data on these rocks are sparse and are limited to $^{40}Ar/^{39}Ar$ studies (Dallmeyer and Lécorché, 1990a). A total gas age of

2,035±11 Ma was obtained for an amphibole concentrate from Saouda Group rocks of the Bou Kerche nappe. Argon dating of muscovites from a garnet-mica schist and a leucocratic gneiss from the Saouda Group gave mixed Mesoproterozoic and upper Paleozoic ages, however these data display internally discordant spectra that suggest thermal disturbance of mineral systems as old as 2,600 Ma (Pitfield and others, 2004). Correlation of mafic metavolcanic rocks in the Zemzem tectonic window of the southern Mauritanides with the Saouda Group of the Inchiri district and a U-Pb zircon age of 2,683±22 Ma on an associated Zemzem metamicrogranodiorite strengthens the probability that rocks of the Bou Kerche nappe are at least Neoarchean age (Pitfield and others, 2004). However, as discussed above, the greenstone successions of the Tasiast-Tijirit terrane are Mesoarchean in age and are approximately 300 million years older than rocks of the Saouda Group. Thus, the association of greenstones of the Saouda Group with comparable rocks in the Tasiast-Tijirit terrane is tenuous. No geochemical data are available for comparison.

There are currently no known Ni-Cu-PGE mineral occurrences of any type present within rocks of the Saouda Group. The dominantly metamafic assemblage contains three major lithologies: amphibolites, metamafites, and chloritic schists. The amphibolites are generally medium to fine grained and are mostly slatey to schistose. Medium grained amphibolites may represent co-genetic micrograbbroic intrusions. A small layered gabbro body associated with serpentinites and metacarbonate rocks (marble) is restricted to the southern limit of exposure of the Saouda Group/Bou Kerch Nappe. The chloritic schists include variably quartzitic chlorite-sericite and calc-chlorite-sericite schists, which contain thin metalimestone horizons (Pitfield and others, 2004). Thin and impersistent BIF and lesser metachert layers are ubiquitous. Without further geochemical data on the metavolcanic rocks or descriptive information on mineral occurrences, the entire Saouda Group must be regarded as permissive of Cu-Ni-PGE or chromite (±PGE).

The Choueima Nappe overthrusts the Bou Kerche Nappe and consists of at least two major volcanosedimentary successions separated by an unconformity. The lower Eizzene Group forms the first succession and is dominated by mafic volcanic rocks overlain by BIF and semipelitic schists. The Eizzene Group is present in two outcrop areas to the north of Akjoujt near the northern margin of the nappe. The lower portion of the Eizzene Group consists of monotonous metabasalts of the Raoui Formation. In contrast to metavolcanic rocks of the Oumachoueima Group, co-genetic intrusive rocks are absent. The overlying Khmeiyat Formation is marked by a regionally extensive BIF at the base followed by an entirely metasedimentary succession characterized by low-grade, pelitic to semi-pelitic schist-phyllites with psammitic subgraywackes, quartzites, and intermittent thin BIF (Pitfield and others, 2004). Based on these descriptions, rocks of the Eizzene Group are not considered permissive of Cu-Ni-PGE or chromite (±PGE) deposits.

The second volcanosedimentary succession of the Choueima Nappe consists of the Oumachoueima Group, which hosts the majority of known mineral occurrences of the Inchiri district. It is the most aerially extensive rock unit present in the district and occupies the majority of the center, northern, and northeastern portion of the Akjoujt nappe pile. It overlies the Amsaga terrane above a major sole thrust fault along the northern margin of the district and is in thrust contact with the overlying Hajar Dekhen-

Kleouat Nappe along a curvilinear western boundary. From its unconformable basal contact with the Eizzene Group, the Oumachoueima Group passes upwards from siliciclastic through pelitic sedimentary rocks into andesite-dacite derived volcaniclastic and proximal volcanic rocks followed by submarine basaltic flows and gabbroic synvolcanic intrusions. BIF units occur at several stratigraphic levels within the group (Pitfield and others, 2004). Aside from rare mafic volcanic rocks and associated (synvolcanic ?) metgabbroic bodies low in the Oumachoueima Group, the major accumulation of mafic volcanic rocks and associated gabbroic intrusive rocks occur in the Akjoujt Formation at the top of the Oumachoueima Group. Intervening rocks are mostly pelitic sedimentary rocks and lesser intermediate to felsic volcanic rocks and are not considered permissive for Cu-Ni-PGE or chromite (±PGE) deposits.

The uppermost unit of the Oumachoueima Group overlies the Lembeitih BIF and consists almost entirely of submarine basalts, microgabbros and their tectonized equivalents of the Akjoujt Formation. The dominant rock type is a fine-grained non-porphyritic tholeiitic metabasalt that is rarely well exposed and occasionally exhibits shapes that may be pillows. The microgabbros, interpreted as synvolcanic intrusives, are almost as common in some areas. The synvolcanic metamicrogabbro intrusions locally form block fields and are amphibolitic, though primary igneous texture is still discernible (Pitfield and others, 2004). In contrast to mafic rocks of the Eizzene and Oumachoueima Groups, the geochemistry of the Akjoujt basalts indicate a change in both composition and volcanic style from subduction related arc affinities to those more closely related to E-MORB or T-MORB magmas.

Due to the complex structural relationships in the Akjoujt nappe pile, age relationships of rocks in the Oumachoueima Group are critical in working out the volcanosedimentary history of the district and consequently the metallogenic history. The prime example is the conflicting age assignments for the Akjoujt Formation basalts. Current structural and stratigraphic reconstructions place the Akjoujt basalts above the Lembeitih BIF at the top of a succession that is generally regarded to be Neoproterozoic in age based on detrital and inherited U-Pb zircon determinations (Pitfield and others, 2004). However, this is in direct conflict with geochronological data from authigenic monazite and xenotime from Guelb Mohgrein mine ore assemblages that are hosted by the Akjoujt Formation. U-Pb dates of 2,492 Ma on monazite and 1,742 Ma on xenotime from the deposit were interpreted as minimum ages of mineralization and remobilization, respectively. Additional conflicting data include a reported K-Ar date of 393 Ma on metamorphic muscovite, K-Ar dates on skarn minerals ranging between 829 and 626 Ma, an Ar-Ar date on amphibolite of 1.7 Ga, and a K-Ar date on metagabbro of 3.6 Ga. (Marutani and others, 2005; Meyer and others, 2006). New detrital zircon data obtained by the USGS during this study, including from sedimentary rocks below the ore-hosting volcanic rocks, show no evidence of material older than Neoproterozoic (fig. 16; Bradley and others, 2015). Numerous workers have commented on the abundance of iron formation in the district and that the general appearance and structural style of the metamafic volcanosedimentary sequences are similar to Archean greenstone sequences. It is likely that tectonic windows of Archean rocks similar to the Tamagot window and the Arhdejit leucotonalite are present in the Akjoujt nappe pile and are as yet unidentified.

In contrast to the absence of base and precious metal occurrences in the other thrust nappes and tectonic windows of the Inchiri district, the Choueima nappe is well

mineralized with over 18 known Au and Cu±Au deposits and occurrences (Marsh and Anderson, 2015) including the currently producing Guelb Mohgrein mine. Most if not all of these occurrences are hosted in Fe-Mg-rich metacarbonate bodies in breccias and shear zones associated with Pan African to Hercynian thrust faulting and appear to be epigenetic, structurally controlled styles of mineralization. They are currently regarded as unusual, carbonate-hosted variants of IOCG deposits. However, possibilities also include skarn, orogenic gold, and VMS deposit types. The association of Cu-Ni-PGE and chromite (±PGE) deposits with these companion deposit types suggests that these rock sequences must be regarded as permissive, however, there are currently no known primary occurrences of Cu-Ni-PGE or chromite (±PGE) in these rocks. Reviews of the characteristics and available data for the known occurrences of the district are therefore provided in companion reports by the USGS (see Goldfarb and others, 2015; Fernette, 2015; Taylor and Giles, 2015a).

Southwest of Akjoujt and Guelb Moghrein are several outcropping laterite units (fig. 17). These units are described as detrital laterite and ferruginous duricrust. The laterite units are spatially associated with rocks mapped as mafic metavolcanic units that may be potential parent rocks for Ni-laterite deposits. The RTP magnetic anomaly map shows the mafic metavolcanic units are magnetic and thus are likely enriched in magnetite through serpentinization. The RTP magnetic anomaly highs also correlate with mapped BIF units. The analytic signal shows a linear high trending east-northeast near outcropping laterite units approximately 20 km southwest of Akjoujt. This area has a favorable magnetic signature for magnetite-rich, mafic metavolcanic units that may represent suitable parent rock necessary to form Ni-laterite deposits within, and proximal to, the mapped weathered units.Further to the southwest, approximately 35 km from Akjoujt, in an area with outcropping laterite units the analytic signal forms a circular cluster of highs about 12 km in diameter. This area contains both mafic metavolcanic and BIF units that are contributing to the analytic signal high. Because the area consists of favorable geologic units that also show favorable magnetic response, along with outcropping laterite deposit, the area is also considered favorable for Ni-laterite deposits.

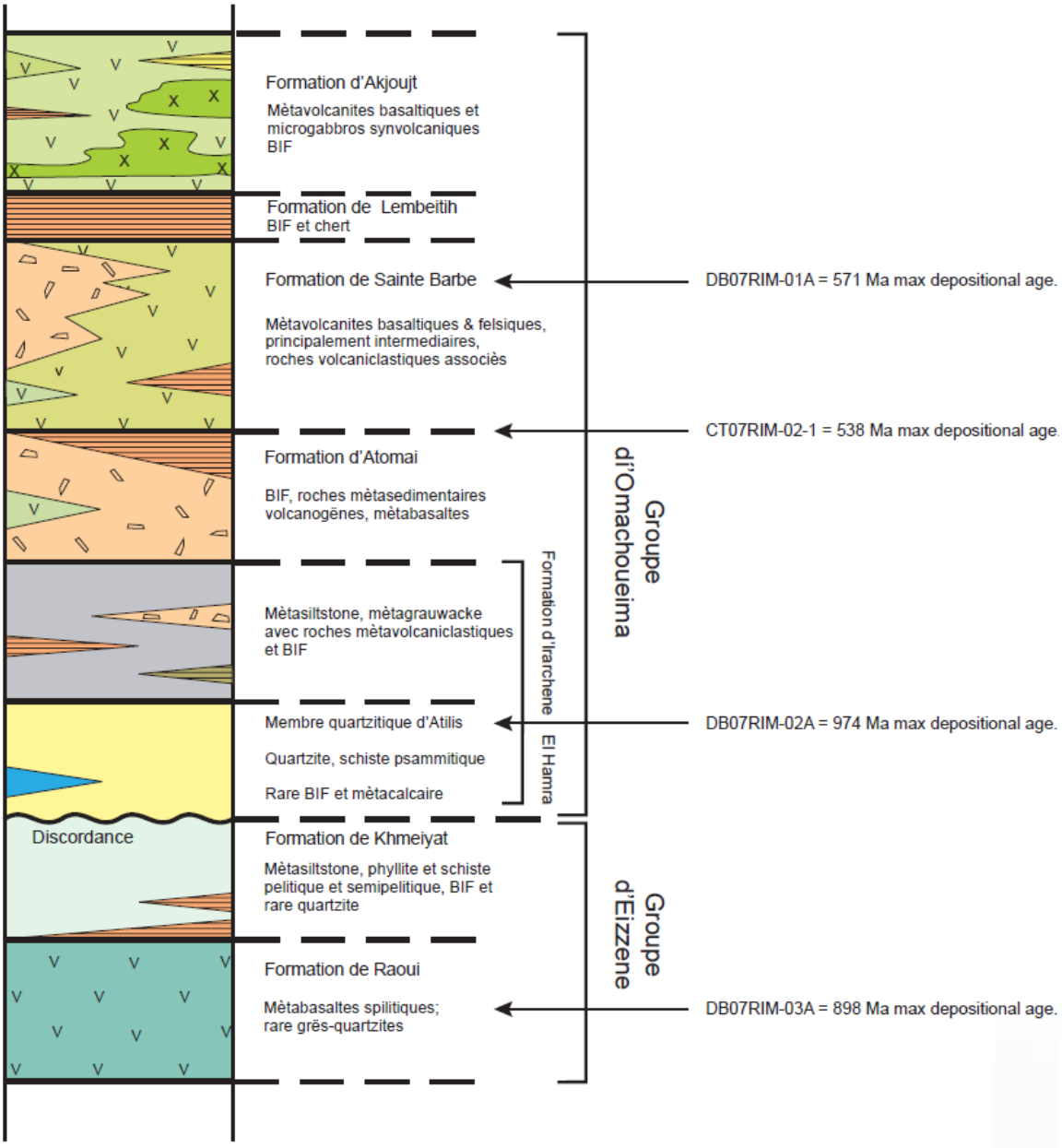

Figure 16. Detrital zircon maximum depositional ages of rock units in the Chouiema nappe. Structural-stratigraphic column from Pitfield and others, 2004.

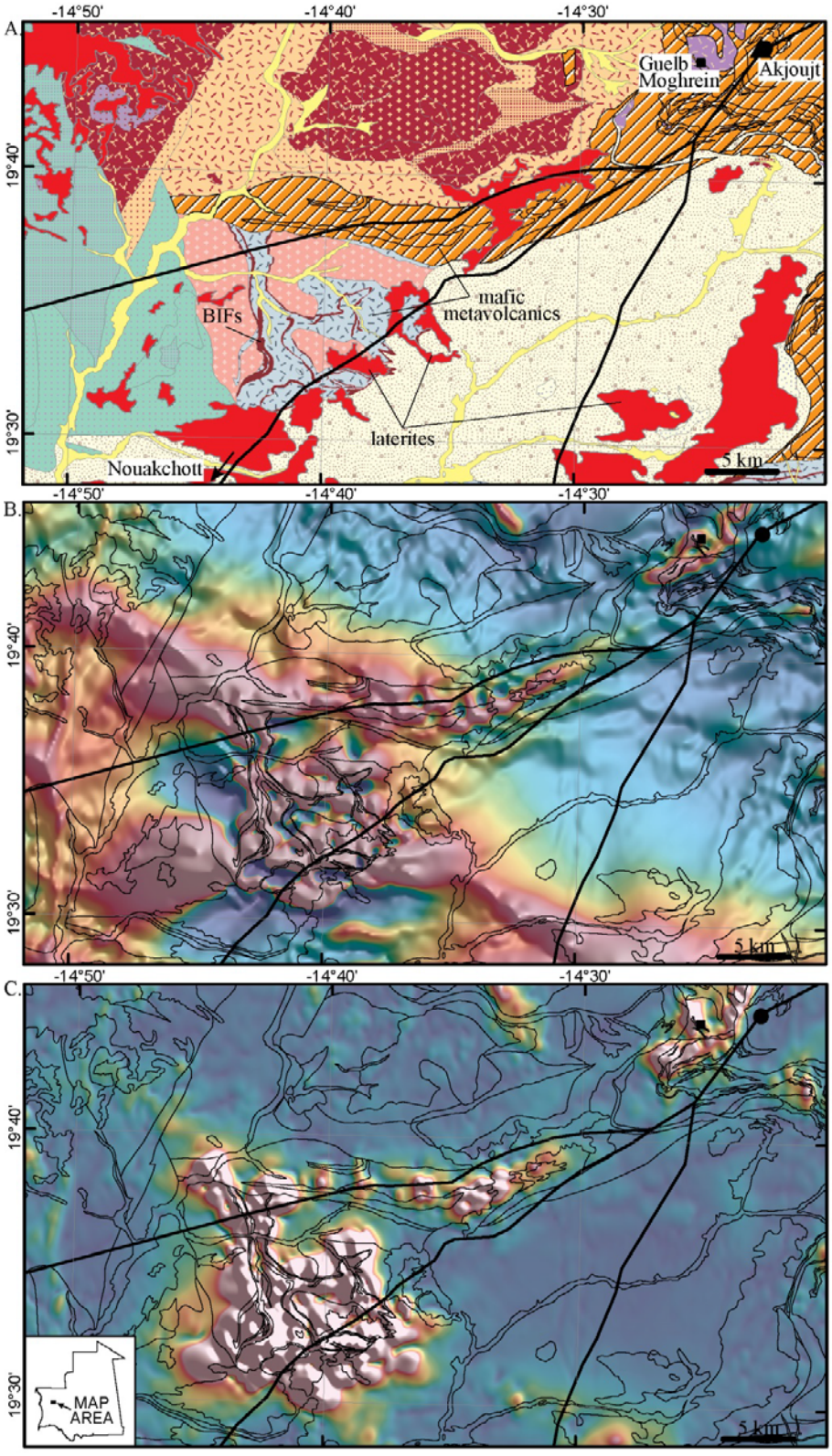

Figure 17. Generalized geology, reduced-to-pole (RTP), and analytic signal maps from the Akjoujt region. *A,* The geology favorable for Ni-laterite deposit formation in the region consists of mapped laterite and mafic metavolcanic units. Also present are BIF. *B,* The RTP map shows mapped

metavolcanic and BIF units correlated with magnetic anomaly highs. Magnetic highs and lows are shown as warm and cool colors, respectively. *C,*. The analytic signal map highlights a linear east-northeast trending high about 20 kilometers (km) southwest of Akjoujt. This anomaly trends for approximately 15 km with more isolated anomalies on the western end. The area contains mapped laterite units, mostly in the east, and is considered favorable for Ni-laterite deposits. The circular cluster of analytic signal anomalies further southwest contains permissive mapped units and is also considered favorable for Ni-laterite deposits. Analytic signal highs and lows are shown as warm and cool colors, respectively.

3.4 Mesoarchean and Paleoproterozoic Mafic-Ultramafic Rocks and Annular Ultramafic Complexes of the Northeastern Rgueïbat Shield

Several areas of the Mesoarchean and Paleoproterozoic portions of the northeastern Rgueïbat Shield, here considered as the area northeast of Zouerate, contain mafic dominated supracrustal rock sequences with associated mafic-ultramafic intrusive rocks that are permissive for Cu-Ni-PGE-Cr deposits.In the Mesoarchean portion of the shield, studies by the BRGM (Marot and others, 2003) suggest that the Zednes Suite and Temmimichate Tsabya Complex are permissive of mafic-ultramafic complexes similar to those described in the Amsaga Complex. The presence of three occurrences of Cr and Cr-Ni in the Paleoproterozoic Gleibat Tenebdar Suite, the Adam Esseder Complex, and the Adam Anajim Suite, respectively, and an additional 17 new disseminated sulfide showings suggest potential for ultramafic complexes in the Paleoproterozoic rocks of the shield.

3.4.1 Mesoarchean Mafic-Ultramafic Rocks of the Zednes Suite and Temmimichate Tsabya Complex

Prospective areas in the BRGM phase I Nord region (Marot and others, 2003) include metadunite bodies in the Mesoarchean portion of the Rgueïbat Shield primarily in the Zednes map sheet and represent an area of potential for chromite and Cu-Ni-PGE deposits in mafic ultramafic complexes that have been suggested to be similar to the Alaska/Urals-type.Eight separate chromite occurrences are present within rocks of the Zednes Suite and Temmimichate Tsabya Complex.The BRGM states that granulitic metagabbros, serpentinized metadunites, and amphibolites within these larger units have geochemical affinities to tholeiitic and boninitic volcanic rocks found in oceanic island arcs (Marot and others, 2003).Additionally, BRGM reports the presence of Ti-V bearing magnetite enrichment as well as nickel sulfides in chromite layers associated with the mafic-ultramafic complexes hosting these occurrences.

Rocks of the Zednes Suite and Temmimichate Tsabya Complex constitute the northeasternmost Mesoarchean portion of the Rgueïbat Shield in the area northeast of the village of Tourine (fig. 18). The area is bounded on the west by the Mesoarchean Tiris Complex, on the north, northeast and east sides by the complex shear zone separating the Mesoarchean portion of the shield from Paleoproterozoic granites and supracrustal sequences of the northeastern shield, and on the south by sedimentary rocks of the Taoudeni Basin. The Zednes Suite is the most voluminous suite of rocks and consists primarily of gneissic tonalite and granodiorite. Gneissic banding is defined by leucosomes of quarztofeldspathic gneiss interbanded with biotite-rich gneiss. However, the unit is described as being heterogeneous and includes tonalitic orthogneiss, pseudoporphyritic monzogranite and numerous mafic enclaves, especially near the contact with the Temmimichate Tsabya Complex (Lahondère and others, 2003). The granitic rocks are not permissive of mafic-ultramafic rock-hosted deposits, however, the included bodies of mafic-ultramafic rocks represent targets for exploration. Because current mapping does not distinguish the mafic-ultramafic bodies as separate mappable units, the entire Zednes Suite must be regarded as permissive.

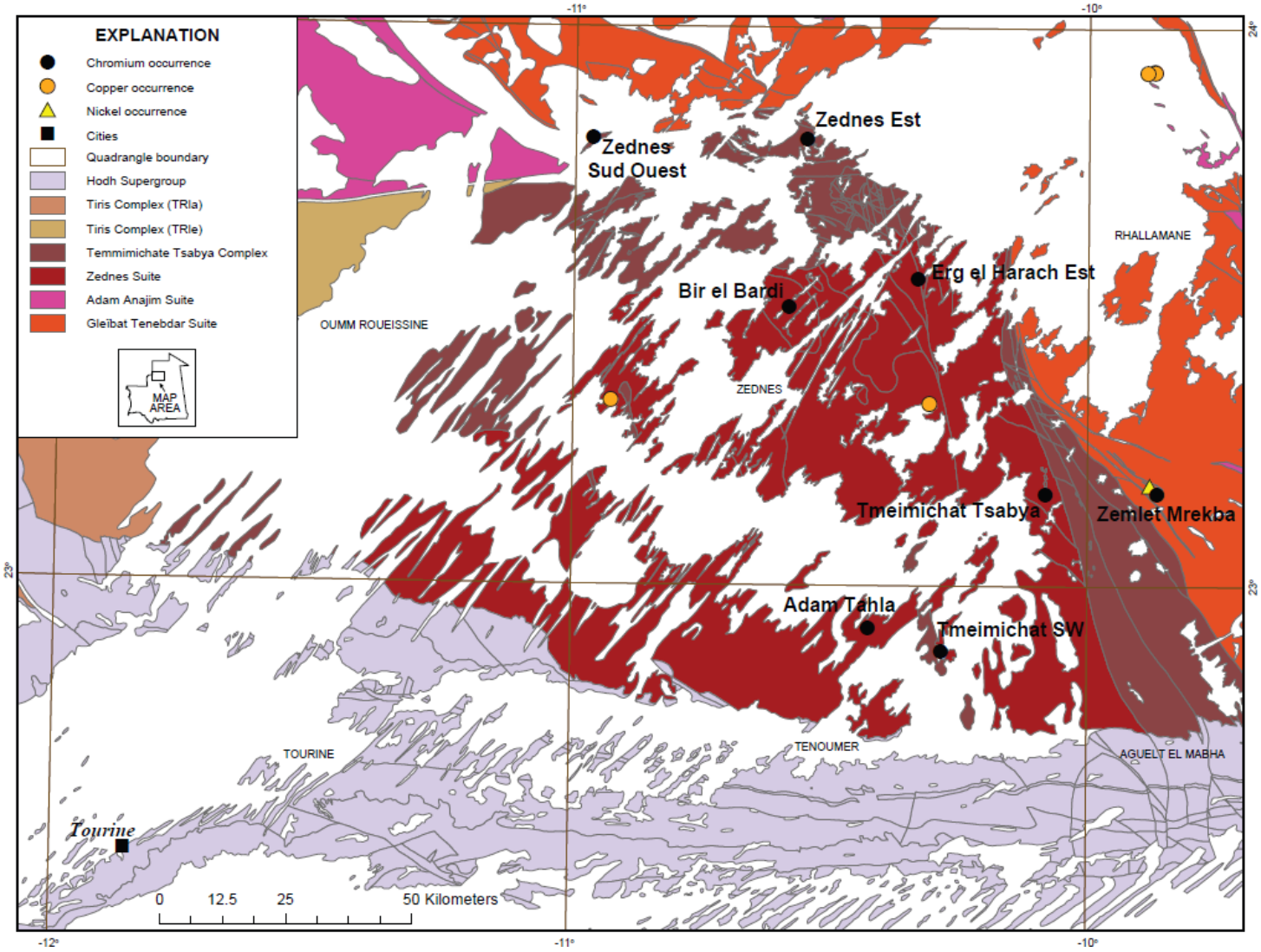

Figure 18. General geology of the Mesoarchean Rgueïbat Shield northeast of Tourine showing mafic-ultramafic rocks of the Zednes Suite and Temmimichate Tsabya Complex and the locations of Cr+Ni occurrences discussed in text.

The Temmimichate Tsabya Complex forms a north-northwest-south-southeast trending margin to the Zednes Suite varying from 1–15 km wide along the northern and northeastern sides of the Zednes Suite. This suite represents a slightly thicker east-west trending margin along the northern and northwestern sides. Primary lithologies are granulite-facies gneisses consisting of hypersthene and diopside (±red garnet) alternating with quartzofeldspathic (leptynite) bands. Topographic relief in the area is limited to low rounded rises and ridges above the extensive deposits of hamada, regolith, and eolian sand deposits. The complex is best exposed in the area around the Tmeimichat Tsabya occurrence where distinguishable petrographic units include serpentinized metadunites, metagabbros, garnet-bearing anorthosites, and quartzofeldspathic gneisses with thin bands of marble (Lahondère and others, 2003). BRGM work in the area defines five mappable units consisting of: (1) serpentinized metadunites that generally appear as low rounded hills or linear low ridges composed almost entirely of silica-carbonate altered brown rock (birbirite) containing 750–2,200 ppm nickel and 700–800 ppm chromium with olivine pseudomorphs in serpentine, carbonate, magnetite, and local accumulations of green spinel; (2) metagabbro and anorthosite with garnet characterized by an absence of orthopyroxene; (3) two-pyroxene-bearing gneiss (metalherzolite) interbanded with leucocratic anorthositic gneiss without garnet and minor biotite, rutile, hornblende, magnetite, pyrite, and apatite; (4) garnet-bearing quartzofeldspathic gneiss (leptynite) and metagabbro; and (5) a banded marble unit 1–2 m thick and several kilometers long associated with metagabbros and amphibolites (Lahondère and others, 2003).While the metadunite unit may be the most favorable mapped unit for the occurrence of Cu-Ni-PGE-Cr deposits in mafic-ultramafic rocks, the ubiquitous presence of both metagabbros and anorthosites in all of these map units with the exception of the marble indicate that all are permissive of mafic-ultramafic rock hosted deposit types.

Of the eight known chromium (±nickel) occurrences in the area, four are located within the Zednes Suite (Bir el Bardi, Erg el Harach Est, Adam Tahla, and Tmeimichat Tsabya) and three are within the Temmimichate Tsabya Complex (Zednes Sud Oueste, Zednes, Est, and Tmeimichat SW). The Zemlet Mrekba occurrence is located within a small enclave of rock mapped as amphibolites and metapyroxenites of the early Birimian Aguelt abd el Maï Complex surrounded by granitic rocks of the Gleibat Tenebdar Suite approximately 4 km east of the contact with the Temmimichate Tsabya Complex. Descriptive comments in the Mauritanian National Mineral Deposits Database (Marsh and Anderson, 2015) suggest that all eight of the occurrences are hosted within Archean ultramafic bodies indicating that there may be a mapping problem associated with the host body at the Zemlet Mrekba occurrence. A ninth unnamed nickel occurrence is located within the same enclave approximately 2 km northwest of the Zemlet Mrekba occurrence.

Descriptive information on the mafic-ultramafic complexes in the Zednes Suite and Temmimichate Tsabya Complex is extremely sparse, making evaluation of the potential of these occurrences to host economic Cu-Ni-PGE-Cr mineralization difficult. Available descriptive information is summarized in table 2 and is drawn from the Mauritanian National Mineral Deposits Database (Marsh and Anderson, 2015). Marot and others (2003) conclude that the boninitic chemistry of rocks in the Temmimichate Tsabya Complex suggests that they may be synorogenic intrusions related to island arc magmatism and that they are therefore most likely to be annular complexes similar to the

Alaska/Urals-type. However this is difficult to evaluate because the majority of the intrusions are apparently little more than supergene accumulations of brown silica-carbonate rock (birbirite) covering low ridges and hills in the otherwise flat regolith. Marot and others (2003) describe exploration of the supergene Ni-PGE potential of these birbirites in the Tenoumer area (near the Adam Tahla occurrence) by Rex Diamond Mining Company in 2000–2001. Testing (presumably by trenching) of two birbiritic gossans yielded values of 0.89 percent Ni and 1.64 g/t PGE+Au over 20 m and a second, 15 m containing 0.61 percent Ni and 1.33 g/t PGE+Au (Marot and others, 2003). No occurrence of either primary Ni-sulfides or of anything more than accessory amounts of chromite have been reported. Economic potential of the primary mafic-ultramafic rocks are untested.

Only one of the occurrences is described as having a circular shape (Zemlet Mrekba; table 2) and of the three that have descriptions of primary host rock, one (Tmeimichat Tsabya) is described as a linear, eight-km-long anorthosite complex, and the other two (Zemlet Mrekba and the nearby unnamed Ni occurrence) are described as consisting of gabbro, troctolite, pyroxenite, and amphibolite. Anorthositic lithologies are rarely observed in Alaska/Urals-type intrusions. Thus, only the Zemlet Mrekba occurrence appears to have characteristics that are vaguely similar to the Alaska/Urals-type of intrusions and Zemlet Mrekba may be mismapped and therefore more likely to be associated with Paleoproterozoic rocks of the Aguelt abd el Maï Complex. In contrast, all of the rocks described are common lithologies in both layered and massive mafic-ultramafic complexes. Until further work on the known occurrences is realized, we suggest that the mafic-ultramafic bodies in the Zednes Suite and Temmimichate Tsabya Complex may be very similar to the anorogenic intrusions previously described in the Amsaga Complex. The location of these occurrences close to a major shear zone also highlights the possibility that they could be dismembered layered intrusions or dikes of Mesoarchean age similar in composition to the Ahmeyim Great Dike in the Tasiast-Tijirit terrane.

Aeromagnetic data collected along 500-m spaced flightlines near the Tmeimichat Tsabya Cr occurrence show a complex pattern of magnetic anomalies (fig. 19). The RTP map shows a mottled pattern of moderate amplitude magnetic anomalies associated with the granodiorite rocks. The north-northwest trending metadunites associated with the Tmeimichat Tsabya Cr occurrence correlate with subtle magnetic anomaly highs. Eight kilometers west of the Tmeimichat Tsabya is a similarly trending linear string of magnetic highs present within the granodiorite and extending to the south under the hamada. The northwest trending tonalite, gneiss, and eastern extent of the metagabbro units correlate with prominent magnetic anomaly highs.

The analytic signal calculates the gradient of the magnetic field and can be used to simplify the interpretation of magnetic anomalies (Nabighian, 1972; Roest and others, 1992). The analytic signal near the Tmeimichat Tsabya Cr occurrence shows highs that strongly correlate with the mapped tonalite, gneiss, and eastern extent of the metagabbro units. The Tmeimichat Tsabya occurrence is located over an analytic signal high. Several other analytic highs of similar dimension are found trending to the north-northwest. The north-northwest trending RTP anomaly west of Tmeimichat Tsabya and within the granodiorite produces strong analytic signal highs.

Magnetic anomalies with amplitudes greater than 500 nanoteslas were identified along flightlines. Such anomalies may represent magnetic material, such as ultramafic rock, within less magnetic material. Such strong anomalies may be subdued during gridding processes, so using original flightline data to map their distribution is preferred. All of the magnetic anomalies identified correlate with analytic signal highs. Such picks may be more focused regions within the analytic signal highs where the most magnetic units occur. A few anomaly picks occur within the eastern edge of the mapped metagabbros. Several anomaly picks occur along the belt of analytic signal highs within the granodiorite. Combined, the mapped geology, RTP, analytic signal, and magnetic anomaly picks may help indicate where the more favorable areas for ultramafic rocks near the Tmeimichat Tsabya chromium prospect occur.

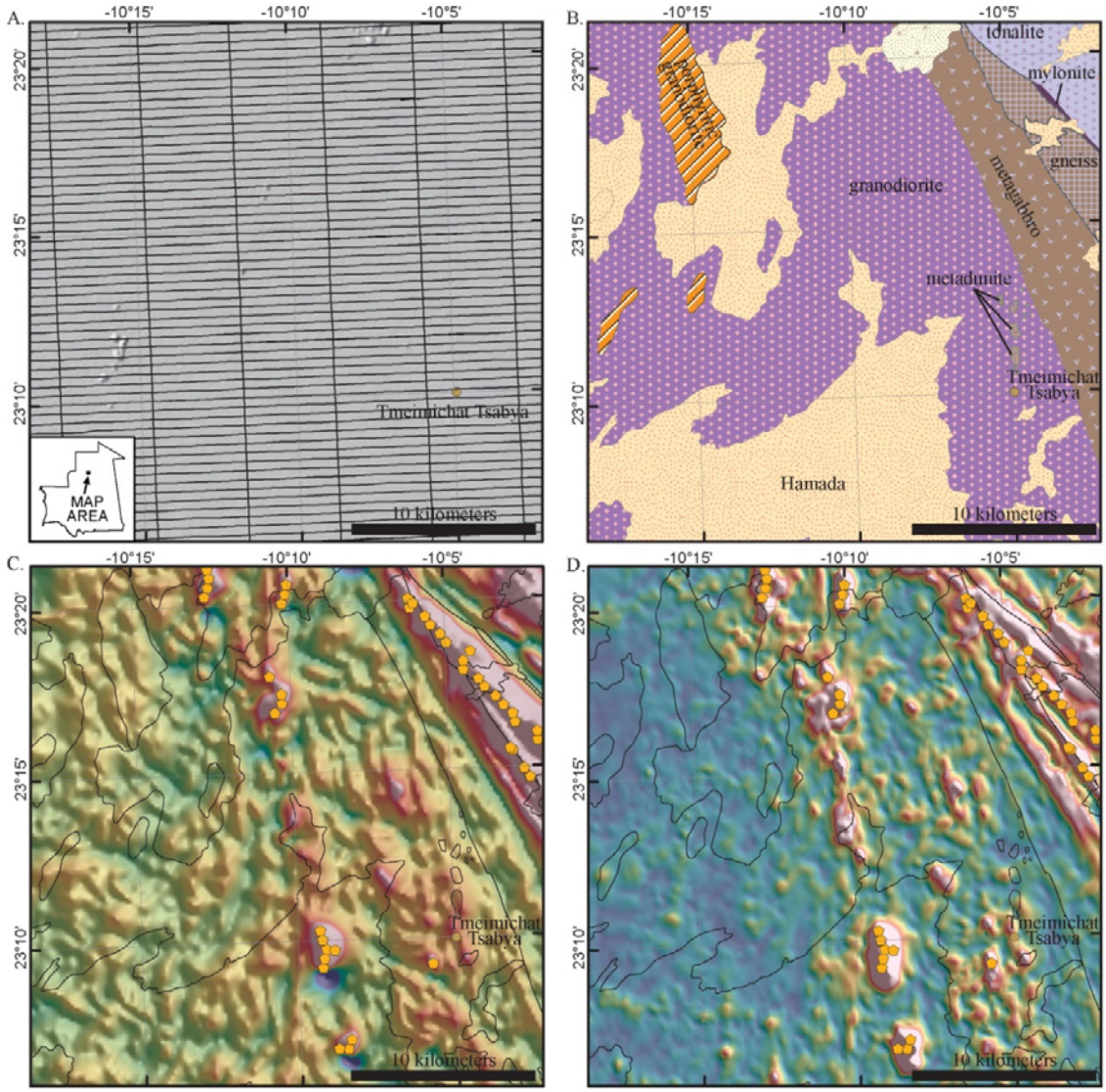

Figure 19. Generalized geology, reduced-to-pole (RTP), and analytic signal, maps near the Tmeimichat Tsabya chromium prospect. *A,* Shaded-relief of digital elevation model and flightline location for the area. *B,* Generalized geologic map showing the distribution of mapped metadunite intrusions hosted in granodiorite rocks. *C,* RTP map showing moderate amplitude magnetic anomaly highs associated with the granodiorite rocks. Metagabbro, tonalite, and gneiss units in the east produce strong, high amplitude magnetic anomalies. Black polygons show outline of mapped units. Orange markers indicate magnetic anomalies > 500 nanoteslas along flightlines. Magnetic highs and lows are shown as warm and cool colors, respectively. *D,* Analytic signal highlighting several areas where the magnetic field is rapidly changing that may reflect ultramafic rocks. In particular, the north-northwest trending analytic signal highs within the granodiorite. Orange markers indicate magnetic anomalies > 500 nanoteslas along flightlines. Analytic signal highs and lows are shown as warm and cool colors, respectively.

3.4.2 Paleoproterozoic Mafic-Ultramafic Complexes of the NW Rgueïbat Shield

Three known occurrences, one of chromite at Dhbeat, a second of disseminated chromite, magnetite and nickel sulfides at Gleibat el Hafeira, and a third of Cr and Ni at Aguelt Adam are located in Paleoproterozoic mafic-ultramafic rocks of the Gleibat Tenebdar Suite, the Adam Esseder Complex, and the Adam Anajim Suite, respectively. All three are described as circular, with or without layering, and are interpreted to belong to the Alaska/Urals-type of intrusions. BRGM studies (Marot and others, 2003) suggest that these occurrences as well as an additional seventeen new disseminated sulfide occurrences mostly associated with gabbroic rocks may represent an additional area in the northwestern corner of the Paleoproterozoic portion of the Rgueïbat Shield that is permissive for the occurrence of Alaska/Urals-type annular ultramafic complexes. Additional complexes and suites of the Paleoproterozoic shield are known to contain similar mapped subunits of mafic-ultramafic intrusive rocks that must be considered equally permissive of arc-related types of Ni-Cu-PGE-Cr deposits despite the absence of known mineral occurrences. Specific subunits of the Rich Anajim, Aguelt abd el Maï, Tsalabia el Khadra, and the Tmeïmichatt Ghallamane Complexes are described below. Due to the small size of these deposit types and the uncertain context or endowments of most of the new occurrences, the potential for economic deposits of this type is currently regarded as low.

The northeastern Rgueïbat Shield is composed of Paleoproterozoic (Birimian) to Neoproterozoic granitoids and supracrustal rocks of the West African Craton. This region is characterized by a series of volcanosedimentary belts and associated batholithic-scale granitic intrusive suites emplaced during the Eburnean orogeny from about 2,150–2,000 Ma. Two major sets of shear zones oriented NNW-SSE and E-W are present and often bound the volcano-sedimentary belts and (or) batholiths. French workers divide the northeastern shield into four major lithologic groupings by age consisting of (1) an early Birimian (>2,150 Ma) group of primarily metamafic volcanosedimentary rocks including from west to east, the Rich Anajim, Aguelt abd el Maï, Ghallamane and Tsalabia el Khadra Complexes; (2) a middle Birimian (2,150–2,120 Ma) group of intrusive granites including from west to east, the Adam Anajim Suite, and the Tin Bessaïs and Tmeïmichatt Ghallamane Complexes; (3) a late Birimian (2,070–2,060 Ma) group of volcanosedimentary sequences of low metamorphic grade including from west to east, the Legleya, Imourène and Blekhzaymat Groups accompanied by similar-aged granites of theGleïbat Tenebdar Suite; and (4) a latest Birimian (2,040–2,000 Ma) group of voluminous magmatic rocks including the Adam Esseder Complex and the Sfariat, Yetti, Bir Moghreïn and Tigsmat el Khadra Suites (Lahondère and others, 2003). With the exception of the Blekhzaymat Group, most of the volcanosedimentary sequences are relatively restricted in area and occur as roof pendants and partitions within and adjacent to the areally extensive granitic batholiths and other intrusive suites primarily in the central area of the northeastern shield (fig. 20).

Geochemical and petrological studies by the BRGM in the Birimian rocks of the northeastern shield suggest overwhelmingly that the entire sequence of supracrustal rocks as well as the voluminous granitic rocks that surround them have subduction-related volcanic arc, intra-arc, and back-arc signatures (Lahondère and others, 2003). These features are consistent with the accretion of island arcs and continued suprasubduction

zone magmatism in a convergent continental margin orogenic setting along and northeast of the Mesoarchean portion of the shield. Such a setting is permissive of a wide variety of mineral deposit types such as orogenic gold (see Goldfarb and others, 2015), VMS (see Taylor and Giles, 2015a), and a variety of Cu-Ni-PGE-Cr deposit types including podiform chromite and magmatic sulfide segregation deposits in ophiolites, suprasubduction zone mafic-ultramafic intrusions, and Alaska/Urals-type annular intrusions.

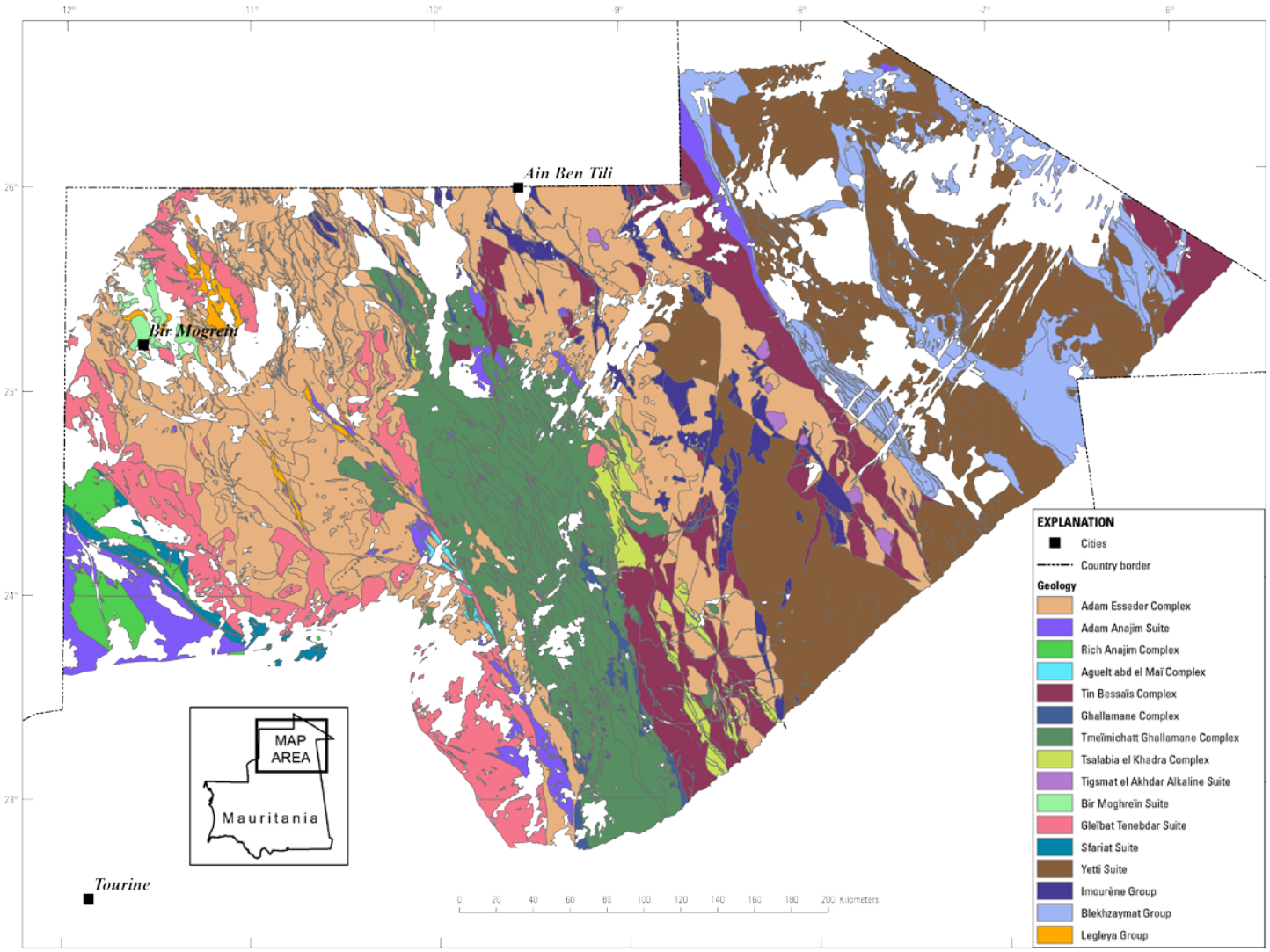

Figure 20. General geology of the Paleoproterozoic (Birimian) portion of the Rgueïbat Shield.

Based on the current state of geologic mapping, igneous rock geochemistry, and identification of mineral deposit types in the northeastern shield, there do not appear to be any ophiolite sequences preserved. However, descriptions of many of the major granitic complexes and supracrustal belts in which mafic volcanic rocks are present indicate that small (tens of meters to several kilometers in diameter) amphibolitic, gabbroic melanocratic to leucocratic, and ultramafic intrusions as well as dikes of the same composition (several meters thick and hundreds of meters to kilometers in length) are present and are widely distributed throughout the Birimian portion of the shield (Lahondère and others, 2003). The widespread nature of small mafic-ultramafic intrusions and the generally poor exposure of rock units creates difficulty in constraining the area of permissive rock units for mafic-ultramafic rock hosted mineral deposits. It is impractical to delineate the whole of the northeastern Rgueïbat Shield as permissive, so in the section that follows we briefly review the descriptive geology of the major igneous complexes and supracrustal belts that have mapped subunits described as gabbroic and ultramafic rocks. These units together are regarded as permissive of the occurrence of either suprasubduction zone or Alaska/Urals-type Cu-Ni-PGE-Cr deposits in the Paleoproterozoic portion of the shield.

Early Birimian granitic complexes and/or groups that contained mapped mafic-ultramafic subunits include the Rich Anajim, Aguelt abd el Maï, and the Tsalabia el Khadra Complexes. The Rich Anajim Complex (fig. 21) is a metamorphosed supracrustal sequence consisting of metapyroxenites, amphibolites, dolomitic marbles, magnetite quarzites and migmatitic paragneiss that constitute broad mapped areas on both sides of the Sfariat belt in the southwestern portion of the Paleoproterozoic shield. The southern outcrop area lies wholly within the granitic rocks of the middle Birimian Adam Anajim Suite and the northern outcrop area lies between the Sfariat Belt and granitic rocks of the Gleibat Tenebdar Suite. The Rich Anajim Complex is divisible into lithostratigraphic packages consisting of gabbros and basalts thought to be of back-arc origin, a set of closely associated ferruginous quartzites and marbles, and a paragneiss suite derived from pelitic and calcareous sandstones.

Mapped mafic-ultramafic subunits within the Rich Anajim Complex (designated as the RAam subunit; Lahondère and others, 2003) occur primarily to the southwest of the Sfariat belt. They are described as pyroxenites, amphibole-pyroxenites, and amphibolites containing diopside + plagioclase + calcite, quartz, sphene, apatite, chlorite, amphibole, epidote, magnetite and zoisite and are primarily associated with banded marbles and pyroxene-bearing (diopside) gneiss (Lahondère and others, 2003). The Aguelt Adam Cr + Ni occurrence is the only known mafic-ultramafic hosted occurrence in the vicinity and is located approximately 4 km to the west of the main mapped subunit body on the border with Western Sahara. The intrusion is described as a circular mass composed of hydrothermally altered gabbronorite, pyroxenite, and troctolite associated with a well exposed anorthosite complex. No visible magnetite or chromite is reported, however the complex is suggested to have potential for chromite (Marsh and Anderson, 2015).

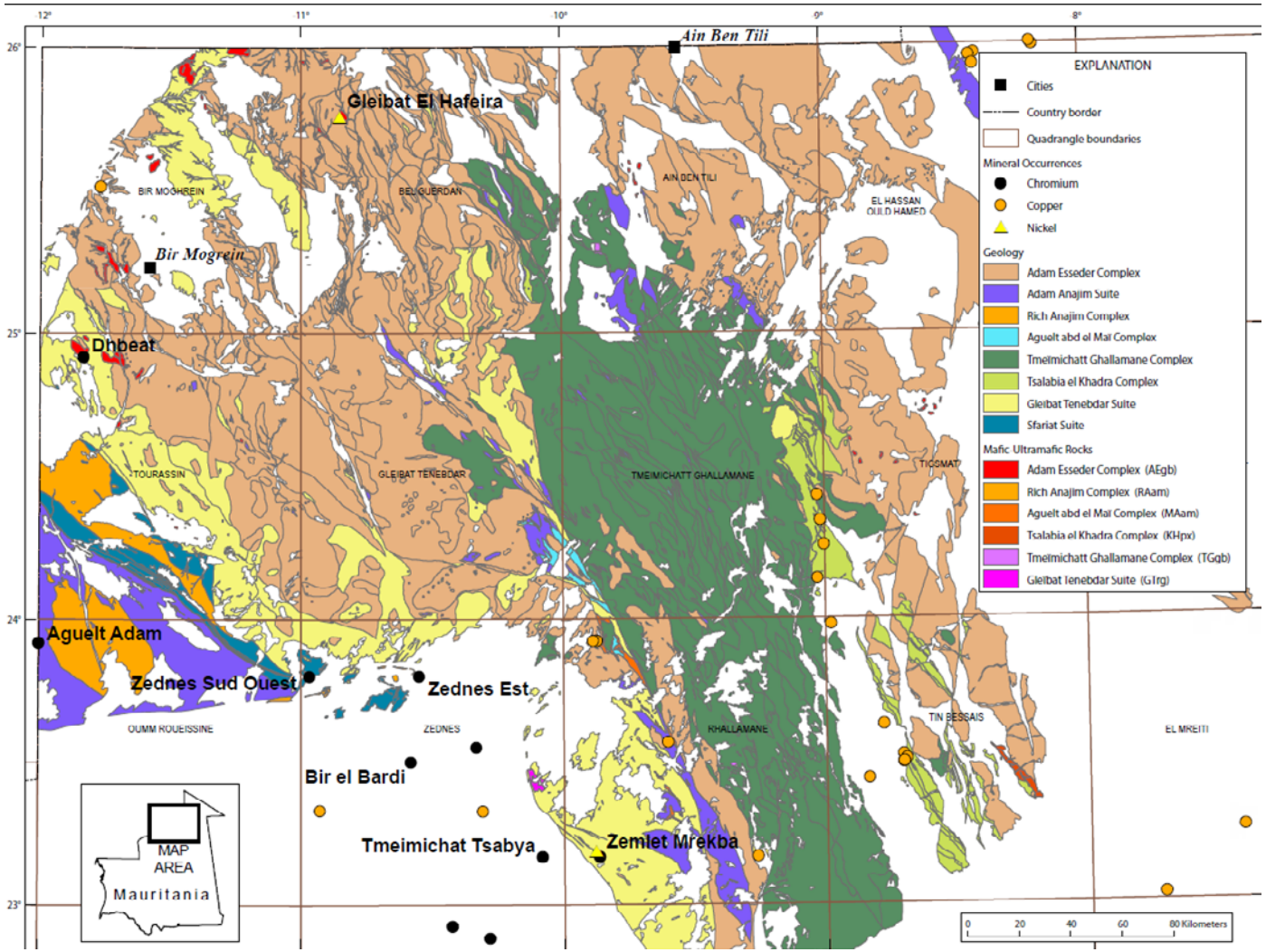

Figure 21. General geology of the northwestern Paleoproterozoic Rgueïbat Shield showing Birimian mafic-ultramafic subunits and the locations of Cr+Ni±Cu occurrences discussed in text.

The Aguelt abd el Maï Complex (fig. 21) is an areally restricted unit occurring as thin partitions, roof pendants, and enclaves of gneissic to mylonitic textured supracrustal rocks between granitic rocks of Adam Esseder and Tmeïmichatt Ghallamane Complexes. The predominant lithologies are a fine grained metamafic rock and dark-colored porphyroclastic rocks with subordinate amphibolites and melagabbros. Metasedimentary rocks include quartzites and calc-silicate gneisses (formerly calcareous sandstones and marbles). The metamafic rocks consist of metamorphosed porphyritic dacites and rhyodacites. The amphibolites contain pyrite partially converted to hematite. The partitions and enclaves are highly attenuated and discontinuous and occur on scales of meters to kilometers in length.Outcrops are wider to the south and contain higher proportions of amphibolites, quartzites, and marbles (Lahondère and others, 2003).

Mapped mafic-ultramafic subunits within the Aguelt abd el Maï Complex (designated as the MAam subunit; Lahondère and others, 2003) occur primarily in the northwestern corner of the Rhall Allamane 1:200,000 map sheet. They are described as primarily consisting of foliated fine grained amphibolites and metapyroxenites containing mostly green hornblende and rare porphyroclasts of pale green clinopyroxene and interstitial granoblastic plagioclase (Lahondère and others, 2003). Minor sphene and partially hematized pyrite is also present. The presence of pyrite in these rocks is suggestive of the possibility of the attainment of sulfur saturation and is therefore favorable for the formation of Cu-Ni sulfides. The Zemlet Mrekba Cr + Ni occurrence described above is the only known mafic-ultramafic hosted occurrence in these rocks and is located approximately 4 km east of the contact with the Temmimichate Tsabya Complex in a small enclave of this subunit. An unnamed nickel occurrence is located within the same enclave approximately 2 km northwest of the Zemlet Mrekba occurrence and is described as a garnierite-bearing birbirite cap to gabbroic and troctolitic rocks (Marsh and Anderson, 2015).

The Tsalabia el Khadra Complex (fig. 21) is an areally more extensive supracrustal sequence located to the east of the Ghallamane Complex in the central part of the northeastern shield. The largest contiguous block is located toward the northern end of its mapped extent and has dimensions of approximately 90 × 20 km. The complex consists of metapyroxenites and metagabbros, mafic metahyaloclastites, amphibolites locally associated with quartzites and lenses of marble, marbles, locally manganiferous quarzites, metaandesites, metarhyolites, epiclastites and tufaceous schists and locally conglomeratic meta-arkoses (Lahondère and others, 2003). The complex is fault bounded to a greater degree than the previously described units and is within or in contact with granitic rocks of the middle Birimian Tin Bessaïs and Tmeïmichatt Ghallamane Complexes and the latest Birimian Adam Esseder Complex.

Mapped mafic-ultramafic subunits within the Tsalabia el Khadra Complex (designated as the KHpx subunit; Lahondère and others, 2003) occur primarily in the eastern Tin Bessias 1:200,000 map sheet. They are described as metapyroxenites and metagabbros (Lahondère and others, 2003) primarily in a single elongate poorly exposed outcrop along the eastern edge of a large diorite body. This outcrop consists of metapyroxenite, cumulate wehrlite, and coarse grained metagabbro. The rocks have a pseudoporphyritic texture that is interpreted as an orthocumulate. Clinopyroxenes appear as squat phenocrysts that are largely altered to amphibole. The amphibole pseudomorphs are associated with cumulate crystals of fayalitic olivine often fringed with magnetite and

intercumulus plagioclase. Secondary minerals include a very clear fibrous amphibole (cummingtonite?), magnesian chlorite, hercynite, pale yellow- brown biotite and clinozoisite. The metapyroxenites and metagabbros are associated with fine grain amphibolites in outcrop. Fine grained foliated amphibolites are ubiquitous throughout the Tsalabia el Khadra Complex and some do have coarse grained textures suggestive of gabbroic intrusive bodies. However, their widespread and undiagnostic occurrence is not very useful in exploration for mafic-ultramafic intrusive rocks and they are not shown in figure 21. There are no known occurrences of Ni, PGE, or Cr in the Tsalabia el Khadra Complex and as with all other copper occurrences in the early Birimian rocks none of the copper occurrences in the Tsalabia el Khadra Complex are associated with the rocks described above.

Geochemical analyses of amphibolites and metabasaltic rocks from all of the early Birimian supracrustal sequences yield N-MORB elemental patterns consistent with their derivation in an oceanic environment. Geochemical characteristics of intermediate volcanic rocks are more consistent with derivation in a calc-alkaline, volcanic arc environment. Together these data are interpreted to represent a back-arc or intra-arc environment of formation of the early Birimian supracrustal sequences of the northeastern shield (Lahondère and others, 2003).

Middle Birimian granitic rocks consisting of the Adam Anajim Suite, and the Tin Bessaïs and Tmeïmichatt Ghallamane Complexes occupy much of the central portion of the Paleoproterozoic Rgueïbat Shield. They are mainly intermediate to felsic granitoids, which are distinguished from the latest Birimian granites by a frequent planar fabric of tectonic and/or magmatic origin. While both the Rich Anajim and Tin Bessaïs Complexes contain tonalitic to granodioritic gneisses with melanosomes of amphibolite, neither complex contains mafic-ultramafic bodies large enough to warrant mapping as a subunit. Tmeïmichatt Ghallamane Complex (fig. 21) has a mapped subunit of mafic-ultramafic lithologies.

Mapped mafic-ultramafic subunits within the Tmeïmichatt Ghallamane Complex (designated as the TGgb subunit; Lahondère and others, 2003) occur primarily as several small (tens of meters to 2 kilometers) subcircular intrusions or as meter-thick rectilinear dikes. They are described as occurring in the Gleibat Tenebdar 1:200,000 map sheet, however, the only discretely mapped body occurs in the southwest corner of the Ain Ben Tili 1:200,000 map sheet (fig. 21). They are described as gabbro with amphibole and biotite/phlogopite and locally abundant pyrite (Lahondère and others, 2003). The presence of pyrite in these rocks is suggestive of the possibility of the attainment of sulfur saturation and is therefore favorable for the formation of Cu-Ni sulfides. However, there are no known mafic-ultramafic rock-related Ni-Cu-PGE-Cr occurrences associated with this subunit.

With the exception of minor mafic-ultramafic enclaves associated with the granitic rocks of the Gleibat Tenebdar Suite, the late Birimian rocks of the Paleoproterozoic Rgueïbat Shield are not permissive for Cu-Ni-PGE-Cr deposits. Late Birimian supracrustal rocks of the Legleya, Imourène, and Blekhzaymat Groups consist primarily of intermediate to felsic eruptive rocks and associated reworked volcanogenic sedimentary rocks. They are permissive of VMS deposits and are discussed in a separate USGS chapter (Taylor and Giles, 2015a).

The Gleibat Tenebdar Suite is represented by gneissic granitoids of tonalitic to granodioritic composition that primarily occur as a belt along the northeastern margin of the Mesoarchean Rgueïbat Shield and as large masses in the northwestern Paleoproterozoic shield to the northeast of the village of Bir Mohgrein (fig. 21). Mapped mafic-ultramafic subunits within the Gleibat Tenebdar Suite (designated as the GTrt and GTrg subunits; Lahondère and others, 2003) occur primarily in the western part of the Rall Amane 1:200,000 map sheet as a large mass consisting of amphibole-bearing gabbros, quartz-rich diorites, tonalites and granodiorites. The gabbroic and dioritic rocks occur primarily in the western portion of the mass against the Archean rocks of the Temmimichate Tsabya Complex. However, because the gabbroic and dioritic units are not discriminated from the tonalites and granodiorites, which are the most common rock types present in the Gleibat Tenebdar Suite, the GTrt subunit is not shown on figure 21. An additional pegmatitic gabbro body (GTrg) approximately 25 km^2 in size occurs in the Zednes 1:200,000 map sheet.

The Dhbeat Cr-Ni-Cu occurrence is the only known occurrence hosted in mafic-ultramafic rocks of the Gleibat Tenebdar Suite and is located approximately 42 km southwest of the village of Bir Mohgrein. The Dhbeat occurrence is described as a layered circular mafic-ultramafic intrusion composed of olivine gabbro, anorthosite, and serpentinite with pyrite and chalcopyrite. The occurrence is, however located near the margin of a large (8 × 3.5 km) gabbroic intrusion belonging to the Adam Esseder mafic-ultramafic subunit described below. A second area of three similar intrusions is noted as occurring approximately 15 km to the east-southeast, however BRGM mapping appear to identify these bodies as mafic-ultramafic rocks of the Adam Esseder Complex as well (Lahondère and others, 2003; Marsh and Anderson, 2015).

Latest Birimian rocks of the Paleoproterozoic Rgueïbat Shield consist primarily of the granitic rocks of the Adam Esseder Complex and the Bir Mohgrein and Yetti Suites. These granitoids represent the widespread calc-alkaline magmatism that occurred at the close of the Birimian orogeny. The voluminous, batholith-scalerocks of this association assimilate and surround all of the older Birimian rocks in the Paleoproterozoic shield (fig. 20). Only the Adam Esseder Complex contains mappable bodies of mafic-ultramafic subunits and includes gabbro, hypersthene gabbro, leucogabbro, quartz diorite, and unspecified ultramafic rocks. The mapped mafic-ultramafic subunits within the Adam Esseder Complex are designated as the AEgb subunit (Lahondère and others, 2003). They are widespread throughout the Paleoproterozoic shield and occur as meter-scale pods to sizeable intrusions up to 10 km in size. Mapped bodies are approximately >0.5 km at minimum. Although widespread, the largest concentration as well as the largest of these intrusions occur in the northwestern portion of the Paleoproterozoic shield between the Dhbeat and Gleibat El Hafeira occurrences in the area surrounding the village of Bir Mohgrein.

Two of the largest intrusives are located north of Bir Mohgrein and are clearly identifiable on satellite imagery. The Dhara el Kelba intrusion is located close to the border with Western Sahara and is described as consisting of medium grained intersertal textured gabbronorite. Mineralogy consists of plagioclase, pyroxene (hypersthene, diallage), magnetite, and minor biotite. Identical hypersthene gabbroic intrusions of similar size are present near the northern edge of the Tourassin 1:200,000 map sheet and appear to be closely associated with the Dhbeat Cr+Ni+Cu occurrence described above.

Accessory minerals include small green amphiboles and the common occurrence of pyrite (Lahondère and others, 2003). Dioritic rocks of this suite are composed of zoned plagioclase, saussuritized green hornblende, green-brown biotite, pyrite, epidote, allanite, and sphene. Quartz gabbros with graphic micropegmatites are predominantly composed of clinopyroxene ± orthopyroxene, calcic plagioclase, amphibole, biotite, and quartz with abundant secondary magnetite and pyrite, epidote, and prehnite.

Inspection of most of the 17 unnamed occurrences without assigned major commodities in the Mauritanian National Mineral Occurrences Database (Marsh and Anderson, 2015) in the Bir Mohgrein, Tourassin, Gleibat, Tenebdar, Bel Guerdan, and western Ain Ben Tili 1:200,000 map sheets, reveal that they are mostly described as minor (<1 percent to trace amounts) disseminated pyrite in gabbroic or dioritic rocks. Additionally, with the exception of three unnamed-unspecified occurrences approximately 15–20 km to the east-southeast of the Dhbeat occurrence, all of these pyrite showings are associated with mafic-ultramafic bodies that are too small to warrant inclusion in the BRGM 1:200,000 scale geologic mapping. The only known mineral occurrence hosted in the mafic-ultramafic rocks of the Adam Esseder Complex is the Gleibat el Hafeira Ni-Cr-Cu occurrence. The occurrence is located at the western margin of a 2.5 × 5 km intrusion described as a circular, stratified, olivine-bearing banded gabbronorite with magnetite, chromite, and approximately 1 percent disseminated sulfides including pyrite, pyrrhotite, and possibly pentlandite (Marsh and Anderson, 2015).

3.5 Ophiolite of the Gorgol Noir Complex in the Southern Mauritanides

Possible magmatic Cu-Ni- (PGE, Co-Au) deposits are known at Kadiar, Diaguili, Oudelemguil, Ndieo, Mbalou, and Hassi Chaggar in the southern Mauritanides where they are also associated with podiform chromite occurrences such as at Diaguili, Selibabi, Tourniat, and Barkeol El Abiod. The majority of these deposits occur in the Gadel Group with the remainder in the Gueneiba Group. The Gadel Group is an ophiolite mélange composed of a structurally complex assortment of mafic volcanic rocks and sedimentary rocks juxtaposed with gabbros and ultramafic rocks. The Gueneiba Group is interpreted to be a rift basin assemblage of mafic volcanic rocks and associated sediments. Both groups are components of the Gorgol Noir Complex.The largest such deposit is in association with the Diaguili prospect where both types of mineralization are present. It is significant that there has been no systematic exploration for PGEs throughout the 450 km length of the Gorgol Noir Complex. This area in particular needs to be evaluated for the possibility of shear zone related hydrothermal enrichment of PGEs in the disrupted segments of the Complex.Considerable uncertainty exists as to the nature of many of the sulfide bearing occurrences, with IOCG (see Fernette, 2015), VMS (see Taylor and Giles, 2015a), and magmatic sulfide segregation-type models all being possible.The BGS suggests that much of the potential for Cu-Ni-PGE's in these rocks may be related to hydrothermal fluids responsible for serpentinization and talc-carbonate alteration of the ultramafic bodies (Gunn and others, 2004).

Field work by the USGS in 2007 resulted in site examinations and limited geochemical studies at Kadiar, which is regarded by the USGS as a mafic-type (Cyprus-type) VMS deposit (Taylor and Giles, 2015a), and Mbalou, a podiform chromite occurrence. Further work is required at the other occurrences to place constraints upon

the origins of these deposits. Due to the small size of podiform chromite deposits in general and the remote location of the known podiform chromite occurrences in the southern Mauritanides, the likelihood that they represent an economic target for mineral development is low. Economic viability would have to be tied to the discovery of PGEs associated with the chromitites and this possibility remains untested. Mafic-ultramafic intrusive rocks of the Gorgol Noir Complex are permissive for magmatic sulfide segregation deposits of Cu-Ni±PGE and the presence of a number of Cu+Ni occurrences in the complex that may be magmatic sulfide segregation-type suggests a moderate potential for the discovery of economic deposits.

The area here referred to as the southern Mauritanides consists of the Mauritanide orogen from about latitude 17º south to the Senegal border. The host rocks in the southern Mauritanides are dominantly Neoproterozoic through Cambrian metasedimentary and metavolcanic units that were accreted to and thrust upon the Gondwanan continental margin during early Paleozoic Pan-African tectonism in West Africa. Collision with the North American craton during Hercynian times (approximately 330–270 Ma) reactivated many of the structures from this earlier collisional orogenesis and formed the Appalachian-Mauritanian belt, which later broke apart during Triassic rifting.

The southern Mauritanides consist of a north-south trending pile of thrust slices of allochthonous and parautochthonous units juxtaposed against the Neoproterozoic to Paleozoic rocks of the western Taoudeni Basin foreland sequence (Le Page, 1988; Pitfield and others, 2004).The parautochthonous zone lies between the foreland and the infrastructural allochthonous zone to the west and consists of deformed sedimentary rocks of the Adrar Supergroup imbricated with local basement inliers or tectonic windows (such as the Zemzem window). The infrastructural allochthonous zone consists of imbricated ophiolites, continental margin rift-facies and calc-alkaline igneous complexes. Two major tectono-stratigraphic divisions are recognized in the southern Mauritanides: (1) the western side of the allochthon consists of calc-alkaline metavolcanic and metasedimentary supracrustal rocks with mainly greenschist facies mineral assemblages, collectively termed the Mbout Supergroup; and (2) an eastern belt consisting of a tectonic melange and associated meta-volcanic and intrusive rocks, termed the Gorgol Noir Complex, typified by greenschist to high- pressure amphibolite facies mineral assemblages (fig. 22; Pitfield and others, 2004).

Dallmeyer and Lécorché (1989, 1990a, b) obtained $^{40}Ar/^{39}Ar$ ages on metamorphic minerals throughout the central and southern Mauritanide Belt and concluded that region had been affected by three orogenic events in Neoproterozoic, Cambrian and Hercynian time.Caby and Kienast (2009) reevaluated the data of Dallmeyer and Lécorché (1989, 1990a, b) and proposed a simpler metamorphic and tectonic history of late Paleozoic (Hercynian) plate convergence, which induced docking of Laurentia against the 670 Ma western arc domain and a compressive, nappe-forming episode correlating with Appalachian deformation at about 300 Ma.

The Mbout Supergroup consists of four parallel north-south trending zones separated by east-directed thrusts. The two outer zones consist of the El Harach Group in the east and the El Fadra Group in the west and are dominantly pelitic metasedimentary sequences. The El Harach Group is essentially a metasedimentary unit with minor metamorphosed bimodal volcanic intercalations in its southern outcrop. The two central

zones consist of the El Ghabra and El Mseigguem Groups and are characterised by intermediate to felsic metavolcanic rocks. Although there are metabasic rocks described in the Bathet Jmel Formation of the El Mseigguem Group and the Oued Erdi Formation of the El Ghabra Group, descriptions (Pitfield and others, 2004) indicate that they are primarily extrusive rocks.Due to the absence of mafic-ultramafic intrusive rocks, the Mbout Supergroup is regarded as non-permissive of Cu-Ni-PGE-Cr deposits and will not be discussed further.

The Gorgol Noir Complex consists of ophiolite and continental margin–rift facies sequences divided into three tectonically imbricated groups, each with characteristic lithologies. The upper western Guidamaka Suite consists of massive gabbro and associated more felsic intrusive rocks. The intrusive suite has many of the characteristics of a plagiogranite association but is metasomatically altered and exhibits some crustal inheritance. The lower eastern Group de Gueneiba consists of a middle-upper greenschist facies oceanic lithospheric or ophiolitic association dominated by metabasaltic rocks. The metabasic rocks have characteristics of submarine tholeiitic basalt but exhibit a more alkaline or transitional within-plate chemistry. The central Gadel Group is interpreted as a melange composed of a range of lithologies including serpentinite and quartzite (Pitfield and others, 2004). It consists of an internally imbricated middle to lower amphibolite facies continental margin rift-facies association containing major tectonic rafts of the Gueneiba Group and is tectonically intercalated with deformed parautochthonous sedimentary rocks of the Taoudeni Basin in the extreme south. The Gadel Group melange occurs structurally below as well as above the Gueneiba Group, which suggests that the metavolcanic rocks form one or more very large units in the form of frontal klippen within the mélange (Pitfield and others, 2004).

Lithologies within the Gadel Group consist of two major associations: (1) a predominantly magmatic association including ultramafic rocks (serpentinites), metabasalts, ferruginous jaspilites, garnet amphibolites, albitites, metagabbros, greenschists, and metacarbonate rocks; and (2) a siliciclastic metasedimentary association consisting of muscovite and kyanite quartzites with or without garnet and staurolite, and pelitic mica schists. Because the Gadel Group is a tectonically imbricated mélange, no lithostratigraphic or tectonostratigraphic succession can be defined. However, in general, a simplified succession of serpentinites associated with talc schists, greenschists, ferruginous quartzites, amphibolites and jaspilites in the west transition eastward into kyanite-staurolite-garnet quartzites and micaschists, muscovite quartzite, muscovitic schists and local amphibolites (Pitfield and others, 2004).

The serpentinite bodies form the main areas of high relief in the group and have a wide range of appearances and variable primary and secondary mineralogy. They are commonly capped by birbiritic gossans that have secondary chert and carbonate filling fractures that separate clasts of the host serpentinite. The serpentinites are usually sandwiched between mylonitic, variably ferruginous quartzites and (or) quartz-muscovite/sericite-schists. Talc-schists invariably form lenticular bodies that are rarely more than several hundred meters in length and are always enclosed by serpentinite. Geochemical profiles for the serpentinites suggest a within plate, non-arc environment of formation. Ferruginous jaspilites and subordinate BIF are common within the Gadel Group melange and form resistant, black- weathered low ridges. They are mostly associated with the pelitic schists, mafic and ultramafic rocks (Pitfield and others, 2004).

Less common metamafic volcanic rocks consist of quartz-chlorite-schists and green amphibole-quartz-plagioclase-schists. All the amphibole and/or epidote schists, epidosites and chlorite schists have a chemical composition close to tholeiitic basalt and have geochemical profiles that are characteristic of within-plate magmas. Tectonically aligned lenses of garnet amphibolite and pyroxenite are present and in contrast to other mafic and ultramafic rocks in the group, exhibit geochemical profiles characteristic of subduction-related volcanic arc rocks. Gneissic quartzofeldspathic schists and feldspathic muscovite schists are also present and are considered to be highly tectonized granitic sheets that are correlated with the Guidamaka Suite. Both mafic volcaniclastic rocks, interpreted as pillow breccias and pelitic schists in the Gadel Group contain local concentrations of malachite (Pitfield and others, 2004).

No direct U-Pb zircon dates are reported for rocks of the Gadel Group. $^{40}Ar/^{39}Ar$ incremental release ages for hornblende and muscovite concentrates suggest that post-metamorphic cooling occurred following distinct Neoproterozoic tectonothermal events at approximately 700-720 Ma and 640-650 Ma (Dallmeyer and Lécorché, 1989). The younger episode is related to the Pan-African 1 continental collision and broadly corresponds to U-Pb dates obtained for the syn- to post-kinematic granitoid suites of Guidamaka (665Ma) and Selibabi (637Ma). Muscovite within Gadel Group lithologies cooled through argon closure temperature between approximately 570 and 595Ma (Pitfield and others, 2004).

The Gadel Group mélange is interpreted to represent a major tectonic suture. The ultramafic rocks represent tectonized oceanic lithosphere. They are commonly associated with ferruginous jaspilites and metacarbonate rocks. The mafic rocks have two distinct geneses: one suite is comparable to the Gueneiba Group metabasaltic rocks with a within-plate chemistry whereas the amphibolites have a composition more typical of a subduction-related volcanic arc derivation. Their association with distal turbidites is consistent with their oceanic origins (Pitfield and others, 2004).

The Gueneiba Group is imbricated with and locally incorporated within the Gadel Group. It is characterized by calc-chlorite schists, chlorite±talc±amphibole schists and deformed metabasalts (pillow lavas and breccias) metamorphosed to middle-upper greenschist facies. The group remains undifferentiated in the southern Mauritanides with the exception of intrusive suites of the Guidamaka Suite. Less common lithologies include quartz-sericite-phyllites, chlorite-quartz-schists, deformed metabasalts with quartz-carbonate segregations associated with pillow breccias, ferruginous jaspilites, metakeratophyres, and massive, fine-grained marble with pyritic clots. Local intercalations of BIF lithologies are present and consist of mm-thick iron-rich seams with magnetite and/or hematite separated by thicker siliceous bands of quartz and chert. Quartz veins are extremely common and a veneer of vein quartz gravel covers large portions of the outcrop area (Pitfield and others, 2004).

Geochemical profiles of major lithologies of the Gueneiba Group show wide variation from patterns consistent with alkaline, within plate tectonic settings to subduction-related volcanic arc patterns. The presence of pillows in the metabasaltic volcanic rocks suggests deposition in a submarine setting. The Gueneiba Group is interpreted to consist of a disrupted ophiolite consistent with the rest of the Gorgol Noir Complex. Intrusive (?) relationships with dated granitic rocks of the Guidamaka Suite suggest a minimum age of 665±2.7Ma (Pitfield and others, 2004).

The Guidamaka Suite is a gabbro-granodiorite suite that forms the uppermost thrust slice of the Gorgol Noir Complex and is locally emplaced within the Gueneiba Group. The dominant rock type is a coarse hornblende gabbro with more felsic lithologies mostly consisting of medium to coarse tonalite-granodiorite. Gabbroic and granodioritic components grade into each other. They are mostly massive rocks that are cut by brittle fractures that are locally infilled by epidote veins. Xenoliths of metabasic schists, hornblendite and quartz-epidote rock are locally abundant and variably assimilated. Geochemical profiles are indicative of a subduction-related arc setting. A sample of microgranodiorite-tonalite gave a U-Pb zircon age of 665± .7Ma (Pitfield and others, 2004). The relationship of the gabbro-granodiorite suite to the other groups is uncertain. The gabbroic suite is intensely deformed at its margins and displays fabrics observed throughout the complex suggesting that it was emplaced prior to or early in the tectonic history. Gabbro is not a common component of the Gadel Group melange. Therefore, the gabbro and other intrusive rocks may be genetically associated with the allochthonous calc-alkaline magmatic arc represented by the Mbout Supergroup (Pitfield and others, 2004).

Based on the above descriptions of mafic and ultramafic intrusive bodies and the presence of mafic-type (Cyprus-type) VMS deposits, podiform chromite deposits, and a number of known Ni±Cu and Cu±Au occurrences in the rocks of the Gadel and Gueneiba Groups and Guidamaka Suite, the entire Gorgol Noir Complex is considered both permissive and favorable for the discovery of Ni-Cu-PGE-Cr deposits.

Numerous metallic mineral occurrences are present in the southern Mauritanides and in addition to podiform chromite include a variety of mineral deposit types such as orogenic gold (see Goldfarb and others, 2015), Guelb Moghrein-like IOCG (see Fernette, 2014), Cu-Ni-PGE-bearing magmatic sulfide deposits, and VMS deposits (see Taylor and Giles, in 2015a). Due to the recognized potential of the region, the area has been the subject of multiple exploration campaigns dating to the first surveys by the BRGM from the mid-1960s to the mid-1970s, followed by various collaborations of the OMRG with the BRGM and a German private company, Otto Gold, through the mid-1990s. In 1995, exploration rights to the M40 concession area consisting of a 20,000 square kilometer (km^2) section of the Southern Mauritanides from just north of the Bou Zrabie and Kadiar occurrences to the border with Senegal. Their work included stream sediment, panned concentrates and BLEG sample surveys, and detailed studies at 28 prospects, using shallow soil sampling, trenching/pitting, rock chip sampling, geophysical surveys and geological mapping. RC drilling (51 holes, 4,180 m) was carried out at several targets with limited diamond drilling (5 holes, 808 m) at a few localities. Over 20,000 geochemical samples were ultimately collected and analyzed (Gunn and others, 2004). As a result of these various programs, the basic geological relationships at many of the more important mineral occurrences have been documented. Below, descriptions of several of the occurrences in the Gorgol Noir Complex that are thought to be possibly of magmatic sulfide segregation Ni-Cu-PGE type are given. None of the described occurrences were visitied by the USGS during fieldwork in 2007. However, Gunn and others (2004) provide excellent descriptions of these occurrences based on their review of previous work and fieldwork during the BGS program in 2003. Their descriptions are provided below with minor modifications.

The Diaguili Occurrence

This prospect is located 6 km northeast of the village of Diaguili, in the Bakel 1:200,000 map sheet close to the international border with Senegal (fig. 22). The copper mineralization was considered by BRGM to be confined to a narrow silicified fault zone in an area of jaspilites, serpentinites, chloritic schists and siltstones exposed on two prominent hills separated by a discordant fault zone (BRGM, 1975). Drilling and other detailed surveys were conducted by BRGM in the mid-1970s. In the first phase one intercept of 23 m @ 2.08 percent Cu was reported between 47.0 and 70.25 m in a zone of oxide and sulfide mineralization. Low tenor Au anomalies were reported in drill and rock samples collected in these early stages of exploration. Subsequently General Gold International S.A. (GGISA) conducted an extensive program of detailed geochemical and geophysical surveys, followed up in 1997 by a program of nine RC holes for a total of 950 m (General Gold International, 1997). The soil geochemistry, carried out at 100 × 20 m centers over a strike length of 3 km, revealed anomalous values of Au and Cu over both the southern and northern hills. In addition significant Au values were reported in soils on the eastern flank of the grid in serpentinite and silicified 'jasperlite'. Sporadic anomalous values of Pb and Zn were also identified. The geophysical surveys included magnetics, IP and EM and identified clearly the underlying ultramafic rocks and indicated the possible presence of disseminated sulfides in one zone. The drilling was designed to test the geological, geochemical and geophysical targets around both the southern and northern hills. However, no economic gold or base-metal mineralization was identified by this drilling program. The best intercept was reported in hole PDDA1 where 450 ppb Au was reported betweeen 32–36 m in the vicinity of the significant Cu-Au intercepts reported in the BRGM campaigns of the mid-1970s. However it should be noted that the original Cu-Au values have never been replicated. The Au soil anomalies on the eastern edge of the grid identified by GGISA have not been tested and clearly merit further investigation.

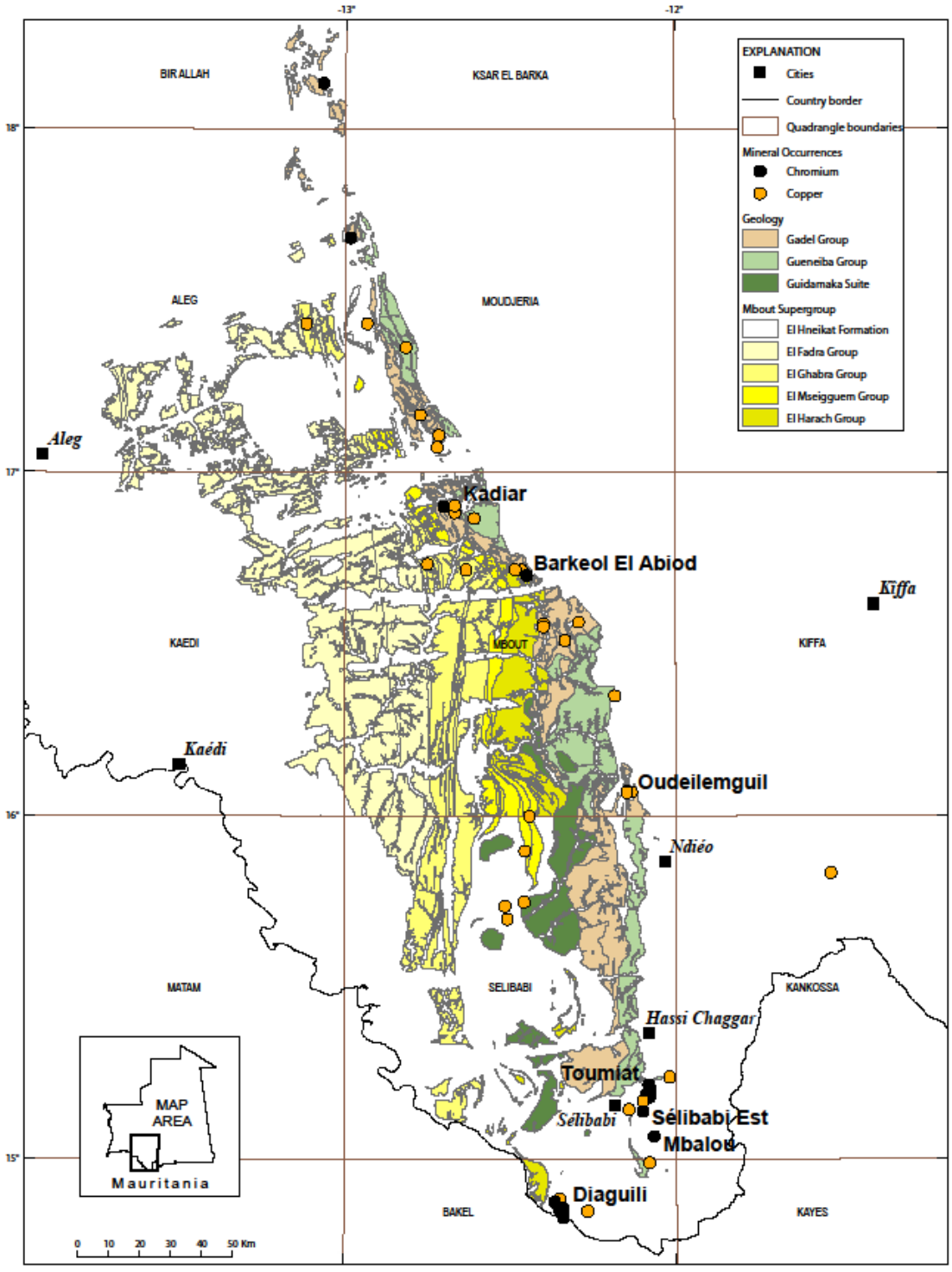

Figure 22. General geology of the southern Mauritanides showing the Mbout Supergroup, the Gorgol Noir Complex and the locations of Cr and Cu-Ni occurrences discussed in text.

The Oudelemguil Occurrence

In the course of systematic prospecting between Barkéol and Diaguili in the period 1983–1986, Otto Gold – OMRG identified numerous minor occurrences of copper chiefly in association with serpentinites and metagabbros of the Gadel Group (OMRG – Otto Gold, 1986). The most important of these discoveries were at Oudelemguil, Ndiéo and Hassi Chaggar.

The Oudelemguil prospect, discovered in 1985 by Otto Gold, is located approximately 19 km north of Oudelemguil village at 16º04'17"N., 12º08'46"W. (fig. 22). There are several Cu occurrences in this area, but the two of most interest are known as the 'Principal Occurrence' and the 'Rasi Occurrence'. Both were examined in detail by Otto Gold in 1984 and 1985, while GGISA carried out limited studies in 1996–1997.

The geology consists of a north–south-trending sequence of metasedimentary rocks enclosing structurally-controlled lenses of mafic volcanic rocks and gabbro. The succession was interpreted by GGISA as a sequence of imbricate thrust sheets with the faults marked by intense quartz veining and brecciation (General Gold International, 1997). The mineralization at the Principal occurrence is found in three narrow zones, each 2–3 m wide, extending over a strike length of about 600 m within a zone about 100 m wide. It consists of disseminations, veinlets and massive bands that follow the schistosity in the metagabbroic host rocks. The massive bands consist of malachite, calcite, quartz and talc and are 20–40 cm thick.

Otto Gold carried out IP, resistivity and magnetic surveys at Oudelemguil but failed to identify significant anomalies that indicated the presence of massive or disseminated sulfide mineralization at shallow depths. Detailed rock chip sampling was carried out at Oudelemguil and in the surrounding area by Otto Gold in 1984–1985. Average values over a width of 25 m were 1.7 percent Cu, 0.13 percent Zn, 4 ppm Ag and 0.5 ppb Au. However maximum values were 35.5 percent Cu and 400 ppm Ag, with several Au values in the range 35–75 ppb. In addition Otto Gold reported locally high values of P, W, Pb, Bi, Co and B in association with other Cu occurrences in the Oudelemguil district (OMRG-Otto Gold, 1986). These element associations suggest the possible influence of late high-level granitoid intrusions (W-Pb-Zn-Bi).

The second zone of Cu mineralization, the Rasi Occurrence, occurs 2 km southeast of the principal occurrence. Here malachite and chalcopyrite occur in lenticular bodies, oriented 340º, up to 100 m long and a few meters wide in ferruginous chloritic mafic metavolcanic rocks adjacent to a coarse-grained gabbro. Intense silicification and quartz veining accompany the copper mineralization. Limited rock chip sampling in this area by GGISA in 1996–1997 failed to identify significant Cu values, but high Au values, up to a maximum of 1,260 ppb with several others containing a few hundred ppb, were reported (General Gold International, 1997). Subsequently GGISA undertook further studies focused on gold in the area. In 1998–1999 they collected 66 stream-sediment samples from an area of 80 km^2 surrounding the Oudelemguil prospect. These samples, and associated rock chip sampling, confirmed the known Cu-Au anomalies in the area but failed to identify any new targets (Gunn and others, 2004).

The Ndiéo Occurrence

The occurrence, located eight km north-west of the village of Ndiéo, at 15º55'12"N., 12º05'33"W., was discovered by Otto Gold in 1985 (OMRG–Otto Gold, 1986) and subsequently investigated in detail in 1989-90 by Otto Gold working in conjunction with OMRG (fig. 22) (OMRG–Otto Gold, 1990). At the surface it consists of malachite and traces of chalcopyrite hosted by metagabbro close to a contact with serpentinite (Gadel Group), both of which are tectonic inclusions in a suite of quartzites and conglomerates belonging to the Djonaba Group.

The copper mineralization occurs in sporadic stringers and centimeter-scale bands in a north-trending zone about 160 m long and 1–5 m wide at surface that dips east at 35º–45º. Associated alteration consists of clay alteration of the gabbro wallrocks, together with local minor silicification and carbonatization. Average values reported in 17 rock chip samples collected in 1985 over a strike length of 140 m were 11.25 percent Cu and 49 ppb Au, accompanied by Ag values below detection.

Five trenches, total length 70 m, were excavated and sampled in detail in 1989 to investigate both the main copper zone and an altered serpentinite-gabbro-contact containing traces of probable pyrrhotite and pentlandite. Detailed geochemical data are not available, but in general, Au and Ag values were very low. In contrast, Cu grades were encouraging with a maximum of 18.2 percent Cu over a true width of 2.5 m reported in one trench. Although its strike extent is uncertain, the small size of the occurrence indicates that there is unlikely to be an economic deposit at Ndiéo. However, detailed geophysical surveys should be undertaken to investigate the possibility of Cu sulfide (±Ni, PGE) targets at depth.

The Hassi Chaggar Occurrence

The Hassi Chaggar copper occurrence is located at 15º22'35"N., 12º02'23"W., about 5 km east-north-east of the village of Hassi Chaggar, close to the eastern boundary of the Selibabi 1:200,000 map sheet (fig. 22). It has a similar structural setting to the Ndiéo occurrence, hosted by serpentinite (Gadel Group) close to a probable faulted contact with sandstones and quartzites.

The mineralization was discovered by Otto Gold in 1986 (OMRG–Otto Gold, 1990). Sampling of five mineralized outcrops gave average Cu values of 1.6 percent Cu, with a maximum Au value of 210 ppb and all Ag values less than 5 ppm. Subsequent trenching (110 m) across the exposed mineralization gave generally disappointing Cu values with the best intercept being 30 m at 0.24 percent Cu, including 0.48 percent Cu over 4 m. Associated Au values are also low with a maximum of 135 ppb. No Ag values exceeding 0.2 ppm were reported.

The mineralization consists of thin films and infillings of malachite and azurite in the serpentinite host rock associated with the development of talc, silicification, ferruginization and thin (1–2 cm) veins of asbestos. The dimensions of the mineralized bodies are unknown, but Otto Gold estimated a maximum strike extent of less than 100 m. The highest Cu values appear to be related to the most altered, talc-bearing sections of the serpentinite. This may be ascribed to hydrothermal fluid flow accompanying shearing.

Two other minor copper occurrences with associated low tenor gold enrichment were discovered near Hassi Chaggar by Otto Gold between 1984 and 1986 (OMRG–Otto

Gold, 1990). Indice 94, also referred to as Houi Damour, is located at 15º27'03"N., 12º04'04"W., about 10 km north-northeast of the village of Hassi Chaggar. The mineralization consist of scattered stringers and thin (centimeter-scale) lenses of malachite trending 160º and dipping towards the west at about 40–60º. It is hosted by chloritic schists in proximity to gabbro and serpentinite. Initial rock chip sampling (6 samples) identified Cu contents up to 15.3 percent, with maximum Au and Ag values of 540 ppb and 4.5 ppm, respectively. Subsequently three trenches, total length 20 m, were excavated in 1989–1990. Channel sampling of these trenches yielded average grades of 2.1 percent Cu and 130 ppb Au over a true width of about 1.5 m. The mineralization has a strike length of about 100 m and is associated with strong silicification and development of Fe oxides. The second occurrence identified by Otto Gold, known as Occurrence 79 or Oued Moudjeri, is located 3 km west-north-west of Hassi Chaggar. Initial rock chip sampling revealed up to 24.2 percent Cu and 1,000 ppb Au, although these are not regarded as representative typical values. Subsequent channel sampling of four trenches (total length 29 m) across the main mineralized zones revealed Cu values in the range 1.5–3.0 percent with Au of 0.8–1.5 ppm. The mineralization consists of scattered disseminations and stringers of malachite and subordinate chalcopyrite distributed along the foliation in the host schistose serpentinite, talc schists and chlorite schists. The schistosity trends 110º and dips towards the south at 75º. The largest mineralized zone, about 100 m long and 30–80 cm thick, has an average Cu content of approximately 2.5 percent. The copper mineralization is accompanied by strong silicification and locally by the development of magnetite and hematite.

The economic potential of the known copper occurrences in the vicinity of Hassi Chaggar village is poor on account of their small size. Furthermore, high Cu and Au values reported in surface samples have probably been enriched by supergene processes and should be treated with caution. Nevertheless these occurrences demonstrate the effectiveness of local structurally controlled hydrothermal processes in producing elevated levels of both copper and gold. PGE may also be enriched in this setting and samples of the exposed mineralization should be checked for PGE anomalies.

The Diagiuli Chromite Occurrence and Other Small Occurrences in the Southern Mauritanides

A few small occurrences of podiform chromite are known in the southern Mauritanides in association with the serpentinites of the Gadel Group. These are located in the north near Moudjeria and in the south near Diaguili and Selibabi. The only descriptions of these occurrences available are those produced by BRGM in the late 1960s and summarized in the 1975 Mineral Plan (BRGM, 1975). USGS field work in 2007 examined the Mbalou podiform chromite occurrence.

The most important podiform chromite occurrences are located near the village of Diaguili, on the Bakel 1:200,000 map sheet. The principal one, 5 km east of Diaguili, at 14º51'00"N., 12º21'00"W., consists of discontinuous steeply dipping lenses of chromitite exposed over a strike length of approximately 500 m, oriented north–south. The largest individual body is 55 m long, with an average thickness of 3 m. Two other lenses exceed 10 m in length. The lenses and the enclosing serpentinite are strongly tectonized and folded. The average grade reported from this locality is 25.5 percent Cr_2O_3 with Cr/Fe 1.61. The vertical extent of the chromite is limited: two boreholes drilled to intersect the

chromitite at 25 m below the ground surface encountered only barren serpentinite. A second occurrence, about 4 km northeast of Diaguili, consists of blocks of chromitite over an area of 80 × 15 m, without any bedrock exposure. The average grade of this material is 34.3 percent Cr_2O_3.

Other small occurrences of chromite occur in serpentinites of the Gadel Group near Sélibabi. The Mbalou podiform chromite occurrence is located approximately 15 km southeast of Sélibabi, at 12º04'W., 15º04'N., on the Sélibabi 1:200,000 map sheet (fig. 22). Several pods of chromitite and scattered chromitite blocks occur over an area of about 100 × 25–30 m including one small exposure (fig. 23). The pods are up to three meters in length. Three trenchs around 10-m long that cross two pods reveals average Cr_2O_3 values are 41.7 percent, with Cr/Fe of 1.8. At Toumiat, 13 km northeast of Sélibabi, chromitite boulders occur over a small area within a serpentinite body. BRGM reported Cr_2O_3 values of 28 percent and Cr/Fe of 1.23 at this locality.

A few small chromite occurrences, mostly loose float blocks, occur associated with serpentinite masses in a similar setting to the west-northwest of Moudjeria, in the Bir Allah 1:200,000 map sheet. The largest body, at Gouerarate (13º04'00"W., 18º08'00"N.), consists of an exposed lens 10 m long and up to 4 m wide. The Cr_2O_3 contents of four samples reported by BRGM are in the range 21.5–36.7 percent Cr_2O_3.

In the southern Mauritanides several ultramafic and serpentinized rock units are mapped within the Gadel and Gueneiba Groups, both of which are obducted ophiolite segments of the Gorgol Noir Complex. In general the RTP magnetic anomaly map shows a speckled pattern of high frequency magnetic anomaly highs and lows in the region (fig. 24). Multiple broad magnetic anomaly highs trending east-northeast are also present. These anomalies are interpreted to reflect deeper, basement rocks trending into and below the sedimentary rocks of the Taoudeni Basin (Finn and Anderson, 2015). The high frequency RTP magnetic anomaly highs spatially correlate with the mapped ultramafic and serpentinized rock units. The RTP magnetic anomaly lows may be related to schists and metapelitic rocks within the mapped unit. The analytic signal also shows strong spatial correlation with mapped ultramafic and serpentized rock units. Several northerly trending analytic signal highs are widespread within the southern Mauritanides. These linear belts are on the order of 10 to 20 km long and are interpreted to reflect ultramafic and serpentinized rock in the southern Mauritanides and help delineate permissive tracks for Ni-laterite deposits that are associated with the weathering of such rocks (fig. 24).

Figure 23. Photograph showing chromite pods at the Mbalou podiform chromite occurrence. The occurrence is hosted in serpentinized rock of the Gadel Group. USGS photo.

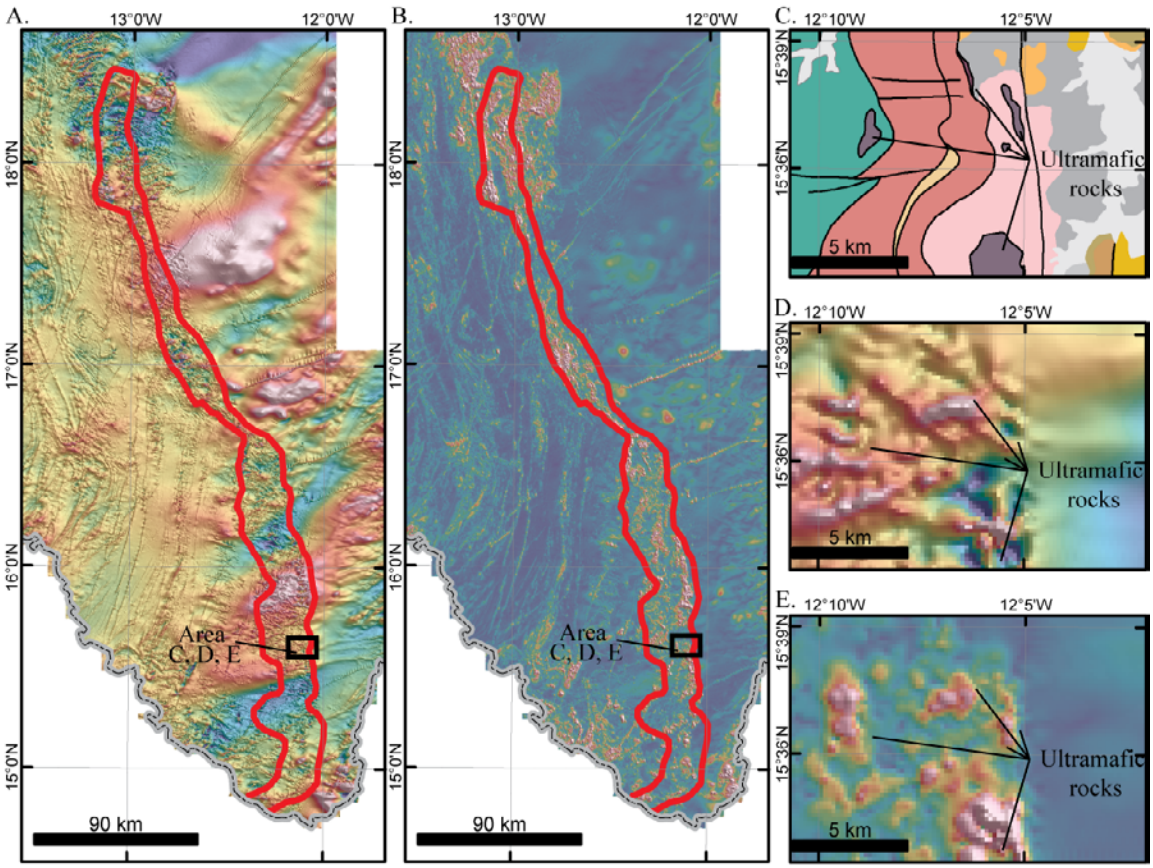

Figure 24. Maps showing aeromagnetic signature of ultramafic rocks in the southern Mauritanides. Red outline encloses rocks of the Mauritanide orogen. *A,* Reduced-to-pole (RTP) magnetic anomaly map. Ultramafic and serpentinized rock are shown as high frequency magnetic anomaly highs. The broad, east-northeast trending magnetic anomaly highs are interpreted as reflecting basement rock. Magnetic highs and lows are shown as warm and cool colors, respectively. *B,* Analytic signal of the RTP data. Ultramafic and serpentinized rock are highlighted and the broad east-northeast anomalies evident in the RTP data are suppressed. Analytic signal highs and lows are shown as warm and cool colors, respectively.*C,* Geologic map of an area within the southern Mauritanides showing distribution of ultramafic rock. *D*, RTP magnetic anomaly map showing detailed high frequency magnetic anomalies associated with ultramafic rock. *E,* Analytic signal highlighting the ultramafic rocks in the southern Mauritanides. *A* and *B* are the same extent. Black box on *A* and *B* shows the extent of *C*, *D*, and *E*.

3.6 Mafic-Ultramafic Sills, Dikes, Laccoliths, and Chimneys of Mauritania

Numerous intrusions of mafic-ultramafic composition and varying morphology are widespread throughout all of the physiographic domains of Mauritania with the exception of the Coastal Basin. They are particularly abundant within the Rgueïbat Shield where several generations of primarily mafic dikes have been recognized in addition to the amphibolites, metagabbros, and ultramafic rocks already described. The majority of the dikes are tholeiitic microgabbros and gabbros with subordinate basalts. Within the Archean shield, both pre- and post-metamorphic dike swarms are defined and the Paleozoic portion of the shield is cut by numerous post-Birimian dikes (Lahondère and others, 2003; Pitfield and others, 2004).

The Archean shield shows a long history of dike emplacement especially in the northwestern portion in the Tasiast-Tijirit and Choum-Rag el Abiod terranes, however, the early premetamorphic dikes are volumetrically insignificant. These include metamafic dikes in Mesoarchean migmatitic gneisses and uncommon anorthositic dikes within the Choum-Rag El Abiod terrane. Post-metamorphic dikes are the most volumetrically important and are most concentrated in a swarm of NE-trending dikes. These are locally so abundant that little of the country rock is exposed, whereas elsewhere dikes are sparse. The emplacement pattern may be directly related to the structure of the country rock. Dikes are abundant in the highly strained zones of foliated gneisses, but are less abundant in lenses of low-strain lithologies such as granites, and migmatitic or charnockitic gneisses. Dikes intruded into the high strain zones are typically narrower than those in the low strain zones. In general, the dikes are oriented NW and NE with the dominant dike trend oriented NE-SW. In the greenstone belts, dikes tend to be oriented NNE parallel to local shear zones. The western margin of the major swarm of NE-trending dikes occurs in the center of the Chami 1:200,000 map sheet. Its eastern margin is concealed beneath sedimentary rocks of the Taoudeni Basin (fig. 25; Pitfield and others, 2004).

Pre- and syn-metamorphic dikes consist of linear anorthosite dikes, dike-like amphibolitized gabbro to microgabbro intrusions, and megacrystic basaltic dikes associated with megacrystic lavas in greenstone belts in the Ahmeyim 1:200,000 scale map sheet. The anorthosites are massive, medium to coarse grained, and consist of >85 percent plagioclase, predominantly andesine, with variable amounts of hornblende. Primary pyroxene (diopside) is replaced by hornblende with accessory sphene, magnetite, rare rutile and zircon with secondary chlorite, zoisite epidote, hornblende, and minor disseminated sulfides. Emplacement of these rocks predate emplacement of the Touijenjert granite complex. The amphibolitized gabbro-microgabbro dikes are medium to coarse grained, dark green to black and are composed of variable amounts of plagioclase, actinolite and relic pyroxene. Virtually all of the pyroxene has been replaced and largely pseudomorphed by green actinolitic amphibole. Geochemically these rocks are very similar to the Ahmeyim Great Dike (described below). The megacrystic basalt dikes were emplaced in the greenstone belts and commonly have an intense shear fabric. They are dominantly composed of actinolite (≥75 percent) with subordinate amounts of plagioclase and clinozoisite and accessory sphene and opaques (Pitfield and others, 2004).

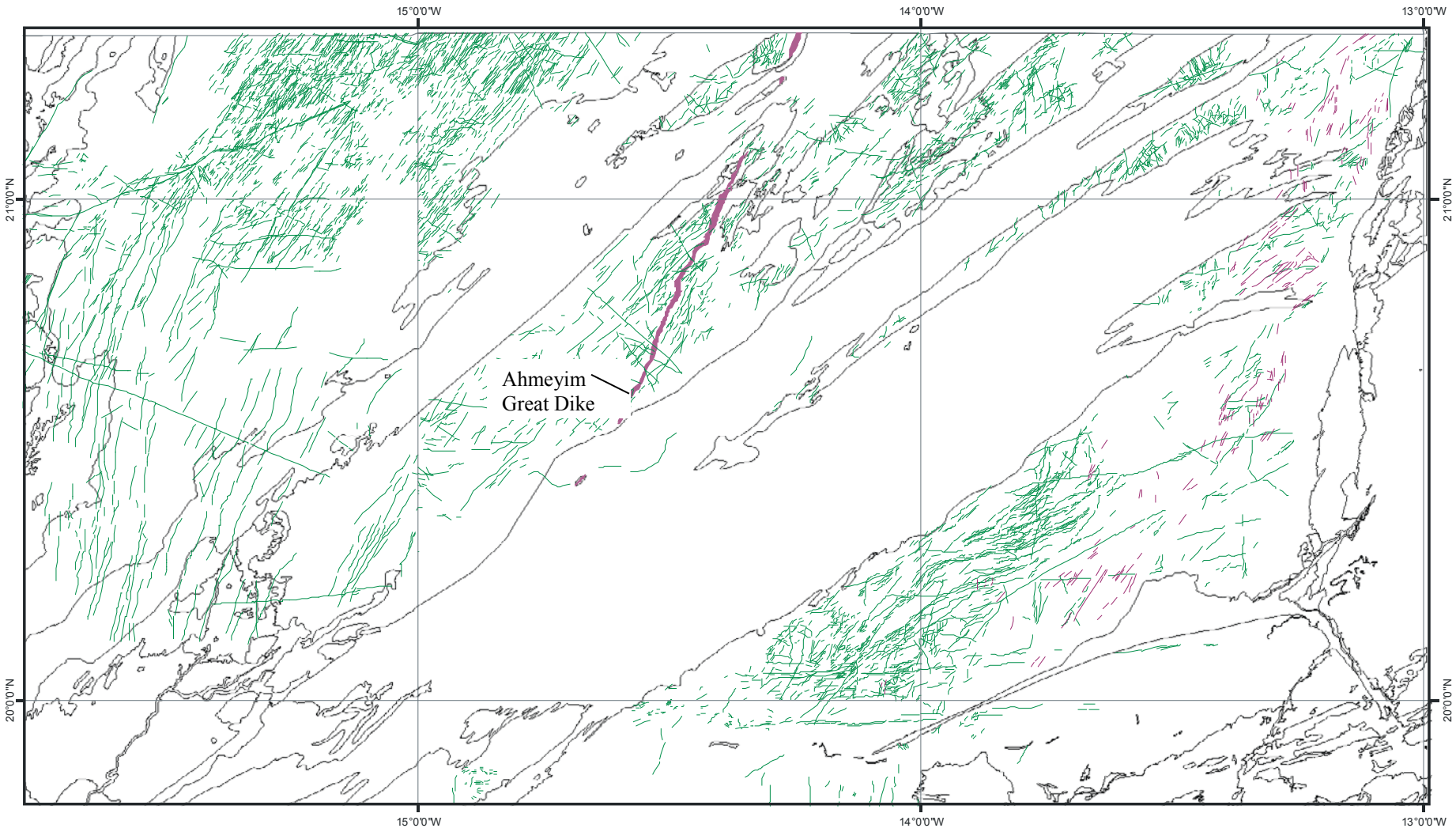

Figure 25. Distribution of dikes in the northwestern portion of the Archean Rgueïbat Shield. Basic dikes are shown in green, anorthosite dikes in the Choum-Rag el Abiod terrane are shown in purple, and the Ahmeyim Great Dike is shown in violet (from Pitfield and others, 2004). Black lines indicate mapped geology.

Post-metamorphic dikes are widespread and are of four types: (1) E-W oriented gabbroic dikes that locally form small hills are located in the southern part of the Atar and Ahmeyim and the Akjoujt 1:200,000 map sheets. They consist of labradorite, pigeonite, hypersthene, augite, sericite and epidote. The E-W dikes are cut by a series of N-S oriented microgabbro dikes and by fissile basic dikes oriented NE-SW. They are also cut by major (commonly mylonitised) NE-SW faults. (2) Fissile basic dikes oriented NNE to NE (dated at 1,949±9 Ma) are the most common and form a major dike swarm through the Choum-Rag El Abiod Terrane and the eastern half of the Tasiast-Tijirit Terrane. The swarm continues northwards into northern Africa. Individual dikes are mostly up to 10 m in thickness although a number of approximately 30-m-thick dikes are present. The dikes have gently curvilinear traces, locally bifurcate and also form an en echelon array in the NW within the main swarm. The majority of dikes are massive, unaltered basalts or microgabbros. They cut the Touijenjert granites and the basal sandstones of the Taoudeni Basin and unconformably overlie the dikes, showing that most are Precambrian in age. The dikes have sharp contacts with their host rocks. (3) N-S and E-W to ENE-WSW trending gabbro dikes are less abundant than the other two dike sets. They form linearly persistent outcrops that can be traced for great distances.Individual ENE-WSW gabbroic dikes (such as the Agada Dike) may be traced for up to several hundred kilometres throughout the western Rgueïbat Shield. The Touyerma Dike in the southern part of the Atar sheet has provided an age of about 1,500 Ma (Dosso and others, 1979). The general, outcrop pattern is rectilinear with dikes intersecting at 90°. In general the N-S and E-W dikes are medium to coarse grained and the ENE-WSW dikes are fine grained. The N-S and ENE-WSW suites of dikes consist of gabbros that are commonly in excess of 20 m wide and rare basalts that are often less than 10 m wide. NE-SW and also NW-SE dikes typically 8–12 m wide are abundant in the Tasiast-Tijirit region. (4) Layered gabbronorite, leucogabbro and gabbrodiorite of the Ahmeyim Great Dike. A major feature of the Tasiast-Tijirit Terrane is a large 030º-trending dike that can be traced for over 100 km before disappearing under sand at both ends. It is up to 4 km thick and exhibits strong vertical layering at its northern end that may suggest it is a compound intrusion. The main lithology is a massive, coarse-grained, equigranular, massive orthopyroxene-gabbro and less common microgabbro. A leucogabbro facies is common (notably on its western side in southernmost exposures) with abundant feldspar. Two pyroxenes and amphibole are locally visible in hand specimen. The gabbros and gabbrodiorites are amphibolitized and consist of sericitized plagioclase and actinolite, which locally contains fresh relics of clinopyroxene and minor amounts of chlorite, quartz, and opaque oxides. Sulfides are conspicuously absent (Pitfield and others, 2004).

Tait and others (2013) have recently obtained a precise age of 2,733±2 Ma (U-Pb baddeleyite) for the Ahmeyim Great Dike. Their work notes the boninitic nature of the Great Dike and suggests that the Dike is part of an Archean Large Igneous Province (LIP) that was present beneath and invaded the West African Craton. Similar ages obtained for gabbroic and other rocks of the Iguilid metagabbro in the Amsaga terrane provide a link to the anorogenic magmatic event that followed granulite facies metamorphism in the Archean Rgueïbat Shield and suggests that the anorogenic melting event was related to LIP underplating of the Archean Rgueïbat Shield. Significantly for Ni-Cu-PGE exploration in the Archean shield, Tait and others (2013) note similarities in

size and composition of the Ahmeyim Great Dike with the younger Great Dike of Zimbabwe. They suggest that the Ahmeyim Great Dike magmas may have been Cu-enriched compared with Primitive Mantle values (using Cu/Zr ratios as a proxy for sulfide accumulation and removal) and may have Ni concentrations similar to or lower than typical continental flood basalts. This suggests that the magmas that formed the Great Dike were fertile and may have undergone sulfur saturation and removal of immiscible magmatic sulfides at some point during its history. In addition to the obviously underevaluated potential of the Ahmeyim Great Dike itself, similar potential must be assumed to apply to other smaller subparallel dikes belonging to this suite throughout the Archean shield (Tait and others, 2013).

BRGM workers in the Paleoproterozoic portion of the Rgueïbat Shield document two types of basic dikes that crosscut all but the very latest phase of granitic magmatism related to the Birimian orogeny (Lahondère and others, 2003). The most common type of dike consists of gabbroic rocks defined alternatively as dolerites or diabases that are generally hydrothermally altered. These dikes are occasionally rich in feldspar (aluminous gabbro), and exibit chloritization and saussuritization of plagioclase. The second type of dikes are andesitic rocks with textures similar to lavas and distinctive textural features including sheaf-textured pyroxene microlites and corneal clinopyroxene rims surrounding phenocrystic orthopyroxenes. Compositionally, the second type of dikes are magnesian andesites or boninites. BRGM authors state that a latest Birimian age for the majority of these dikes is well established based on commingling relationships between latest Birimian granites and gabbroic dikes as well as crosscutting relationships between the dikes and the latest Birimian episode of pegmatite and aplite dikes emplaced at approximately 2,020 Ma (Lahondère and others, 2003). Dike swarms are particularly well developed on the Tourassin, Gleïbat Tenebdar and Bel Guerdan 1:200 000 scale map sheets. In the Tourassin map sheet the dikes are generally oriented NNW-SSE or NE-SW and are localised to the south and north of parallel 24°35'N., respectively. On the Gleïbat Tenebdar map sheet, most dikes are oriented NNE-SSW with a N-S component or NE-SW with an ENE-WSW component. In the northwestern quadrant of the Bel Guerdan map sheet NE-SW or ENE-SSW oriented dikes are very abundant. In general, all of the dikes are relatively small with widths in meters to tens of meters. They show up well in Landsat imagery and are generally linear, rectilinear, or gently arcuate in shape with lengths of tens to hundreds of meters (Lahondère and others, 2003).

In detail, the latest Birimian dikes range from ultrabasic to intermediate composition and include picrobasalts, basalts, trachybasalts, basaltic andesites and basaltic trachyandesites. The ultrabasic rocks are in the compositional domain of komatiites, however, coarse grain size in these rocks are suggestive of cumulate textures. In general, the suite of latest Birimian dikes are strongly heterogeneous in composition but are primarily subalkaline in nature. They generally exhibit subduction related volcanic arc signatures probably inherited from melting of the Birimian crust (Lahondère and others, 2003).

Numerous post-tectonic basic dikes cut the Mauritanide belt in the central and southern Mauritanides in addition to the mafic-ultramafic intrusions of the Gorgol Noir Complex described above. They are more numerous and widespread in the Central Mauritanides where dikes less than approximately 3 m thick are present but are too small to map unless they occur as closely spaced swarms (Pitfield and others, 2004). A large

number of N-S to NNE-SSW-trending dikes cut across the Akjoujt nappe pile and associated thrust boundaries. A subordinate NE-SW-trending set commonly follow late faults. Dikes of both trends cut the parautochthonous sediments of the Nouatil Group to the north and east of the Akjoujt nappe pile. The dikes are predominantly basic and depending on their size range from gabbro through microgabbro to basalt. Many of the thicker dikes consist of a coarse- grained gabbro interior that grades outward through microgabbro to basaltic chilled margins. A prominent swarm of N-S trending microgabbro dikes cut the western side of the Akjoujt nappe pile. In a 2.75 km E-W section, the BGS logged 12 dikes ranging in thicknesses from 2 to 45 m (Pitfield and others, 2004).

Post-tectonic basic dikes in the southern Mauritanides cut all major units but are concentrated in a main N-S trending swarm about 15–20 km wide along the 13ºN meridian through rocks of the El Fadra Group. To the east, dike trends become more scattered, with trends of E-W, NW-SE, and NE-SW present cutting rocks of the Gorgol Noir and the parautochthon. All of the dikes consist of massive microgabbro that varies from nearly pristine olivine gabbro to amphibolitized gabbro in which all of the pyroxene and olivine has been replaced and pseudomorphed by actinolite (Pitfield and others, 2004).

Mafic intrusions of Lower Jurassic age occur over extensive areas of both the northeastern and southeastern sections of the Taoudeni Basin.They consist of sills and sheeted complexes, dikes, laccoliths, and chimneys that intrude the Neoproterozoic to Cambrian sedimentary rocks and are overlain by the Nema Group of Middle to Upper Jurassic age. Although not directly dated, a hornblende-bearing granophyric microgranite dike that crosscuts the Akjoujt nappe pile yielded a U-Pb zircon age of 199.1±3.6Ma (Pitfield and others, 2004). These mafic intrusions are a component of the Central Atlantic Magmatic Province (CAMP), the 200 Ma tholeiitic dikes, sills, and lava flows associated with the breakup of Pangea (Marzoli and others, 1999), which included a LIP melting event related to opening of the Atlantic Ocean. They are predominantly composed of gabbro and microgabbro with lesser diorite and are cut by veins of leucogranite. In both areas as well as the border region south of Ayoun El Autrous these intrusions are associated with numerous Cu ± Au occurrences of unknown type that could be a variety of deposit types including sedimentary copper, epithermal vein, or magmatic segregations (similar to the Norilsk type; see Taylor and Giles, 2015c).They are included here as permissive for magmatic Cu-Ni- (PGE, Co-Au) deposits, provided that large conduits or feeder dikes can be located (see below). Further work will be required to determine whether they may have economic significance. Chimneys are notable features of the Chegga region in the northeastern Taoudeni Basin where they protrude above the sedimentary rocks and localize several minor copper occurrences (Chegga Guettatira, Kreb en Naga, Kreb en Naga SW; described in Taylor and Giles, 2015c). In the southeastern Taoudeni, two major massifs (the Amourj and Agouenit massifs) consisting of coalescing sills or laccoliths make up the hilly region to the south and southwest of the village of Nema. At least one copper occurrence is associated with these laccolith massifs (Nejam-Medroume; Taylor and Giles, 2015c).

In summary, there appears to be at least three and probably four generations of mafic dike emplacement within Mauritania: (1) a late Mesoarchean to Neoarchean event (approximately 2,750 Ma) related to anorogenic magmatism and deep crustal melting

beneath the Tasiast-Tijirit and Choum-Rag el Abiod terranes, (2) a Paleoproterozoic (≥1,500 Ma) suite that was emplaced following the Birimien orogeny, (3) a Late Neoproterozoic to Early Cambrian (570–550 Ma) suite emplaced during the period of uplift and cooling following the Pan African 1 event and immediately prior to the onset of the Pan African II event, and (4) a Lower Jurassic (200 Ma) suite related to the CAMP emplaced during proto-Atlantic rifting.At present, only the basic dikes of Jurassic age that cut sedimentary strata in the Taoudeni Basin are known to be associated with minor metallic mineral occurrences. Due to their small size and lack of evidence for differentiation or layering, they are generally regarded as unlikely to be permissive of significant economic accumulations of magmatic sulfides. However, a few larger dikes that exhibit layering and other favorable geochemical characteristics, such as the Ahmeyim Great Dike are present. These larger dikes have untested potential for Ni-Cu-PGE-Cr deposits.

4 Permissive Tracts for Ni, Cu, PGE, and Cr Deposits in Mafic-Ultramafic Rocks in Mauritania

Based on the USGS synthesis of PRISM data for the chromium and Cu-Ni (± Co, Au) potential of Mauritania, tracts considered permissive for deposits broadly classified as mafic-ultramafic-hosted deposits are shown on figure 26. Criteria for the delineation of these tracts is based upon permissive geology as described in BGS (Gunn and others, 2004; Pitfield and others, 2004) and BRGM (Marot and others, 2003) reports and is broken out primarily at the complex or suite level or group level and at the formation level where possible. A second major criteria for selection of tracts is the distribution of known occurrences of chromite, asbestos, copper, and nickel where they are hosted within permissive host rocks.There are currently no occurrences containing PGE's listed in the Mauritanian National Inventory of Mineral Occurrences. Eight tracts are defined as follows: In the Mesoarchean rocks of the southwestern Rgueïbat Shield, (1) a tract is drawn that is permissive for Ni-Cu-PGE deposits within the supracrustal sequences currently lumped into the Lebzenia Group in the Tasiast-Tijirit terrane.More specifically, the Sebkhet Nich Formation and the correlative Talhayet Formation encompasses the currently known mafic volcanic sequences and associated ultramafic rocks within the greenstone belts and are host to known nickel and asbestos occurrences. This tract encompasses the seven separate greenstone belts of the Tasiast-Tijirit terrane and their extension under cover based upon aeromagnetic data represents the total area regarded as permissive of ultramafic rock-hosted deposits. Mapped areas of either the Sebkhet Nich or Talhayet Formations represent more favorable areas for the occurrence of such deposits, (2) A tract is drawn upon the Amsaga Complex of the Choum-Rag El Abiod terrane, representing an area of potential for chromite and Cu-Ni-PGE deposits in layered ultramafic complexes, (3) In the Inchiri district of the central Mauritanides, a separate tract is drawn on the Mesoarchean Saouda Group of the Choum-Rag El Abiod terrane,(4) In the Akjoujt nappe pile of the Inchiri district a tract is drawn that includes the mafic-ultramafic intrusive rocks of the Agoualilet Group, the Amleila Suite (currently mapped as a correlative of the Guidamaka Suite) and the Adam el Bouje Formation, Treïfiyat Formation, Toueirja Subgroup, and the Akjoujt Formation, (5) in the Mesoarchean portion of the Rgueïbat Shield, a tract is drawn in the Zednes map sheet and represents an

area of potential for chromite and Cu-Ni-PGE deposits in ultramafic complexes similar to those described in the Amsaga Complex.This tract is drawn upon rocks of the Zednes Suite and the Temmimichate Tsabya Complex, (6) In the Paleoproterozoic portion of the northwestern Rgueïbat Shield, a tract is drawn collectively upon specific mapped mafic-ultramafic rock units of the Gleibat Tenebdar and Adam Anajim Suites, and the Adam Esseder, Rich Anajim, Aguelt abd el Maï, and the Tsalabia el Khadra Complexes that together, represent small widespread targets that are permissive for occurrences of the Alaska/Urals-type annular ultramafic complexes in a large area of the Paleoproterozoic shield. Specific mapped subunits include: the RAam subunit in the Rich Anajim Complex, the MAam subunit in the Aguelt abd el Maï Complex, the KHpx subunit in the Tsalabia el Khadra Complex, the TGgb subunit in the Tmeïmichatt Ghallamane Complex, the GTrg subunit in the Gleibat Tenebdar Suite, and the AEgb subunit in the Adam Esseder Complex, (7) In the southern Mauritanides, a tract is drawn upon the Gorgol Noir Complex, an ophiolite mélange composed of a structurally complex assortment of mafic volcanic rocks and sediments juxtaposed with gabbros and ultramafic rocks.The majority of the deposits within this tract occur in the Gadel Group with the remainder in the Gueneiba Group. Intrusive rocks of the Guidamaka Suite are also considered permissive and are included in the tract, (8) Finally a very large and poorly constrained tract is drawn upon mafic intrusions of Lower Jurassic age that occur over extensive areas of both the northeastern and southeastern sections of the Taoudeni Basin.Rocks within this tract consist of Jurassic intrusive rocks defined by the designators Md and Mg. They are associated with poorly understood copper occurrences that are probably related to hydrothermal activity during intrusion of the dikes, sills, laccoliths, and chimneys and due to their generally small size and lack of layering or differentiation are regarded as having relatively low potential. Similarly small and widespread sills and dikes of multiple ages related to several episodes of LIP magma generation are present throughout the Rgueïbat Shield and Mauritanide belt. They are also shown on the map, however, the vast majority of them are regarded as having very low potential for hosting economic Ni-Cu-PGE-Cr-bearing magmatic sulfide segregation deposits. Only a very small subset of larger dikes related to these dike swarms, such as the Ameyim Great Dike, are regarded as having potential for economic deposits.

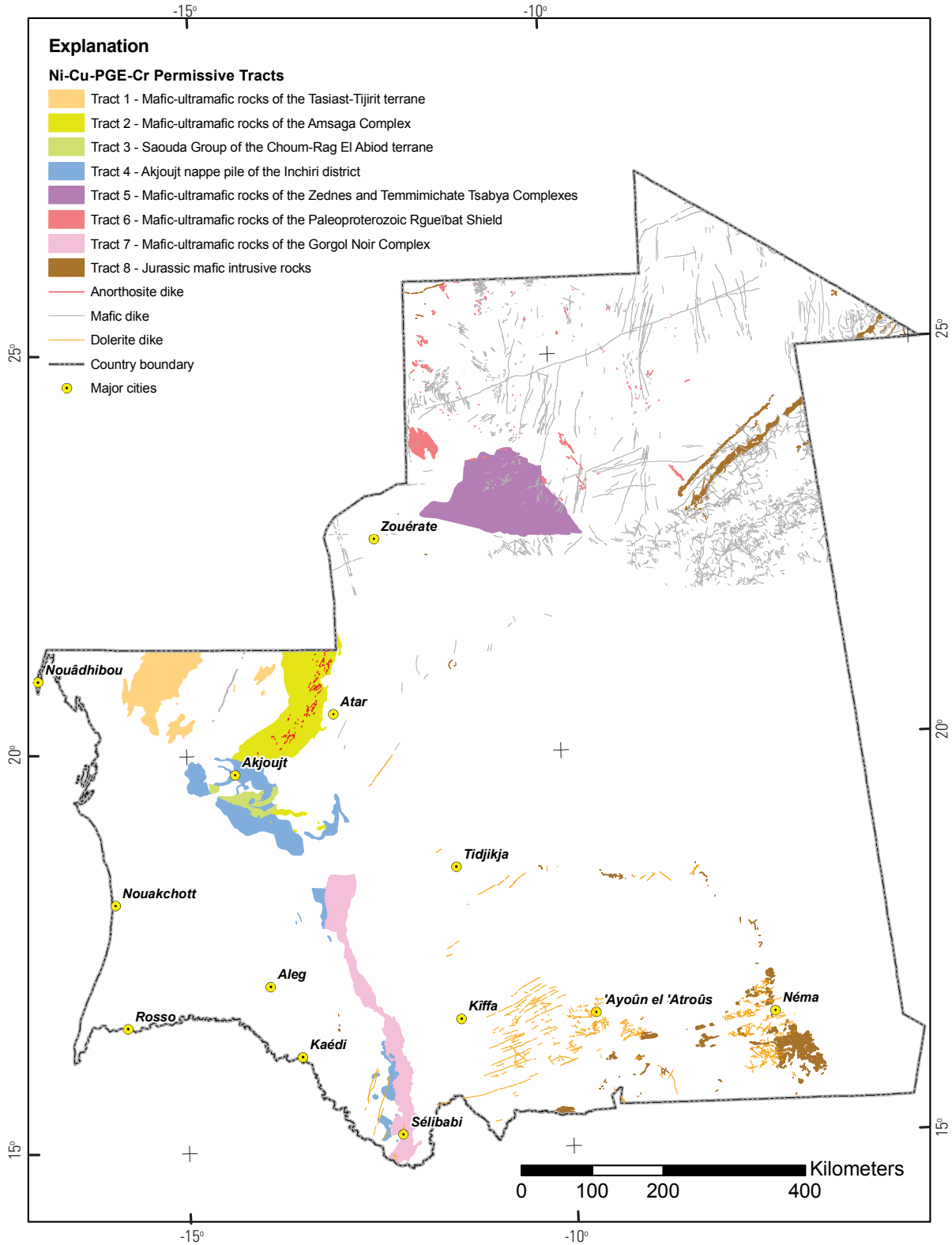

Figure 26. Permissive geology for Ni-Cu-PGE-Cr deposits in mafic-ultramafic rocks in Mauritania.

Table 3. Chromium and nickel occurrences in the Mesoarchean Zednes Suite and Temmimichate Tsabya Complex of the Rgueïbat Shield. Descriptions from Marsh and Anderson (2015).

Name	Metals Detected	Host Complex	Host Lithology	Descriptive Comments
Bir el Bardi	Cr + Ni	Zednes	Archean ultramafic intrusive complex	Birbirite.
Erg el Harach Est	Cr + Ni	Zednes	Archean ultramafic intrusive complex	Birbirite.
Adam Tahla	Cr	Zednes	Birrimian conglomerate	Silica-cemented conglomerate close to the Tenoumer circular structure consisting of serpentinite, rhyodacite, and granite
Tmeimichat Tsabya	Cr + Ni	Zednes	Archean ultramafic intrusive complex	Anorthosite complex; 8 km long birbirite. XY location imprecise. Birbirite found in regolith by USGS in 2007. No visible chromite.
Zednes Sud Ouest	Cr + Ni	Temmimichate Tsabya	Archean ultramafic intrusive complex	Birbirite. No visible chromite.
Zednes, Est	Cr + Ni	Temmimichate Tsabya	Archean ultramafic intrusive complex	Birbirite.
Tmeimichat SW	Cr + Ni	Temmimichate Tsabya	Archean ultramafic intrusive complex	Birbirite. XY location imprecise. Occurrence not found by BRGM in 2004.
Zemlet Mrekba	Cr + Ni	Aguelt abd el Maï	Archean mafic-ultramafic intrusive complex	Circular intrusive complex with gabbro, troctolite, pyroxenites; chloritic amphibolite crosscut by pegmatitic quartz veins.
Unnamed	Ni	Aguelt abd el Maï	Archean gneiss and ferruginous quartzite	Foliated gabbro/troctolite. Lattice-textured silica-carbonate-garnierite covers several hundred m².

5 Conclusions

Potential for PGE's, chromium, and Cu-Ni (± Co, Au) deposits in Mauritania exists within mafic-ultramafic rocks in several areas of the Rgueïbat Shield, the central and southern Mauritanides, and in association with Jurassic mafic intrusive rocks of the northeastern and southeastern Taoudeni Basin. Eight permissive tracts have been drawn based upon permissive geology at the complex, suite, group, or formation level and upon specific mapped subunits of mafic-ultramafic intrusive rocks within the larger units where applicable. The distribution of known occurrences thought to belong to several types of mafic-ultramafic hosted, magmatic segregation class of deposits are described and highlighted when present within each of the defined permissive tracts.

6 References

Ahmed, A.H., Arai, Shoji, Abdel-Aziz, Y.M., Ikenne, Moha, and Rahimi, Abdellatif, 2009, Platinum-group elements distribution and spinel composition in podiform chromitites and associated rocks from the upper mantle section of the Neoproterozoic Bou Azzer ophiolite, Anti-Atlas, Morocco: Journal of African Earth Sciences, v. 55, p. 92–104, doi:10.1016/j.jafrearsci.2009.02.005.

Albers, J.P., 1986, Descriptive model of podiform chromite, *in* Cox, D.P., and Singer, D.A., eds., Mineral deposit models: U.S. Geological Survey Bulletin 1693, p. 34.

Arai, Shoji, 1992, Chemistry of chromian spinel in volcanic rocks as a potential guide to magma chemistry: Mineralogical Magazine, v. 56, p. 173–184.

Arif, Mohammed, and Qasim Jan, M., 2006, Petrotectonic significance of the chemistry of chromite in the ultra-mafic complexes of Pakistan: Journal of Asian Earth Sciences, v 27, issue 5, p. 628–646.

Ba Gatta, A., 1982, Contribution à l'étude géologique et minéralogique du gissement d'Akjoujt (Mauritanie): Universite d'Orleans, Ph.D. dissertation, 162 p.

Baranov, Vladimir, and Naudy, Henri, 1964, Numerical calculation of the formula of reduction to the magnetic pole: Geophysics, v. 29, issue 1, p. 67–79, doi: 10.1190/1.1439334.

Barnes, D.F., 1986, Gravity data indicate large mass and depth of the gabbro body at Haines, *in* Bartsch-Winkler, Susan, and Reed, K.M, eds., Geologic studies in Alaska by the U.S. Geological Surveyduring 1985: United States Geological Survey, Circular 978, p. 88–92. [Available at http://pubs.er.usgs.gov/publication/cir978.]

Barnes, S.J., 2006, Komatiite-hosted nickel sulfide deposits—Geology, geochemistry, and genesis: Society of Economic Geologists Special Publication, v. 13, p. 51–118.

Blakely, R.J., 1995, Potential theory in gravity and magnetic applications: Cambridge University Press, 441 p.

Blakely, R.J., Jachens, R.C., Simpson, R.W., and Couch, R.W., 1985, Tectonic setting of the southern Cascade Range as interpreted from its magnetic and gravity fields: Geological Society of America Bulletin, v. 96, p. 43–48.

Blakely, R.J., and Simpson, R.W., 1986, Approximating edges of source bodies from magnetic or gravity anomalies: Geophysics, v. 51, no. 7, p. 1494–1498.

Bradley, D.C., O'Sullivan, Paul, Cosca, M.A., Motts, H.A., Horton, J.D., Taylor, C.D., Beaudoin, Georges, Lee, G.K., Ramezani, Jahan, Bradley, D.B., Jones, J.V., and

Bowring, Samuel, 2015, Synthesis of geological, structural, and geochronologic data (phase V, deliverable 53), chap. A *of* Taylor, C.D., ed., Second projet de renforcement institutionnel du secteur minier de la République Islamique de Mauritanie (PRISM-II): U.S. Geological Survey Open-File Report 2013–1280-A, 328 p., http://dx.doi.org/10.3133/ofr20131280/. [In English and French.]
Brew, D.A., Karl, S.M., Barnes, D.F., Jachens, R.C., Ford, A.B. and Horner, R., 1991, A northern Cordilleran ocean-continent transect—Sitka Sound, Alaska, to Atlin Lake, British Columbia: Canadian Journal of Earth Science, v.28, 840–853.
Buddington, A.F., and Chapin, Theodore, 1929, Geology and mineral deposits of southeastern Alaska: U.S. Geological Survey Bulletin 800, 398 p.
Bureau de Recherches Géologiques et Minières (BRGM), 1975, Plan Minéral de la République Islamique de Mauritanie: Ministere de la Planification at du Développement Industriel, June 1975, 554 p.
Butt, C.R.M., 2005, Geochemical dispersion process and exploration models: Canberra, Cooperative Research Center for Landscape Environments and Mineral Exploration (CRCLEME). [Available at http://www.crcleme.org.au/RegExpOre/6-models.pdf.]
Cabri, L.J., ed., 1981, Platinum-group elements—Mineralogy, geology, recovery: Canadian Institute of Metallurgy, Special Volume 23, 267 p.
Caby, Renaud, and Kienast, J.R., 2009, Neoproterozoic and Hercynian metamorphic events in the Central Mauritanides—Implications for the geodynamic evolution of West Africa: Journal of African Earth Sciences, v. 53, issue 3, p. 122–136.
Cambell, Geoff, 2011, Exploration geophysics of the Bushveld Complex in South Africa—The leading edge: Society for Exploration Geophysicists, v. 30, no. 6, p. 622–638.
Cawthorn, R.G., Barnes, S.J., Ballhaus, Christian, and Malitch, K.N., 2005, Platinum group element, chromium, and vanadium deposits in mafic and ultramafic rocks, *in* Hedenquist, J.W., Thompson, J.F., H., Goldfarb, R.J., and Richards, J.P., eds., Economic Geology, 100th anniversary volume, 1905–2005: Society of Economic Geologists, Littleton, Colo., United States, p. 215–249.
Chardon, D., Davy, P., Choukroune, P., and Cobbold, P.R., 1997, Thermal experiments of Rayleigh-Taylor instabilities in the continental lithosphere [abs.]: Eos, Transactions of the American Geophysical Union, no. 78, p. 713.
Clark, D.A., 1999, Magnetic petrology of igneous intrusions—Implications for exploration and magnetic interpretation: Exploration Geophysics, v. 30, p. 5–26.
Crocket, J.H., 1981, Geochemistry of the platinum-group elements, *in* Cabri, L.J., ed., Platinum-group elements—Mineralogy, geology, recovery: Canadian Institute of Metallurgy, Special Volume 23, p 47–64.
Dallmeyer, R.D., and Lécorché, J.P., 1989, $^{40}Ar/^{39}Ar$ polyorogenic mineral age record within the central Mauritanide orogen, West Africa: Geological Society of America Bulletin, v. 101, p. 55–70.
Dallmeyer, R.D., and Lécorché, J.P., 1990a, $^{40}Ar/^{39}Ar$ polyorogenic mineral age record in the northern Mauritanide orogen, West Africa: Tectonophysics, v. 177, p. 81–107.
Dallmeyer, R.D., and Lécorché, J.P., 1990b, $^{40}Ar/^{39}Ar$ polyorogenic mineral age record within the southern Mauritanide orogen (M'bout-Bakel Region), West Africa: American Journal of Science, v. 290, p. 1136–1168.
Dosso, L., Vidal, P., and Sichler, B., 1979, Age précambrien de dolerites de la Dorsale Reguibat (Mauritanie): Paris, C.R., Acad. Sci., Sér D, 288, p. 739–742.

Dowling, S.E., and Hill, R.E.T., 1998, Komatiite-hosted nickel sulphide deposits, Australia: AGSO Journal of Australian Geology and Geophysics,v. 17, 121–128.
Duke, J.M., 1983, Magmatic segregation deposits of chromite: Geoscience Canada, v. 10, no. 1, p.133–143.
Duke, J.M., 1996, Podiform (ophiolitic) chromite, *in* Eckstrand, O.R., Sinclair, W.D., and Thorpe, R.I., eds., Geology of Canadian Mineral Deposit Types: Geological Society of America, The Geology of North America, v. P-1, p. 621–624.
Dumas, J.P., 1971, Recherche de gîtes de nickel sulfuré au Tasiast et au Tijirit (Mauritanie): Rapport Bureau de Recherches Géologiques et Minières (BRGM), 71 DAK 001.
Economou-Eliopoulos, Maria, 1996, Platinum-group element distribution in chromite ores from ophiolite complexes—Implications for their exploration: Ore Geology Reviews, v. 11, no. 6, p. 363–381.
Economou-Eliopoulos, Maria, 2003, Apatite and Mn, Zn, Co-enriched chromite in Ni-laterites of northern Greece and their genetic significance: Journal of Geochemical Exploration, v. 80. p. 41–54.
Evans, D.M., Barrett, F.M., Prichard, H.M., and Fisher, P.C., 2011, Platinum-palladium-gold mineralization in the Nkenja mafic-ultramafic body, Ubendian metamorphic belt, Tanzania: Mineralium Deposita, v. 47, p. 175–196.
Fernette, G.L., 2015, Iron oxide copper-gold deposits in the Islamic Republic of Mauritania (phase V, deliverables 79), chap. M *of* Taylor, C.D., ed., Second projet de renforcement institutionnel du secteur minier de la République Islamique de Mauritanie (PRISM-II): U.S. Geological Survey Open-File Report 2013–1280-M, 21 p., http://dx.doi.org/10.3133/ofr20131280/. [In English and French.]
Finn, C.A., and Anderson, E.D., 2015, Synthesis of geophysical data (phase V, deliverable 55), chap. B *of* Taylor, C.D., ed., Second projet de renforcement institutionnel du secteur minier de la République Islamique de Mauritanie (PRISM-II): U.S. Geological Survey Open-File Report 2013–1280-B, 60 p., http://dx.doi.org/10.3133/ofr20131280/. [In English and French.]
Foley, J.Y., Light, T.D., Nelson, S.W., and Harris, R.A., 1997, Mineral occurrences associated with mafic-ultramafic and related alkaline complexes in Alaska, *in* Goldfarb, R.J., and Miller, L.D., eds., Mineral deposits of Alaska: Economic Geology Monograph 9, p. 334–354.
Freyssinet, P.H., 1994, Prospection aurifère dans le Tasiast-Tijirit (Mauritanie), Etude géomorphologique : Rapport Bureau de Recherches Géologiques et Minières (BRGM), 1278–DR 94.
General Gold International, S.A., 1997, Mauritania South Project Mining Prospection Permit M40: Annual Report 1996–1997, August, 1997.
Goldfarb, R.J., Marsh, E.E., Anderson, E.D., Horton, J.D., Finn, C.A., and Beaudoin, Georges, 2015, Mineral potential tracts for orogenic, Carlin-like, and epithermal gold deposits in the Islamic Republic of Mauritania, (phase V, deliverable 69), chap. H *of* Taylor, C.D., ed., Second projet de renforcement institutionnel du secteur minier de la République Islamique de Mauritanie (PRISM-II): U.S. Geological Survey Open-File Report 2013–1280-H, 19 p., http://dx.doi.org/10.3133/ofr20131280/. [In English and French.]

Gunn, A.G., Pitfield, P.E.J., Mckervey, J.A., Key, R.M., Waters, C.N., and Barnes, R.P., 2004, Notice explicative des cartes géologiques et gîtologiques à 1/200 000 et 1/500 000 du Sud de la Mauritanie, Volume 2—Potentiel Minier: Direction des Mines et de la Géologie (DMG), Ministère des Mines et de l'Industrie, Nouakchott.

Helmy, H.M., and Mogessie, Aberra, 2001, Gabbro Akarem, Eastern Desert, Egypt—Cu-Ni-PGE mineralization in a concentrically zoned mafic-ultramafic complex: Mineralium Deposita, v. 36, p. 58–71.

Himmelberg, G.R., and Loney, R.A., 1995, Characteristics and petrogenesis of Alaskan-type ultramafic-mafic intrusions, southeastern Alaska: U.S. Geological Survey Professional Paper 1564, 47 p. [Available at http://pubs.er.usgs.gov/publication/pp1564.]

Irvine, T.N., 1965, Chrome spinel as a petrogenetic indicator, Part II, Petrologic applications: Canadian Journal of Earth Sciences, v. 2, p. 648–671.

Irvine, T.N., 1967, Chrome spinel as a petrogenetic indicator, Part I, Theory: Canadian Journal of Earth Sciences, v. 4, p. 71–103.

Irvine, T.N., 1974, Petrology of the Duke Island ultramafic complex, southeastern Alaska: Geological Society of America Memoir 138, 240 p.

Jan, M.Q., and Windley, B.F., 1990, Chromian spinel-silicate chemistry in ultramafic rocks of the Jilal Complex, northwestern Pakistan: Journal of Petrology, v. 31, p. 667–715.

Johan, Z., 2002, Alaskan-type complexes and their platinum-group element mineralization, *in* Cabri, L.J., ed., The geology, geochemistry, mineralogy, and mineral beneficiation of platinum-group elements: Canadian Institute of Metallurgy, Special Volume 54, p. 579–618.

Key, R.M., Loughlin, S.C., Gillespie, M., Del Rio, M., Horstwood, M.S.A., Crowley, Q.G., Darbyshire, D.P.F., Pitfield, P.E.J., and Henney, P.J., 2008, Two Mesoarchaean terranes in the Reguibat Shield of NW Mauritania: Geological Society of London Special Publication 297, p. 33–52.

Kleinkopf, M.D., 1985, Regional gravity and magnetic anomalies of the Stillwater Complex area, *in* Czamanske, G.K., and Zientek, M.L., eds., The Stillwater Complex, Montana—Geology and Guide: Butte, Montana Bureau of Mines and Geology Special Publication 92, p. 33–38.

Krause, J., Brugmann, G.E., and Pushkarev, E.V., 2007, Accessory and rock forming minerals monitoring the evolution of zoned mafic-ultramafic complexes in the central Ural Mountains: Lithos, v. 95, p. 19–42.

Krause, J., Brugmann, G.E., and Pushkarev, E.V., 2011, Chemical composition of spinel from Uralian-Alaskan-type mafic-ultramafic complexes and its petrogenetic significance: Contributions to Mineralogy and Petrology, v. 161, p. 255–273.

Lahondère, D., Thieblemont, D., Goujou, J.-C., Roger, J., Moussine-Pouchkine, A., LeMetour, J., Cocherie, A., and Guerrot, C., 2003, Notice explicative des cartes géologiques et gîtologiques à 1/200 000 et 1/500 000 du Nord de la Mauritanie, v. 1: Direction des Mines et de la Géologie (DMG), Ministère des Mines et de l'Industrie, Nouakchott.

Lee, C.A., and Parry, S.J., 1988, Platinum-group element geochemistry of the Lower and Middle Group chromitites of the eastern Bushveld Complex: Economic Geology, p. 83, p. 1127–1139.

Le Page, Alain, 1988, Rock deformation associated with the displacement of allochthonous units in the central segment of the Caledono-Hercynian Mauritanide Belt (Islamic Republic of Mauritania and eastern Senegal): Journal of African Earth Sciences, v. 7, p. 265–283, doi:10.1016/0899-5362(88)90073-5.
Maier, W. and Barnes, S.-J., 2008, Platinum-group elements in the UG1 and UG2 chromitites, and the Bastard reef, at Impala platinum mine, western Bushveld Complex, South Africa—Evidence for late magmatic cumulate instability and reef construction: South African Journal of Geology, v. 111, p. 159–176.
Marsh, E.E. and Anderson, E.D., 2011, Ni-Co laterite deposits: U.S. Geological Survey Open-File Report 2011–1259, 9 p.
Marsh, E.E., Anderson, E.D., 2015, Database of mineral deposits in the Islamic Republic of Mauritania (phase V, deliverables 90 and 91), chap. S *of* Taylor, C.D., ed., Second projet de renforcement institutionnel du secteur minier de la République Islamique de Mauritanie (PRISM-II): U.S. Geological Survey Open-File Report 2013–1280-S, 9 p., Access database, http://dx.doi.org/10.3133/ofr20131280/. [In English and French.]
Marot, A., Stein, G., Artigan, D., and Milési J.-P., 2003, Notice explicative des cartes géologiques et gîtologiques à 1/200 000 et 1/500 000 du Nord de la Mauritanie, Volume 2—Potentiel Minier: Direction des Mines et de la Géologie (DMG), Ministère des Mines et de l'Industrie, Nouakchott.
Marutani, Masaharu, Higashihara, Masami, Watanabe,Yasushi, Murakami,Hiroyasu, Kojima Gen, and Dioumassi, Boubou, 2005, Metallic ore deposits in the Islamic Republic of Mauritania: Shigen-Chishitsu, The Society of Resource Geology, v.55, p. 59–70.
Marzoli, Andrea, Renne, P.R., Piccirillo, E.M., Ernesto, Marcia, Bellieni, Giuliano, and De Min, Angelo, 1999, Extensive 200-million-year-old continental flood basalts of the Central Atlantic Magmatic Province: Science, v. 284, no. 5414, p. 616–618.
McLaren, C.H., and De Villiers, J.P.R., 1982, The platinum-group chemistry and mineralogy of the UG-2 chromitite layer of the Bushveld Complex: Economic Geology, v. 77, p. 1348–1366.
Meyer, F.M., Kolb, Jochen, Sakellaris, G.A., and Gerdes, Axel, 2006, New ages from the Mauritanides belt—Recognition of Archean IOCG mineralization at Guelb Moghrein, Mauritania: Terra Nova, v. 18. P. 345–352.
Muller, Y., 1972, Mission nickel sulfure du Tasiast (Mauritanie occidentale): Rapport Bureau de Recherches Géologiques et Minières (BRGM), 73 RME 025 AF.
Nabighian, M.N., 1972, The analytic signal of two-dimensional magnetic bodies with polygonal cross-section—Its properties and use for automated anomaly interpretation: Geophyisics, v. 37, no. 3, p. 507–517.
Naldrett, A.J., 1989, Magmatic sulfide deposits: New York, Oxford University Press, 196 p.
Noble, J.A., and Taylor, H.P., Jr., 1960, Correlation of the ultramafic complexes of southeastern Alaska with those of other parts of North America and the world, 21st International Geologic Congress, Copenhagen, Denmark: International Geologic Congress, Copenhagen, Denmark, Reports, p. 188–197.
O'Connor, E. A., Pitfield, P. E. J., Schofield, D. I., Coats, S., Waters, C., Powell, J., Ford, J., Clarke, S., and Gillespie, M., 2005, Notice explicative des cartes géologiques et gîtologiques à 1/200 000 et 1/500 000 du Nord-Ouest de la Mauritanie, Direction des

Mines et de la Géologie (DMG), Ministere des Mines et de l'Industrie, Nouakchott, 398 p.
OMRG–Otto Gold, 1986, Récherche minière entre Moudjeria et Diaguili: Mauritanian Office for Geological Research rapport final 1983–1986.
OMRG–Otto Gold, 1990, Specific mining exploration in the Mauritanides—Provisional Final Report Geochemistry and Geophysics, 1989/1990 campaign, July 1990: Mauritanian Office for Geological Research.
Page, N.J., Rowe, J.J., and Haffty, Joseph, 1976, Platinum metals in the Stillwater Complex, Montana: Economic Geology, v. 71, p. 1352–1363.
Pitfield, P.E.J., Key, R.M., Waters, C.N., Hawkins, M.P.H., Scholfield, D.I., Loughlin, S. and Barnes, R.P., 2004, Notice explicative des cartes géologiques et gîtologiques à 1/200 000 et 1/500 000 du Sud de la Mauritanie, volume 1—Géologie: Direction des Mines et de la Géologie (DMG), Ministère des Mines et de l'Industrie, Nouakchott.
Potrel, Alain, Peucat, J.J., and Fanning, C.M., 1998, Archean crustal evolution of the West African Craton—Example of the Amsaga Area (Reguibat Rise)—U-Pb and Sm-Nd evidence for crustal growth and recycling: Precambrian Research, v. 90, p.107–117.
Ripley, E.M., Li, C., and Thakurta, J., 2005, Magmatic Cu-Ni-PGE mineralization at a convergent plate boundary—Preliminary mineralogic and isotopic studies of the Duke Island Complex, Alaska, *in* Mao, Jingwen, and Bierlein, F.P., eds., Mineral Deposit Research—Meeting the Global Challenge, Proceedings of the Eighth Biennial SGA meeting, August 18–21, 2005, Beijing, China: Berlin, Heidelberg, Springer Verlag, p. 49–51.
Rocci, G., Bronner, G, and Deschamps, M., 1991, Crystalline basement of the West African Craton, *in* Dallmeyer, R.D., and Lécorché J.P., eds., The West African Orogens and Circum-Atlantic Correlatives: Berlin, Heidelberg, Springer Verlag, p.31–61.
Roedder, P.L., 1994, Chromite—From the fiery rain of chondrules to Kilauea Iki lava lake: Canadian Mineralogist, v. 32, p.729–746.
Roest, W.R., Verhoef, Jacob, and Pilkington, Mark, 1992, Magnetic interpretation using the 3D analytic signal: Geophysics, v. 57, no. 1, p. 116–125.
Salpeteur, I., 2005, Perspectives minières dans le Sud de la Mauritanie, Levé géologique de l'extrême sud de la Mauritanie (projet PRISM): Direction des Mines et de la Géologie (DMG), Ministère des Mines et de l'Industrie, Nouakchott, et rapport Bureau de Recherches Géologiques et Minières (BRGM), RC-54132-FR, Orléans, 100 p.
Samama, J.-C, 1986, Ore fields and continental weathering (Evolution of ore fields series): New York, Van Nostrand Reinhold Co., 326 p.
Singer, D.A., Page, N. J, and Lipin, B.R., 1986, Grade and tonnage model of major podiform chromite, *in* Cox, D.P., and Singer, D.A., eds., Mineral Deposit Models: U.S. Geological Survey Bulletin 1693, 379 p. [Available at http://pubs.usgs.gov/bul/b1693/html/bullfrms.htm.]
Sutphin, D.M., Ford, A.B., Karl, S.M., Duttweiler, K.A., and Finn, C.A., 1992, Probabilistic estimates of metal endowment in undiscovered deposits for selected deposit types in the Sitka, Alaska, 1:250,000-scale quadrangle, *in* Bliss, J.D., ed., Developments in mineral deposit modeling: U.S. Geological Survey Bulletin 2004.
Tait, J., Straathof, G., Soderlund, U., Ernst, R.E., Key, R., Jowitt, S.M., Lo, K., Dahmada, M.E.M., and N'Diaye, O., 2013, The Ahmeyim Great Dike of Mauritania—A newly dated Archaean intrusion: Lithos, v. 174, p. 323–332.

Taylor, C.D., and Giles, S.A., 2015a, Mineral potential for volcanogenic massive sulfide deposits in the Islamic Republic of Mauritania, (phase V, deliverable 77), chap. L *of* Taylor, C.D., ed.,Second projet de renforcement institutionnel du secteur minier de la République Islamique de Mauritanie (PRISM-II): U.S. Geological Survey Open-File Report 2013–1280-L, 70 p., http://dx.doi.org/10.3133/ofr20131280/. [In English and French.]

Taylor, C.D., and Giles, S.A., 2015b, Mineral potential for incompatible element deposits hosted in pegmatites, alkaline rocks, and carbonatites in the Islamic Republic of Mauritania (phase V, deliverable 87), chap. Q *of* Taylor, C.D., ed., Second projet de renforcement institutionnel du secteur minier de la République Islamique de Mauritanie (PRISM-II): U.S. Geological Survey Open-File Report 2013–1280-Q, 41 p., http://dx.doi.org/10.3133/ofr20131280/. [In English and French.]

Taylor, C.D., and Giles, S.A., 2015c, Mineral potential for sediment-hosted copper deposits in the Islamic Republic of Mauritania (phase V, deliverable 75), chap. K *of* Taylor, C.D., ed., Second projet de renforcement institutionnel du secteur minier de la République Islamique de Mauritanie (PRISM-II): U.S. Geological Survey Open-File Report 2013–1280-K, 53 p., http://dx.doi.org/10.3133/ofr20131280/. [In English and French.]

Taylor, H.P., Jr., 1967, The zoned ultramafic complexes of southeastern Alaska, *in* Wyllie, P.J., ed., Ultramafic and related rocks: New York, John Wiley, p. 97–118.

Taylor, H.P., Jr., and Noble, J.A., 1960, Origin of ultramafic complexes in southeastern Alaska, 21st International Geologic Congress, Copenhagen, Denmark: International Geologic Congress, Copenhagen, Denmark, Reports, 1960, p. 175–187.

Taylor, H.P., Jr., and Noble, J.A., 1969, Origin of magnetite in zoned ultramafic complexes in southeastern Alaska: Economic Geology Monograph 4, p. 209–230.

Tistl, M., 1994, Geochemistry of platinum-group elements of the zoned ultramafic Alto Condoto Complex, northwest Colombia: Economic Geology, v. 89, p. 158–167.

Tsoupas, G., and Economou-Eliopoulos, Maria, 2008, High PGE contents and extremely abundant PGE-minerals hosted in chromitites from the Veria ophiolite complex, northern Greece: Ore Geology Reviews, v. 33, p. 3–19.

Valeton, I., Biermann, M., Reche, R., and Rosenberg, F., 1987, Genesis of nickel laterites and bauxites in Greece during the Jurassic and Cretaceous, and their relation to ultrabasic parent rock: Ore Geology Reviews, v. 2, p. 359–404.

Viljoen, M.J., 1999, The nature and origin of the Merensky Reef of the western Bushveld Complex based on geological facies and geological data: South African Journal of Geology, v. 102, no. 3, p. 221–239.

Wyllie, P.J., ed., 1967, Ultramafic and related rocks: New York, John Wiley, 464 p.

Zaccarini, F., Pushkarev, E.V., and Garuti, G., 2008, Platinum-group element mineralogy and geochemistry of chromitite of the Kluchevskoy ophiolite complex, central Urals (Russia): Ore Geology Reviews, v. 33, p. 20–30.

ISSN 2331-1258 (online)
http://dx.doi.org/10.3133/ofr20131280